

MANF AND CDFN AS THERAPEUTIC TARGETS FOR BIPOLAR DISORDER

ESTABLISHING THE ROLE OF MESENCEPHALIC ASTROCYTE-DERIVED
NEUROTROPHIC FACTOR (MANF) AND CEREBRAL DOPAMINE
NEUROTROPHIC FACTOR (CDNF) AS THERAPEUTIC TARGETS FOR BIPOLAR
DISORDER

By

SHREYA PRASHAR

H.BSc.

A Thesis

Submitted to the School of Graduate Studies

in Partial Fulfilment of the Requirements

for the Degree

Master of Science

McMaster University

© Copyright by Shreya Prashar, June 2017

Master of Science (2017) - Neuroscience

McMaster Integrative Neuroscience & Discovery Study (MiNDS) Program

McMaster University

Hamilton, Ontario

TITLE: Establishing the Role of Mesencephalic Astrocyte-derived Neurotrophic Factor
(MANF) and Cerebral Dopamine Neurotrophic Factor (CDNF) as Therapeutic
Targets for Bipolar Disorder

AUTHOR: Shreya Prashar, H.BSc. (Biology & Psychology), McMaster University

SUPERVISOR: Dr. Ram K. Mishra

COMMITTEE: Dr. Benicio N. Frey

Dr. Bhagwati Gupta

NUMBER OF PAGES: xvi, 117

ABSTRACT

Bipolar disorder (BD) is a chronic mood disorder affecting ~1-2% of the global population, characterized by cycling moods of mania and depression. The exact pathogenesis of BD is unknown; however, it has been established that endoplasmic reticulum (ER) stress plays an important role. It is known that BD patients have abnormal activity and expression of ER stress proteins in several brain regions. There exists a need for a definitive diagnostic test for the early detection of BD as it is often misdiagnosed for other conditions including unipolar depression and schizophrenia. Understanding the underlying mechanisms and therapeutic targets being used by BD treatments will be helpful in establishing a diagnostic test. The current gold standard for BD treatment includes Lithium (LiCl) prescription, along with other mood stabilizers such as Valproic acid (VPA) and antipsychotics such as Olanzapine. Current therapies only relieve symptoms and are unable to stop disease progression. Neurotrophic factors (NTFs) are naturally occurring proteins that are responsible for the maintenance, differentiation, and survival of neurons. Cerebral dopamine NTF (CDNF) and Mesencephalic astrocyte-derived NTF (MANF) belong to a novel class of NTFs specific to dopaminergic neurons. This study investigated the role of CDFN and MANF as therapeutic targets for bipolar disorder in *SH-SY5Y* cells and Sprague Dawley rats, as well as determining the endogenous mRNA levels of CDFN and MANF in BD patients. We demonstrated that common BD mood stabilizers – LiCl and VPA – significantly increased the mRNA expression of MANF and CDFN *in vitro*. Additionally, we also established that these mood stabilizers alter the NTFs expression in different rat brain regions including pre-frontal cortex (PFC) and cortex. These findings

suggest that BD drug treatments potentially act via NTFs in order to relieve symptoms. Thus it highlights the importance of further investigating the interaction between neurotrophic factors and bipolar disorder.

*I dedicate this work to my parents for their hard work and unconditional love.
From you, I have learned to never give up, and work hard and honestly.
Your efforts have made me capable of being here today.
Thank you for always believing in me.*

ACKNOWLEDGEMENTS

First and foremost, I would like to thank my supervisor, Dr. Ram Mishra, for trusting me and giving me this wonderful opportunity to conduct my Master's research in his lab. Throughout the duration of my graduate experience, Dr. Mishra has always been there to support, guide, and encourage me in all aspects. His genuine interest in the well-being and success of his students reflects in the manner he provides supervision. He always provided opportunities, allowing me to enhance my academic and personal growth. I am extremely thankful for all his advice and guidance over the last two years, and I hope I have lived up to his expectations.

I would also like to thank my undergraduate supervisor, Dr. Bhagwati Gupta, for his support, and for encouraging my interest in research. While conducting my undergraduate thesis research in your lab, I truly started to enjoy research. Without your guidance, I would not have been here today. I would also like to thank Dr. Benicio N. Frey, for his constant support, guidance, and enthusiasm in my project over the course of my graduate studies. You have helped me understand what it means to be genuinely interested in learning and research.

I am extremely lucky to have had the opportunity to work with all of the Mishra lab members. You made the past two years fly by quickly with all the laughs and Sushi lunches. The Mishra Lab would not have been the same without any of you – Ashley, Omar, Roohie, Sharon, Joella, Kos, Luke, Heta, Ritesh, Jay, Khaled, Brett, and Dima. Thanks for being a super MiNDS Thunderbuddy Ashley! And a special thank you to Khaled for helping me run the crazy number of qPCRs in the limited amount of time. It would not have been

possible without your help. Thank you to Crystal (honorary Mishra lab member) for not only the cell images, but for always being kind and supportive, and making the last two years memorable. I would also like to thank members of the West-Mays lab for being super welcoming and helpful every time I stopped by their lab to use their equipment for our experiments.

Thank you to all of my friends for your constant encouragement and for listening to me talk endlessly about neurotrophic factors. You have all become masters of CDFN and MANF now. Hanan, Sukhi, Soumya, Pavithra, Lisa, Davinder, Farhat, and Michele – these past two years would not have been the same without any of you. Thank you being there for me throughout this process. A special shoutout to my cousin, Juhi, for her amazing artistic abilities that always come handy!

Last but not least, thank you to my parents and brother for encouraging me every step of the way. Thank you for being my support system, and always having faith in my abilities. This would not have been possible without your help and understanding. Thank you for understanding why cell work often took precedence over important birthday celebrations and vacations. Bhaiya, thank you for being an amazing role model. You made this whole process much easier with your support. Thank you to my grandparents for keeping me grounded and reminding me to be thankful for all of my blessings. I hope I have made you all proud.

Table of Contents

ABSTRACT	iii
ACKNOWLEDGEMENTS	vi
LIST OF FIGURES	x
LIST OF TABLES	xiii
ABBREVIATIONS	xiv
Chapter 1	1
1.1 Overview of Neurotrophic Factors: CDNF and MANF	2
1.1.1 Structure	4
1.1.2 Function.....	10
1.2 Bipolar Disorder	12
1.2.1 Prevalence and Symptomology.....	12
1.2.3 Implications of Neurotrophic Factors in Bipolar Disorder	13
1.2.4 Bipolar Disorder Treatments.....	15
1.3 SH-SY5Y Cells	17
Chapter 2	20
2.1 Objective	21
2.2 Materials and Methodology	21
2.2.1 SH-SY5Y Cells – Drug Treatments.....	21
2.2.2 RNA Extraction from Cells.....	22
2.2.3 cDNA Synthesis from SH-SY5Y Cells’ RNA.....	23
2.2.4 Reverse Transcription PCR (RT-PCR)	26
2.2.5 Real-Time Quantitative Reverse Transcription PCR (RT-qPCR)	28
2.2.6 Statistical Analysis	28
2.3 Results	32
2.3.1 Effect of Lithium and VPA on neurotrophic factors expression in SH-SY5Y cells	32
2.4 Discussion	34
Chapter 3	38
3.1 Objective	39
3.2 Materials and Methodology	39
3.2.1 Rats study 1 – December 2016 (N = 22).....	39
3.2.2 Drug Treatments.....	40
3.2.3 Sacrifice, Blood Collection, and Tissue Dissection	40
3.2.4 Rats study 2 – March 2017 (N=16).....	41
3.2.5 Behavioural Test – Open Field Task.....	41
3.2.6 RNA Extraction from Rat Tissues	43
3.2.7 cDNA Synthesis from Rat Tissues’ RNA	44
3.2.8 Reverse Transcription PCR (RT-PCR)	44
3.2.9 Real-Time Quantitative Reverse Transcription PCR (RT-qPCR)	48
3.2.10 Statistical Analysis	49
3.3 Results	60

3.3.1 Body Weight Change Due to Drug Administration – Cohort 1	60
3.3.2 Levels of Drug Treatments in Rats’ Blood Plasma – Cohort 1	61
3.3.3 Effect of Lithium and VPA on CDNF and MANF mRNA expression in rat PFC	62
3.3.4 Effect of Lithium and VPA on CDNF and MANF mRNA expression in rat Striatum	63
3.3.5 Effect of Lithium & VPA on Hippocampus CDNF and MANF mRNA expression	64
3.3.6 Effect of Lithium & VPA on CDNF and MANF mRNA expression in rat Cortex	65
3.3.7 Effect of Lithium and VPA on GAPDH mRNA expression in Striatum, Hippocampus, Cortex, and PFC.	66
3.3.8 Body Weight Change Due to Drug Administration – Cohort 2	67
3.3.9 Levels of Drug Treatments in Rats’ Blood Plasma – Cohort 2	68
3.3.10 Open-Field Task – Behavioural Data	69
3.3.11 Effect of Lithium and VPA on CDNF mRNA expression in rat PFC	71
3.3.12 Effect of Lithium and VPA on MANF mRNA expression in rat PFC	72
3.3.13 Effect of Lithium and VPA on CDNF and MANF mRNA expression in rat Hippocampus	73
3.3.14 Effect of Lithium and VPA on CDNF and MANF mRNA expression in rat Striatum	74
3.3.15 Effect of Lithium and VPA on CDNF and MANF mRNA expression in rat Cortex ..	75
3.3.16 Effect of Lithium and VPA on CDNF and MANF mRNA expression in rat mPFC ..	76
3.3.17 Effect of Lithium and VPA on CDNF and MANF mRNA expression in rat Amygdala	77
3.3.18 Effect of Lithium and VPA on GAPDH mRNA expression in PFC and mPFC	78
3.3.19 Effect of Lithium and VPA on GAPDH mRNA expression in rat Hippocampus and Amygdala	79
3.3.20 Effect of Lithium and VPA on GAPDH mRNA expression in rat Striatum and Cortex	80
3.4 Discussion	81
Chapter 4	85
4.1 Objective.....	86
4.2 Materials and Methodology.....	87
4.2.1 Blood Samples Collection and Preparation.....	87
4.2.2 cDNA Synthesis from Blood RNA	87
4.2.3 Reverse Transcription PCR (RT-PCR)	87
4.2.4 Real-Time Quantitative Reverse Transcription Polymerase Chain Reaction (RT-qPCR)	88
4.2.5 Statistical Analysis	89
4.3 Human Blood Samples – RT qPCR Results.....	92
4.3.1 CDNF mRNA Expression in Blood	92
4.3.2 MANF mRNA Expression in Blood	95
4.3.3 GAPDH mRNA Expression in Blood	98
4.4 Discussion	101
4.5 Conclusion	104
References.....	105

LIST OF FIGURES

Figure 1. BLAST sequence alignment of MANF.....	3
Figure 2. Phylogenetic Tree for CDFN and MANF in different species.....	5
Figure 3. Schematic representation of human MANF & CDFN proteins' primary structure.....	7
Figure 4. NMR solution structure of human MANF.	8
Figure 5. NMR solution structure of human CDFN.	9
Figure 6. Wild-type SH-SY5Y cells before and after differentiation.....	19
Figure 7. Sample drug treatment setup for 6-well plate.....	24
Figure 8. Sample experimental timeline.	25
Figure 9. Gel electrophoresis of human CDFN gene.....	30
Figure 10. Gel electrophoresis of human MANF gene.....	31
Figure 11. CDFN mRNA expression in <i>SH-SY5Y</i> cells treated with Lithium and VPA. ...	32
Figure 12. MANF mRNA expression in <i>SH-SY5Y</i> cells treated with Lithium and VPA. .	33
Figure 13. Sample diagram of open-field chamber.	42
Figure 14. Gel electrophoresis of rat CDFN, MANF and GAPDH genes.....	47
Figure 15. Standard Curve output for RT-qPCR.	50
Figure 16. C _t values for RT-qPCR.....	51
Figure 17. Amplification plot for RT-qPCR.....	52
Figure 18. Dissociation curve for RT-qPCR.....	53
Figure 19. Rat Striatum.....	54
Figure 20. Rat Pre-Frontal Cortex (PFC).....	55

Figure 21. Rat Cortex.....	56
Figure 22. Rat Hippocampus.	57
Figure 23. Rat Amygdala.....	58
Figure 24. Rat Medial Pre-Frontal Cortex (mPFC).	59
Figure 25. Effects of Lithium and VPA on rats’ body weight.....	60
Figure 26. Levels of drug treatments in blood plasma from rats- cohort 1.	61
Figure 27. NTFs mRNA expression in PFC of rats treated with Lithium and VPA.	62
Figure 28. NTFs mRNA expression in striatum of rats treated with Lithium and VPA. ..	63
Figure 29. NTFs mRNA expression in hippocampus of rats treated with Lithium and VPA.	64
Figure 30. NTFs mRNA expression in Cortex of rats treated with Lithium and VPA.....	65
Figure 31. GAPDH mRNA expression in brain regions of rats treated with Lithium and VPA.	66
Figure 32. Effects of Lithium and VPA on rats’ body weight – cohort 2.....	67
Figure 33. Levels of drug treatments in blood plasma from rats- cohort 2.	68
Figure 34. Locomotion data from the open-field behavioural task.	69
Figure 35. Rearing data from open-field behavioural task.	70
Figure 36. CDNF mRNA expression in PFC of rats treated with Lithium and VPA.....	71
Figure 37. MANF mRNA expression in PFC of rats treated with Lithium and VPA.....	72
Figure 38. NTFs mRNA expression in hippocampus of rats treated with Lithium and VPA.	73
Figure 39. NTFs mRNA expression in striatum of rats treated with Lithium and VPA. ..	74

Figure 40. NTFs mRNA expression in cortex of rats treated with Lithium and VPA.	75
Figure 41. NTFs mRNA expression in mPFC of rats treated with Lithium and VPA.	76
Figure 42. NTFs mRNA expression in amygdala of rats treated with Lithium and VPA.	77
Figure 43. GAPDH mRNA expression in rats PFC & mPFC treated with Lithium and VPA.	78
Figure 44. GAPDH mRNA in rats hippocampus & amygdala treated with Lithium and VPA.	79
Figure 45. GAPDH mRNA in rats striatum and cortex treated with Lithium and VPA. ..	80
Figure 46. CDNF mRNA expression in human blood samples (<21 years).	92
Figure 47. CDNF mRNA expression in human blood samples (21 – 49 years).....	93
Figure 48. CDNF mRNA expression in human blood samples (49+ years).	94
Figure 49. MANF mRNA expression in human blood samples (<21 years).	95
Figure 50. MANF mRNA expression in human blood samples (21 – 49 years).....	96
Figure 51. MANF mRNA expression in human blood samples (49+ years).	97
Figure 52. GAPDH mRNA expression in human blood samples (<21 years).	98
Figure 53. GAPDH mRNA expression in human blood samples (21 – 49 years).....	99
Figure 54. GAPDH mRNA expression in human blood samples (49+ years).	100

LIST OF TABLES

Table 1. Human CDNF and MANF primer sequences.....	27
Table 2. Forward and reverse primer sequences for rats.....	46
Table 3. Forward and reverse primer sequences for human samples.....	91

ABBREVIATIONS

6-OHDA	6-hydroxydopamine
ARMET	Arginine-rich, mutated in early stage tumors
ANOVA	Analysis of variance
BAX	BCL2 associated X
BBB	Blood-brain-barrier
BD	Bipolar disorder
CAF	Central Animal Facility
CALR	Calreticulin
cDNA	Complementary DNA
CDNF	Cerebral dopamine neurotrophic factor
ChAT	Choline acetyl transferase
D2R	Dopamine receptor subtype 2
D3R	Dopamine receptor subtype 3
DA	Dopamine
DAergic	Dopaminergic
DAT	Dopamine transporter
ER	Endoplasmic reticulum
ERK	Extracellular signal-regulated kinase
FBS	Fetal bovine serum
GAPDH	Glyceraldehyde 3-phosphate dehydrogenase

GFLs	Glial family of ligands
GSK-3	Glycogen synthase kinase-3
HDAC	Histone deacetylase
IP	Intraperitoneal
IP ₃	Inositol 4,5-Triphosphate
Ku70	Ku antigen p70 subunit
LiCl	Lithium chloride
MANF	Mesencephalic astrocyte-derived neurotrophic factor
MAPK	Mitogen-activated protein kinase
mPFC	Medial prefrontal cortex
MPP ⁺	1-methyl-4-phenyl-pyridinium ion
MPTP	1-methyl-4-phenyl-1,2,3,6- tetrahydropyridine
NAA	N-acetyl aspartate
NRT	No-reverse-transcription
NTC	No template control
NTF	Neurotrophic factor
PCR	Polymerase chain reaction
PD	Parkinson's disease
PFC	Pre-frontal cortex
PI3K	Phosphatidylinositol 3-kinase
PKC	Protein kinase C
RT	Reverse transcription

RT-PCR	Reverse transcription polymerase chain reaction
RT-qPCR	Real-time quantitative reverse transcription PCR
SCG	Superior cervical ganglion
TH	Tyrosine hydroxylase
UPR	Unfolded protein response
VMAT	Vesicular monamine transporter
VPA	Valproic acid

Chapter 1

Introduction to Neurotrophic Factors and Bipolar Disorder

1.1 Overview of Neurotrophic Factors: CDNF and MANF

Neurotrophic factors (NTFs) are secreted proteins that are important in the development, differentiation and survival of neurons (Lindholm & Saarma, 2010). NTFs are specific to the subset of neurons that they affect. Mesencephalic astrocyte-derived neurotrophic factor (MANF) and cerebral dopamine neurotrophic factor (CDNF) are two NTFs which display neuroprotective properties for dopaminergic (DAergic) neurons (Lindholm & Saarma, 2010). MANF and CDNF are conserved between different species from *C. elegans* to humans (**Figures 1 and 2**), and they are structurally different than members of the other families of NTFs (Lindholm et al., 2008; Palgi et al., 2009). CDNF and MANF have been demonstrated to be essential for the development of DAergic neurons in studies conducted *in vivo* with drosophila and zebrafish (Chen et al., 2012; Palgi et al., 2012). Along with being extracellularly secreted as a trophic factor, both MANF and CDNF mainly localize in the endoplasmic reticulum (ER), making them functionally distinct from the classical, target-derived secreted NTFs (Apostolou et al., 2008).

1.1.1 Structure

Petrova and colleagues first discovered the novel secreted human protein called MANF in 2003, and it was originally known as arginine-rich, mutated in early stage tumors (ARMET). Human MANF is a 20 kDa protein, composed of 179 amino acids including a 21 amino acids signal peptide which directs it to the ER (**Figure 3**) (Mizobuchi et al., 2007). Upon cleavage of the signal peptide, the mature form of human MANF is formed which is 158 amino acids, located on chromosome 3 (Petrova et al., 2003). The mature MANF protein contains two domains of 39 and 109 amino acids (**Figure 3**), along with eight cysteine residues which are conserved from *C. elegans* to humans (**Figure 1**) (Petrova et al., 2003). The N-terminal of MANF protein is responsible for mediating neurotrophic functions specific to dopaminergic neurons (Lindholm and Saarma, 2010). The secondary structure of MANF is composed mainly of alpha-helices and random coils which make up 84% of the structure (Petrova et al., 2003). MANF's C-terminal domain consists of three alpha-helices ($\alpha 6$, $\alpha 7$, $\alpha 8$), where helices $\alpha 7$ and $\alpha 8$ form a helix-loop-helix DNA binding motif (**Figure 4**) (Hellman et al., 2011). Similarly, the C-terminal domain of CDFN consists of two alpha-helices ($\alpha 6$ and $\alpha 7$), and their structure is similar to MANF's C-terminal domain (**Figure 5**) (Latge et al., 2015). In mature human MANF, helices $\alpha 7$ and $\alpha 8$ are linked by a cysteine bridge which is an important functional motif located in a CXXC motif¹²⁷CKGC¹³⁰ (**Figures 3 and 4**). This cysteine bridge plays an essential role in the intracellular survival-promoting activity of MANF (Matlik et al., 2015). In mature human CDFN, the corresponding location is motif¹³²CRAC¹³⁵ (Hellman et al., 2011).

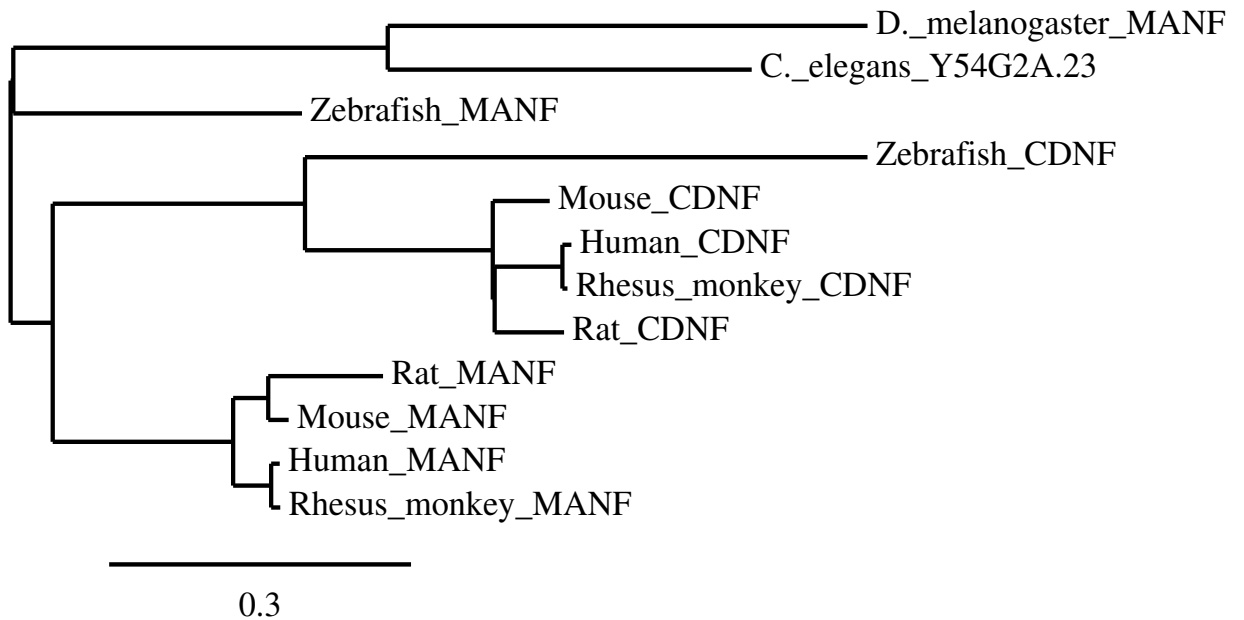


Figure 2. Phylogenetic Tree for CDNF and MANF in different species.

This phylogenetic tree shows the inferred evolutionary relationships between MANF and CDNF genes in various species. This tree was created using the free online phylogeny software, TreeDyn, by LIRMM (Dereeper et al., 2008).

CDNF (also referred to as ARMETL1) is a vertebrate specific paralog of MANF, first discovered by Lindholm and colleagues in 2007. Both MANF and CDFN are structurally and functionally unique, such that they lack the pro-sequence required by other classical NTFs for enzymatic activation. Additionally, unlike the mature glial family of ligands (GFLs) which contain seven cysteine residues, both MANF and CDFN contain eight conserved cysteine residues, and their spacing is conserved from vertebrates to invertebrates (Airaksinen and Saarma, 2002, Lindholm et al., 2007; Petrova et al., 2003). These eight cysteine residues form four di-sulphide bridges in the CDFN/MANF family of proteins (Hoseki et al., 2010; Lindholm et al., 2008, 2007; Parkash et al., 2009). CDFN contains a 26 amino acids long signal peptide in the N-terminal, which directs CDFN to the ER, and upon its cleavage, the mature protein is formed (**Figure 3**) (Lindholm et al., 2007, Petrova et al., 2003).

The mature human CDFN protein consists of 161 amino acids, and it is identical to human MANF with a 61% amino acid identity, and it has 46% similarity with *C. elegans* MANF protein (Latge et al., 2015, Lindholm and Saarma, 2010). Comparatively, human MANF has a 50% amino acid identity with *C. elegans* MANF protein. Together, CDFN and MANF form a novel evolutionary conserved protein family displaying neurotrophic activities. Vertebrates contain both CDFN and MANF genes, whereas invertebrates such as *C. elegans* and *D. melanogaster* contain a single gene more closely resembling MANF than CDFN (**Figure 2**) (Lindholm et al., 2007 and Palgi et al., 2009).

Similar to MANF, CDFN consists of two well-folded domains which are linked by a loop with intermediate flexibility (**Figure 5**). These domains consist of amino acid

residues 10 – 100, and residues 111-157 (Latge et al., 2015). The N-terminus of the CDNF protein (residues 9 – 107) contains two surface patches which embrace active site due to their increased conformational dynamics (Latge et al., 2015). Both MANF and CDNF have homologous N-terminal domains which are composed of 5 α -helices, and a 3_{10} helix (**Figures 4 and 5**). Additionally, the C-terminal of both MANF and CDNF contains two conserved active sites which corresponds to their intracellular mode of action (Latge et al., 2015). However, in comparison to MANF’s well-folded C-terminal, the C-terminus of CDNF is intrinsically disordered.

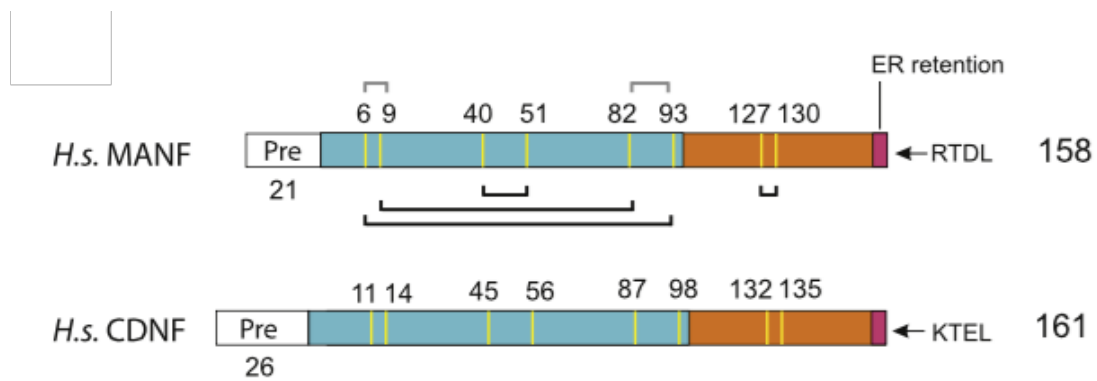


Figure 3. Schematic representation of human MANF & CDNF proteins’ primary structure.

The blue areas represent the saposin-like domains, followed by the SAP-like domain in orange. The eight conserved cysteine residues are marked with yellow bars, and numbered according to the sequence of the mature protein. The black connecting lines represent the di-sulphide bridges according to Parkash et al., 2009. *H.s.*- Homo sapiens. (Image adapted from Lindahl et al., 2017).

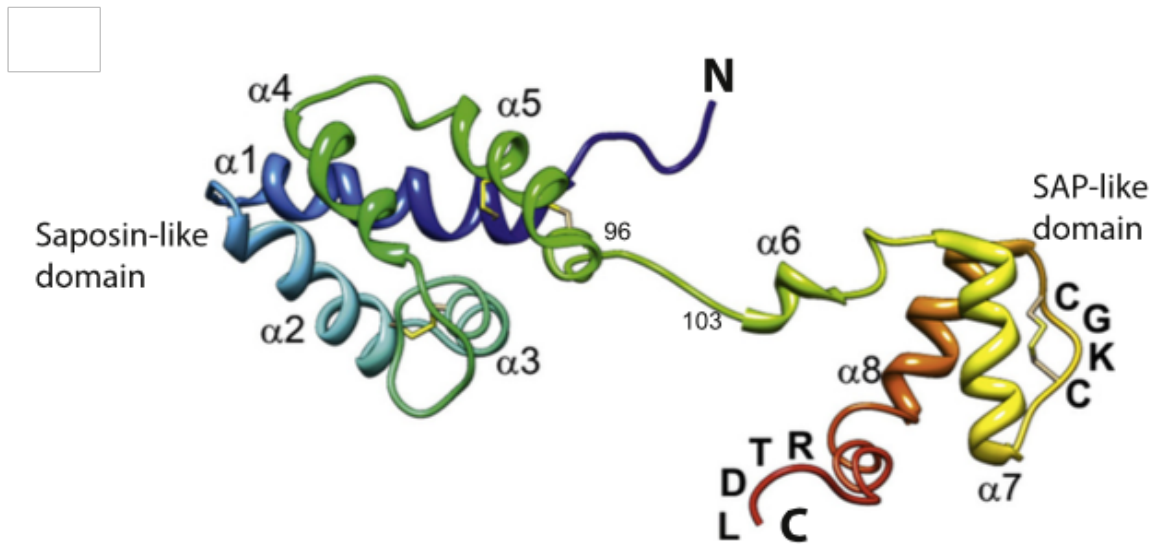


Figure 4. NMR solution structure of human MANF.

The image displays the saposin-like N-terminal domain (residues 1-95), and the SAP-like C-terminal domain (residues 96-158). The linker region is indicated in green with numbered residues from 96-103. CXXC motif and ER-retention signal are also indicated.

N- amino-terminus, C- carboxy-terminus. (*Image adapted from Lindahl et al., 2017*).

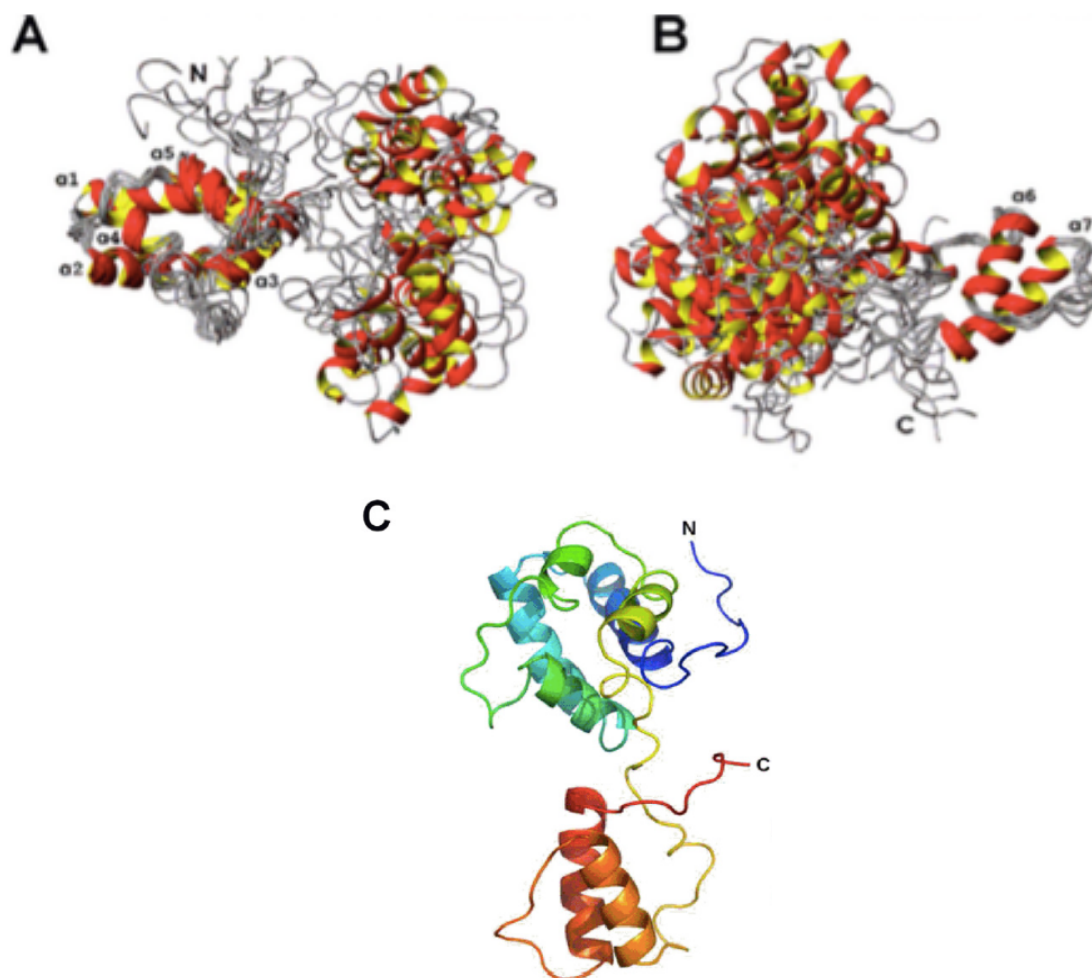


Figure 5. NMR solution structure of human CDNF.

(A) Represents the N-terminal domain structure as a result of superposition of 10 conformers on residues 10 – 100. (B) Represents the C-terminal domain structure as a result of superposition of 10 conformers on residues 110 – 150. Seven conserved α -helices are labelled in images A and B. (C) Shows the representative conformer of the three-dimensional structure of full-length CDNF. The colour change from blue to red in this image corresponds with a change in sequence from the N-terminus to the C-terminus. The N and C terminal are also labelled in the image. (*Image adapted from Latge et al., 2015*).

1.1.2 Function

Previous studies have established the neuroprotective and neurorestorative effects of CDNF in the functioning of DAergic neurons (Lindholm et al., 2007). MANF also plays a protective role in cerebellar Purkinje cell degeneration (Yang et al., 2014). In addition to their neuroprotective roles, MANF and CDNF also play important roles in the endoplasmic reticulum as they both contain a C-terminal sequence which is similar to the ER retention signal, allowing them to be partially retained in the ER (Apostolou et al., 2008 and Raykhel et al., 2007). The therapeutic mechanism of CDNF has been suggested to prevent ER stress-related damage in *in vitro* models (Cheng et al., 2013). Similarly, MANF has also been established as an ER stress response protein in animal studies (Tadimalla et al., 2008). MANF appears to have transcriptional regulation similar to that of GRP78 and GRP94, which are both heat shock proteins found in the ER (Tadimalla et al., 2008).

The structure of MANF protein corresponds to its bi-functional properties, such that the N-terminal domain is responsible for mediating the neurotrophic functions, and the C-terminal domain mediates the ER functions (Hellman et al., 2011; Henderson et al., 2013; Parkash et al., 2009). The ER-retention signals in the C-terminal domains allow CDNF and MANF to localize in the ER and thus potentially play a role in maintenance of ER homeostasis (Apostolou et al., 2008). MANF is especially highly expressed in secretory tissues with high ER protein folding load (Lindahl et al., 2017). Studies show evidence that MANF knockdown in cultured cells results in the activation of the unfolded protein response (UPR), suggesting an important role of MANF in ER protein homeostasis (Apostolou et al., 2008). Similarly, MANF knockout in mice and fruitflies displayed similar

results, supporting the role of MANF protein in maintenance of ER stress response pathways (Lindahl et al., 2014, Palgi et al., 2012). Despite MANF's two domains being responsible for different activities, it is the full length MANF protein which is required for the biological effect. In a study conducted by Lindström and colleagues, it was observed that only mature full-length MANF was able to rescue larval lethality in *Drosophila* (Lindström et al., 2013). Additionally, despite having structural and functional similarities, CDFN and MANF perform several different actions such that unlike MANF, CDFN was unable to rescue the lethal phenotype in the mutants (Lindström et al., 2013). Similarly, the overexpression of MANF and CDFN in the substantia nigra of a rat model of Parkinson's disease (PD) had synergistic effects, suggesting that these proteins may act via different mechanisms (Cordero-Llana et al., 2015).

The C-terminal domain of MANF is closely similar in structure to the SAP domain of Ku70 (Ku antigen p70 subunit) protein (Hellman et al., 2011). Ku70 prevents apoptosis by keeping the cytoplasmic pro-apoptotic BCL2 associated X (BAX) protein inactive (Sawada et al., 2003). Thus, it is hypothesized that MANF displays its anti-apoptotic activity by interacting with the BAX protein. Upon microinjection of MANF complementary DNA (cDNA) or its C-terminal domain into nuclei of mouse superior cervical ganglion (SCG) neurons, it was found to protect them against BAX-mediated apoptosis (Hellman et al., 2011). However, it was interesting to observe that addition of MANF directly to the culture medium did not have survival promoting effects on SCG neurons (Hellman et al., 2011). Additionally, CDFN displays similar neuroprotective properties as MANF, by inhibiting BAX-dependent apoptosis in PC12 cells, as well as by

modulating the activation of caspase-3 (Mei and Niu, 2014). Additionally, CDFN also displayed neuroprotective and restorative properties for primary cultures of DAergic neurons and cultures of differentiated neuron 2a (N2a) cells, against α -synuclein oligomers-induced toxicity (Latge et al., 2015). Thus, it is important to determine the mechanism by which MANF and CDFN displays their neuroprotective activities, as well as determine compounds which may increase the levels of these neurotrophic factors.

1.2 Bipolar Disorder

1.2.1 Prevalence and Symptomology

Neuropsychiatry is a branch of medicine that deals with mental disorders attributable to diseases of the nervous system. Bipolar disorder is a chronic mood disorder affecting approximately 1% of the population, characterized by cycling episodes of mania and depression (Hayashi et al., 2009). It is a serious, recurrent psychiatric illness which causes unusual shifts in individual's mood, energy, and increased impulsivity, and risky behavior (Hirschfeld et al., 2003). These include higher probability of alcohol abuse, sexual indiscretion, and excessive spending, among others. Consequently, this results in increased prevalence of suicide, homicide, accidents, and death from natural causes (Keck et al., 2003, Dilsaver et al., 1994, Strakowski et al., 1996, Osby et al., 2001). Due to the severe changes in moods, there exists a burden on individuals' lifestyle with respect to financial insecurity, as well as physical and emotional strain in relationships with family and friends. Additionally, according to the national institute of mental health (NIMH),

patients with bipolar disorder are also at a higher risk for thyroid disease, migraine headaches, heart disease, diabetes, obesity, and other physical illnesses.

Currently, BD is diagnosed based on self-reporting and behavioural observations (Frey et al. 2013). This method often leads physicians to misdiagnose patients that only seek treatment for their depressive symptoms (Singh & Rajput, 2006). Thus, a biological marker will prove to be a vital tool in the diagnosis of this illness. These markers are measurements of biological processes, disease states or responses to treatment (Frey et al., 2013). Biological markers can improve the accuracy of diagnosis and allow for the assessment of disease progression. A biological target of interest contributing to the pathophysiology of BD is the altered expression of neurotrophic factors.

1.2.3 Implications of Neurotrophic Factors in Bipolar Disorder

Neurotrophins are fragile, hydrophilic molecules that have a very short *in vivo* half life upon administration (<2min). They can not be manually administered as a method of treatment due to their poor ability to cross the blood-brain-barrier (BBB) (Zuccato et al., 2009). There exists a need to design recombinant carrier proteins that will administer these NTFs across the BBB in a receptor-mediated delivery. Alternatively, drug treatments which increase the levels of these important NTFs can act as an easier and more efficient method of neuroprotection in neurodegenerative and neuropsychiatric disorders. There exists an urgent need to explore these areas of research in order to find a potential therapeutic treatment. Neuronal cell death can occur due to a deficiency of neurotrophins, as well as oxidative stress, DNA damage, and altered gene expression among other factors (Autry et

al., 2012; Zuccato et al., 2009; Nagahara et al., 2011). Currently, most of the therapeutic treatments for neuropsychiatric diseases focus on ameliorating disease symptoms and slowing down its progression, rather than targeting the original neuronal cell loss. Thus, it is important to determine mechanisms that underlie these disorders in order to prevent neuronal death, and rescue diseased neurons by activating neuroprotective and neurogenesis pathways (Aron et al., 2011).

The lack of sufficient NTFs leads to neuronal death, also referred to as apoptosis, due to the inability to survive and maintain synaptic contacts with their target tissue (Lindholm & Saarna, 2010). One of the primary goals of NTFs research is to be able to administer them to patients in a safe and targeted manner, in order to prevent the degeneration of DAergic neurons (Sullivan & Toulouse, 2011).

The dopaminergic system has been implicated in BD pathophysiology, based on imaging and pharmacological studies, making NTFs affecting the DAergic neurons a key area of research (Cousins et al, 2009). Additionally, studies have demonstrated that individuals with bipolar disorder (BD) have an impaired ER stress response (Hayashi et al., 2009). As mentioned earlier, CDFN has been shown to protect against endoplasmic reticulum stress-induced apoptosis (Cheng et al., 2013). Thus, CDFN and MANF could potentially act as therapeutic targets, and increasing the levels of these NTFs could help alleviate BD symptoms by regulating the ER stress response. However, currently there are no studies examining CDFN expression in an *in vitro* model of *SH-SY5Y* cells. *SH-SY5Y* cells are a human neuroblastoma cell-line that possesses characteristics of DAergic neurons upon differentiation, and thus, the *SH-SY5Y* cell-line is being proposed as an *in vitro* model

for this study. The results from this study regarding MANF and CDNF's therapeutic abilities can also be applicable for other disorders involving the degeneration of DAergic neurons, such as Parkinson's disease.

1.2.4 Bipolar Disorder Treatments

Currently, lithium is the most commonly used therapeutic agent for BD, and anticonvulsants such as valproic acid, carbamazepine, and lamotrigine are also effective in treating BD symptoms (Goodwin, 2003). There is also evidence that antipsychotics such as, olanzapine, risperidone, and haloperidol are better at treating manic episodes than anticonvulsants and lithium (Geddes and Miklowitz, 2013). Thus, antipsychotic agents can be useful when treating short-term clinical symptoms. However, lithium remains as the dominant treatment due to strongest evidence for long-term relapse prevention (Geddes and Miklowitz, 2013). In majority of cases, patients are prescribed a combination of several different mood stabilizers, antipsychotics, and anti-depressants to treat both manic and depressive episodes. In one study, the combined treatment with olanzapine and fluoxetine, an anti depressant, increased improvement of symptoms when compared to treatment with olanzapine alone (Tohen et al., 2003). Similarly, the combination of lithium and VPA treatment proved to be more effective in treating symptoms than treatment with VPA alone (Geddes et al., 2011). Consequently, these results suggest that these drug treatments potentially work synergistically.

The mechanisms underlying the BD symptomology are complex and there still remains uncertainty. However, understanding the biological mechanisms of the drug

treatments provide us with useful insights into the underlying mechanisms. Some antipsychotics function by modulating the dopaminergic D2 receptors (Cousins et al., 2009). Additionally, based on biochemical studies conducted in various *in vitro* models, it has been established that several different signal transduction pathways are involved. In *SH-SY5Y* neuroblastoma cell line, lithium and VPA affect glycogen synthase kinase-3 (GSK-3), histone deacetylase (HDAC), and protein kinase C (PKC) (Abukhdeir et al., 2003 and Chen et al., 2000). However, other studies did not find the effect of VPA on these pathways, and established that VPA acts via the extracellular signal-regulated kinase/mitogen-activated protein kinase (ERK/MAPK) pathway (Daniel et al., 2005 and Yuan et al., 2001). The ERK/MAPK pathway is also implicated in neuronal survival by other neurotrophic factors (Daniel et al., 2005). It appears that the effect of VPA treatment is cell-type specific since VPA inhibited the GSK-3 pathway in *SH-SY5Y* cells, but this was not observed in neuronal cells (Chen et al., 2000 and Williams et al., 2002). However, implications of lithium treatment on GSK-3 are well established, as lithium inhibits the GSK-3 pathway by directly competing with magnesium, which is needed for GSK-3 activity (Ryves and Harwood, 2001). Overall, a better understanding of the underlying pathways can help determine therapeutically relevant sites of action to develop new drug treatments.

1.3 *SH-SY5Y* Cells

SH-SY5Y cells belong to a human neuroblastoma cell line that possesses characteristics of DAergic neurons upon differentiation (Krishna et al., 2014). *SH-SY5Y* cells were first derived from the parental line *SK-N-SH*, which originated from a metastatic bone tumor biopsy. The *SK-N-SH* cells were subcloned three times to result in the *SH-SY5Y* cell line (Kovalevich and Langford, 2013). The undifferentiated cell cultures consist of both floating and adherent cells, which continuously proliferate and lack mature neuronal markers (Pahlman et al., 1984). The morphology of undifferentiated *SH-SY5Y* cells is represented by neuroblast-like, non-polarized cell bodies with few, truncated processes (**Figure 6a**). Additionally, these cells tend to grow in clusters and often form clumps as they grow on top of each other (Pahlman et al., 1984). Comparatively, differentiated *SH-SY5Y* cells cluster less and have a more pyramidal shaped cell body, along with formation and extension of neurites (**Figure 6b**).

Retinoic acid is one of the most commonly used methods for differentiating *SH-SY5Y* cells into more neuronal-like morphology. Retinoic acid is a vitamin A derivative known to possess powerful growth inhibiting and cellular-differentiation-promoting properties (Melino et al., 1997). To induce differentiation, most commonly a concentration of 10 μM retinoic acid is administered in serum-free or low-serum medium, for approximately 3-5 days with some variations in concentrations suggested (Pahlman et al., 1984, Cheung et al., 2009). For the purposes of this study, a final concentration of 10 μM retinoic acid was administered in culture medium supplemented with 1% fetal bovine serum (FBS), for 9 days. In addition to the change in morphology, there are several other

benefits of differentiating *SH-SY5Y* cells, including the synchronization of cell cycle, allowing for a homogeneous neuronal cell population (Encinas et al., 2000). This synchronization allows for a fixed cell density since differentiation of *SH-SY5Y* cells causes a reduction in their proliferation rate (Encinas et al., 2000). Additionally, treatment with retinoic acid activates the phosphatidylinositol 3-kinase (PI3K)/Akt signaling pathway, and upregulates the anti-apoptotic Bcl-2 protein, both of which promote survival of *SH-SY5Y* cells (Lopez-Carballo et al., 2002, Itano et al., 1996). Cells differentiated with retinoic acid are also less prone to toxin-mediated cell death induced by 6-hydroxydopamine (6-OHDA), 1-methyl-4-phenyl-1,2,3,6-tetrahydropyridine (MPTP), and 1-methyl-4-phenylpyridinium ion (MPP⁺) (Cheung et al., 2009).

Differentiation causes *SH-SY5Y* cells to convert from immature catecholaminergic neurons to mature cholinergic neuronal phenotype (Kovalevich and Langford, 2013). This results in an increased expression of choline acetyl transferase (ChAT) activity and vesicular monoamine transporter (VMAT) expression (Lopes et al., 2010, Presgraves et al., 2004). However, both undifferentiated and differentiated cells express several dopaminergic neuronal markers including tyrosine hydroxylase (TH), dopamine transporter (DAT), and dopamine receptor subtypes 2 and 3 (D2R and D3R) (Kume et al., 2008, Arun et al., 2008). The combination of these neuronal marker expressions, and morphological changes makes differentiated *SH-SY5Y* cells an ideal *in vitro* candidate for this study.

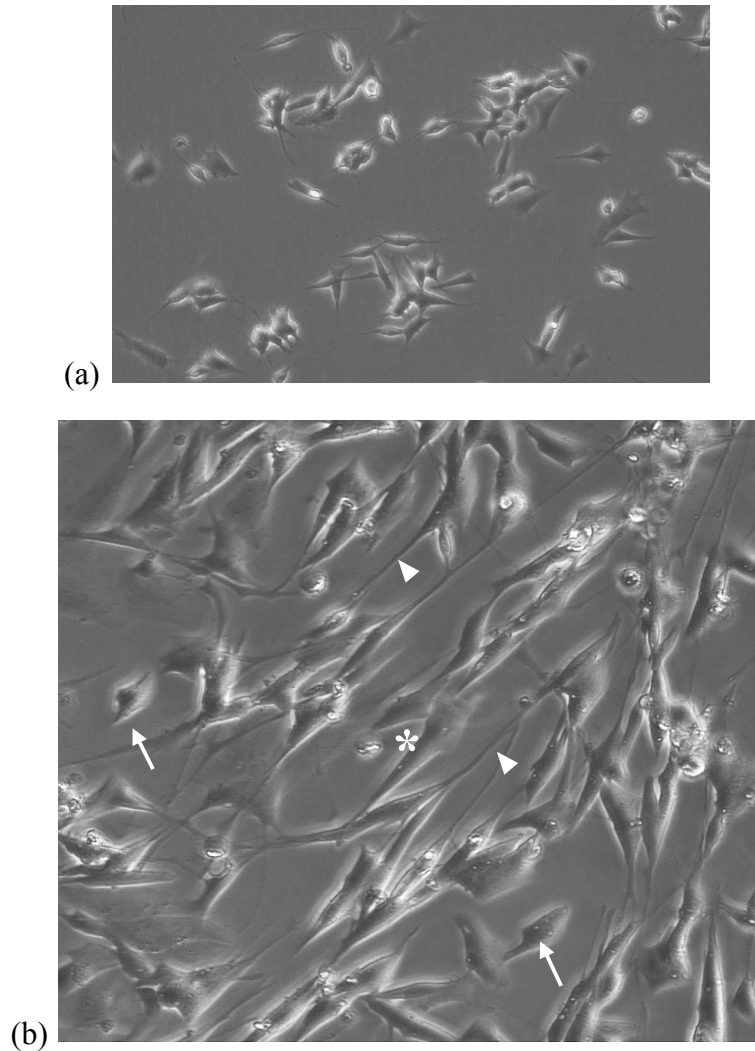


Figure 6. Wild-type SH-SY5Y cells before and after differentiation.

Morphology of SH-SY5Y cells (a)undifferentiated and (b)post-differentiation with 10 μ M retinoic acid. (b)Differentiated cells contain two morphologies (“S” and “N”). The S-type is indicated with arrows, and is more epithelial-like with no processes. The N-type is indicated with an asterick and is more neuronal-like with pyramidal shaped cell bodies and long processes (arrowheads). Cell-seeding concentration was 1.625x10⁵ cells/mL, passage 14, visualized at magnification 10x. Images were provided by Dr. Fahnstock’s lab at McMaster University (Carl Zeiss Microscopy GmbH, 2011, United States).

Chapter 2

Investigation of Neurotrophic Factors in an *in vitro* model of differentiated *SH-SY5Y* cells

2.1 Objective

Investigating CDNF and MANF mRNA expression in differentiated *SH-SY5Y* cells treated with lithium chloride and valproic acid

The objective of this study is to conduct a screening for the role of neurotrophic factors, MANF and CDNF, in an *in vitro* model for bipolar disorder. In order to conduct this screening assay, *SH-SY5Y* cells were treated with different drug treatments, and the corresponding effect on the levels of neurotrophic factors' mRNA expression was measured. The aim of this study is to determine whether commonly prescribed mood stabilizers for BD affect the levels of NTFs, as a mechanism of ameliorating symptoms. It is hypothesized that the drug treatments of lithium chloride (3 mM) and valproic acid (1 mM) will increase the mRNA expression of the NTFs in the *SH-SY5Y* cells. The results from this study can be significant in determining the potential use of NTFs as a therapeutic target for BD human patients. Due to their dopaminergic neuroprotective role, CDNF and MANF could also serve as a potential therapeutic target for neurodegenerative disorders with degeneration of dopaminergic neurons such as Alzheimer's disease and Parkinson's disease. NTFs can potentially be used to halt the progression of these disorders.

2.2 Materials and Methodology

2.2.1 *SH-SY5Y* Cells – Drug Treatments

SH-SY5Y, a human neuroblastoma cell line, was used as an *in vitro* model to investigate the effect of mood stabilizers on the levels of neurotrophic factors. To test this hypothesis, *SH-SY5Y* cells were treated with 3 mM lithium (LiCl) or 1 mM valproic acid

(VPA), which are commonly prescribed mood stabilizers. Cells were cultured in DMEM/F12 medium supplemented with 10% fetal bovine serum (FBS), 1% L-Glutamine and 1% Pen-Strep at 37°C in 5% CO₂ humidified incubation chamber, and subsequently plated in 6-well plates at a density of 3.25x10⁵ cells/well. After 24 hours of seeding, cells were differentiated for 9 days with 10µM retinoic acid. Along with retinoic acid, the differentiation media consisted of DMEM/F12 supplemented with 1% N₂ Supplement, 1% L-Glutamine, 1% Pen-Strep, and 1% FBS. The differentiated cells were treated on day 10 with drug treatments for 24 hours (**Figure 7**). Following the 24-hours drug treatment, cells were harvested and total RNA was extracted (**Figure 8**).

2.2.2 RNA Extraction from Cells

Total RNA was extracted using TRIzol reagent (Thermo Fisher Scientific, Catalog# 15596018). The cell pellet was homogenized 20 times in 1mL TRIzol solution, with a 21G needle and 1 mL syringe. The homogenized solution was then incubated at room temperature for 5 minutes. Following the incubation, 0.2ml of chloroform was added per 1 ml of Tri-pure isolation reagent, and shaken for 15 seconds. Samples were then incubated for 20 minutes at room temperature, and then centrifuged at 12000g for 15 minutes at 4°C. Following the centrifugation, the colourless RNA phase was removed and transferred to a 1.5ml eppendorf, and 0.5ml of isopropanol was then added to these eppendorf tubes. Samples were then inverted 10 times to mix the components in the tube. Samples were again incubated at room temperature for 10 minutes and then centrifuged for 10 minutes at 12000 g at 4°C. Supernatant was then discarded, and 1ml of 75% ethanol was added to each sample, vortexed thoroughly and centrifuged at maximum speed for 15 minutes at 4°C.

Supernatant was again discarded and pellet was air-dried for 5-10 minutes. The dried RNA pellet was then resuspended in 20µl of DEPC-Treated RNase-free water, and heated at 55°C for 10 minutes in a pre-heated water bath. The samples were then quickly centrifuged and vortexed before checking their RNA quantity and purity, using a Beckman Spectrophotometer DU-640 measuring absorption at 260 nm and 280 nm. The extracted RNA was then treated with DNase I enzyme (ThermoFisher Scientific, Catalog# EN0521) to enhance purity by removing genomic DNA. RNA purity and quantity was again determined using the Beckman Spectrophotometer DU-640 measuring absorption at 260 nm and 280 nm.

2.2.3 cDNA Synthesis from *SH-SY5Y* Cells' RNA

The DNase-treated RNA was then converted to complementary DNA (cDNA) by reverse transcription (RT) using the qScript cDNA SuperMix (QuantaBio, Catalog# 95048-100). During cDNA synthesis, negative RT controls were also created for randomly chosen samples by using the DNase-treated RNA without the addition of reverse transcriptase enzyme. This acted as a verification for the RT-PCR specificity as well as a check for any DNA contamination. All of the reactions occurred at the following thermal profile conditions: 5 minutes at 25°C, followed by 30 minutes at 42°C, and lastly 5 minutes at 85°C, with a final hold at 4°C.

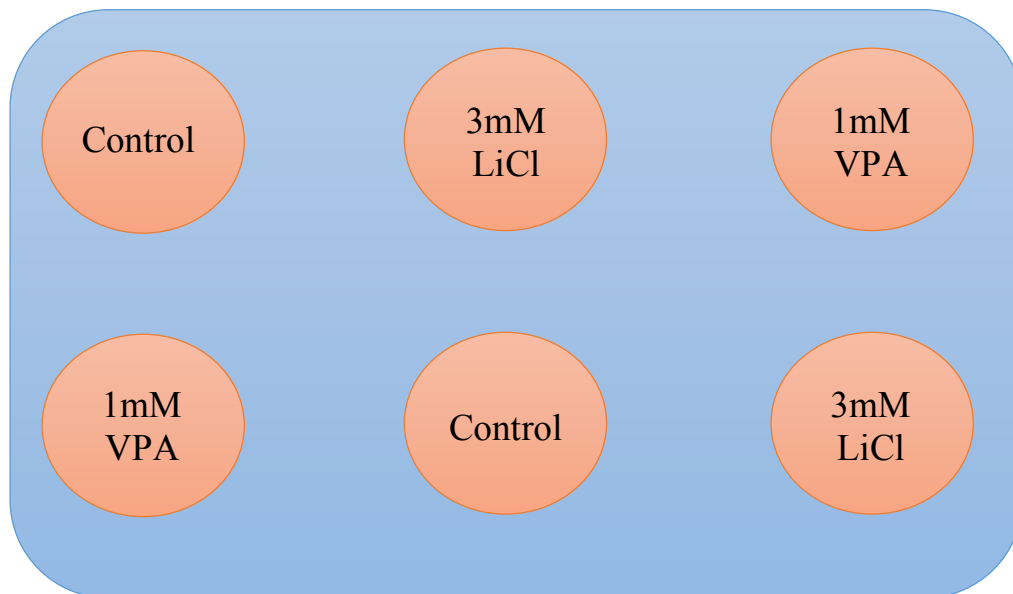


Figure 7. Sample drug treatment setup for 6-well plate.

SH-SY5Y cells were seeded at a concentration of 3.25×10^5 cells/well. Treatments were administered on Day 10, and randomized in different wells during replication trials.

Day 1 Seed Cells 3.25 x 10 ⁵ cells/well	2 Add 10uM Retinoic acid	3 Observe cells	4 Observe cells and change ½ media	5 Observe cells	6 Observe cells and change ½ media	7 Observe cells
8 Observe cells and change ½ media	9 Observe cells	10 Add Drug Treatments (3mM LiCl or 1mM VPA)	11 Harvest Cells (24-hours post treatment)	12 Extract RNA from cells	13 Synthesize cDNA from RNA	14 Run RT-qPCR for gene 1
15 Run RT-qPCR for gene 2						

Figure 8. Sample experimental timeline.

The cell differentiation process began on day 2 with the addition of retinoic acid. After 9-days of differentiation, *SH-SY5Y* cells were treated with LiCl or VPA drug treatments on Day 10.

2.2.4 Reverse Transcription PCR (RT-PCR)

The CDNF and MANF gene amplicons were detected by amplifying 50 ng of RT product using the Invitrogen Platinum Taq High Fidelity DNA Polymerase (Catalog #: 11304-111) with appropriate primers. The PCR amplifications were conducted under the following parameters: initial denaturation at 94°C for 2 minutes 30 seconds, followed with 40 cycles of 94°C for 30 seconds, 57°C for 30 seconds, and 72°C for 40 seconds. The amplification ended with a final extension for 7 minutes at 72°C. The primers for MANF and CDNF were synthesized at MOBIX lab facility (McMaster University, Hamilton, ON), and verified using gel electrophoresis by running the amplicon on a 1.5% agarose gel (**Figures 9 and 10**). The band of interest was then sent for sequencing at the McMaster MOBIX lab. The primers listed in **Table 1** were used for the RT-PCR analysis. Representative RT-PCR products showed 100% homology with the genes of interest – human CDNF and MANF. Concentration of the gene amplicons were then quantified and used for making the absolute standard curve dilutions when running the quantitative RT-PCR.

Primer Sequence (5' → 3')	Product Size	Accession Number
CDNF Fwd: GGGCCGACTGTGAAGTATGT	210 bp	NM_001029954
CDNF Rev: GGCATATGCACACTCATTGG		
MANF Fwd: TCACATTCTCACCAGCCACT	236 bp*	NM_006010
MANF Rev: CAGGTCGATCTGCTTGTCATAC		

Table 1. Human CDNF and MANF primer sequences.

Forward and reverse primer sequences used for RT-PCR and RT-qPCR analysis of CDNF and MANF genes in *SH-SY5Y* cells. *MANF primers as described by *Cheng et al., 2014*.

2.2.5 Real-Time Quantitative Reverse Transcription PCR (RT-qPCR)

The mRNA expression for CDNF and MANF was quantified using RT-qPCR with QuantiFast SYBR Green fluorescent dye PCR kit (Qiagen, Catalog# 204056). The primers listed in **Table 1** were used for the RT-qPCR analysis. RT-qPCR was used to determine absolute copy numbers of CDNF and MANF mRNA in cell samples. The cDNA for the *SH-SY5Y* cells were amplified in triplicate for each sample, using Stratagene MX3000P cycler with an initial PCR activation step at 95°C for 5 minutes. Next, the cDNA was denatured through 40 cycles of denaturation at 95°C for 10 seconds, followed by a combined annealing and extension step for 30 seconds at 60°C. This was followed by melting curve analysis where the qPCR produced a single peak for each product. This allowed for verification of the PCR specificity for each product. Each reaction had a volume of 25µl containing 60ng of total RNA. An absolute standard curve was generated using varying concentrations of cDNA ranging from 1pg to 10ag with 10-fold serial dilutions. Real-time RT-PCR conditions were optimized to ensure amplifications efficiencies remained constant over the course of the run. Components of the RT-qPCR reaction mix were as follows: 12.5ul of QuantiFAST SYBR green (QIAGEN), 5µl each of the 5µM forward and reverse primers (described in **Table 1**), 2µl of sample cDNA, and 0.5µl of nuclease-free water to a final volume of 25µl.

2.2.6 Statistical Analysis

The fold change difference in absolute copy numbers of CDNF and MANF between treated samples and controls was analyzed. MX3000P software performs analysis of data obtained by the RT-qPCR to quantify the copy number of the target sequence in

each sample by comparing it with the standard curve copy numbers. Real-Time PCR experiments were performed in triplicates which were averaged prior to analysis. All statistical analyses were conducted using the GraphPad Prism 6.0 software (GraphPad Software, San Diego, California, USA). Outlier detection was performed prior to analyses using GraphPad Outlier Tool. One-way analysis of variance (ANOVA) with Tukey's post-hoc test was conducted to determine significance between groups, and a p-value of ($p < 0.05$) was considered statistically significant. Data shown is expressed as mean \pm standard deviation (S.D.).

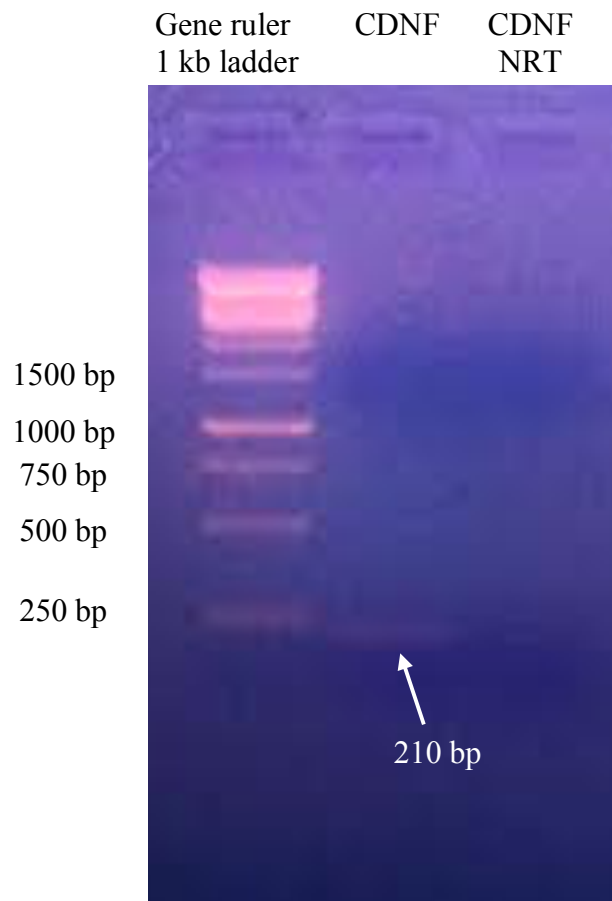


Figure 9. Gel electrophoresis of human CDNF gene.

Amplified PCR products for human CDNF gene was run on 1.5% agarose gel along with a no-reverse-transcription (NRT) control. Only one band of interest was observed in the CDNF lane, and no bands were observed in the NRT control lane.

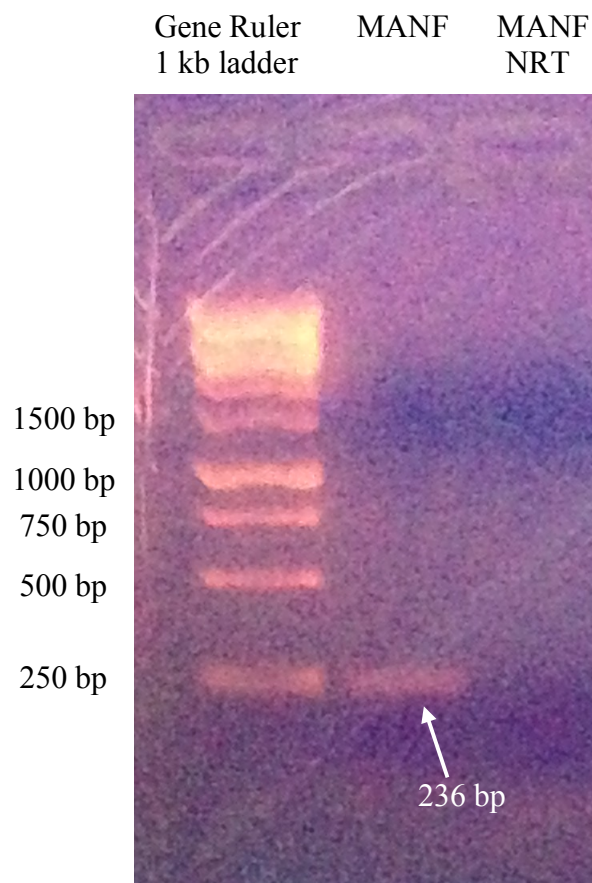


Figure 10. Gel electrophoresis of human MANF gene.

Amplified PCR products for human MANF gene was run on 1.5% agarose gel along with an NRT control. Only one band of interest was observed in the MANF lane, and no bands were observed in the NRT control lane.

2.3 Results

2.3.1 Effect of Lithium and VPA on neurotrophic factors expression in *SH-SY5Y* cells

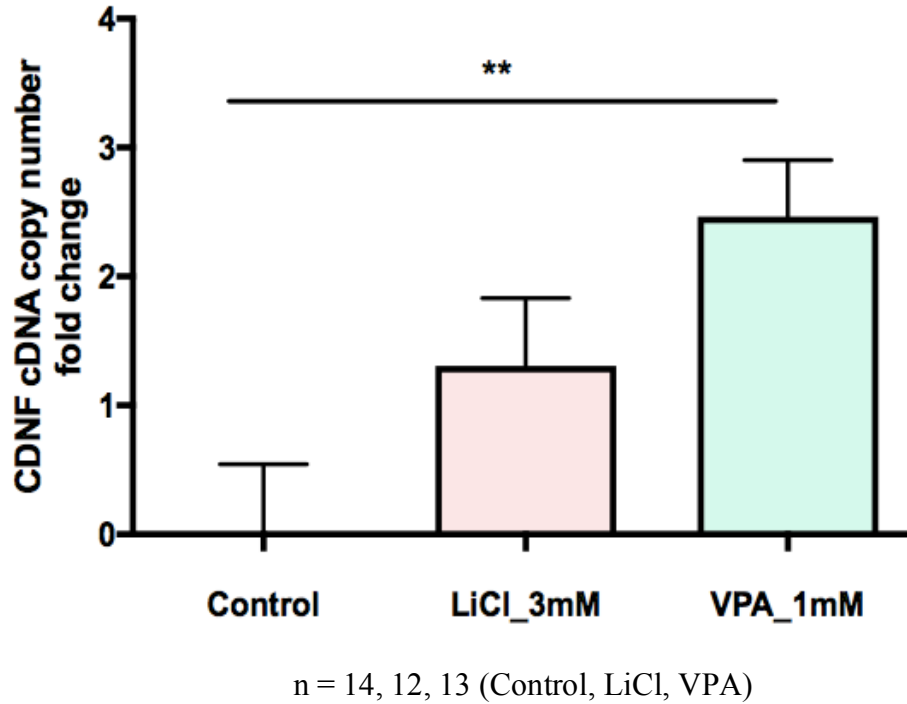
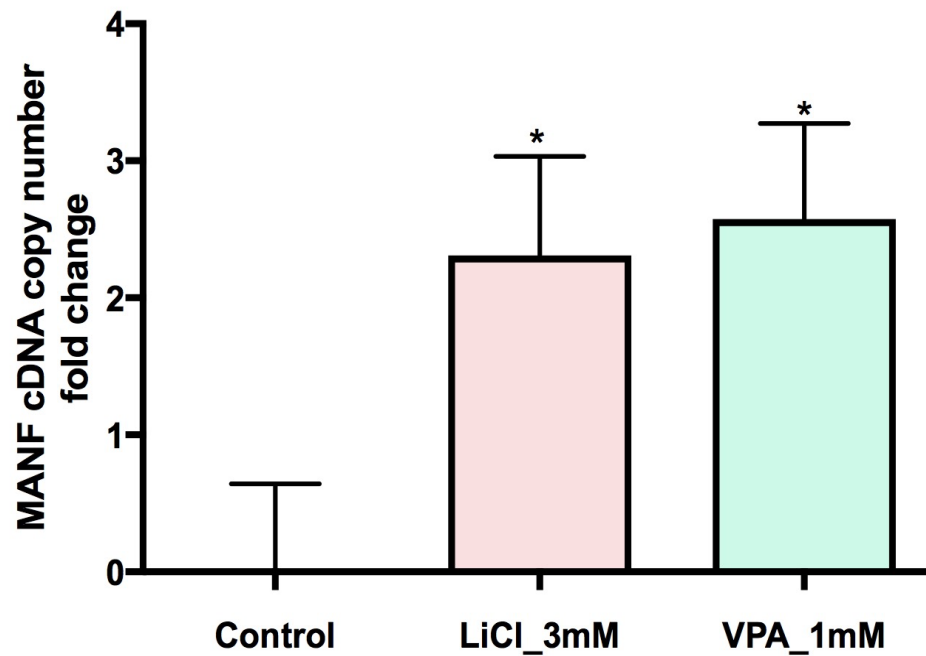


Figure 11. CDNF mRNA expression in *SH-SY5Y* cells treated with Lithium and VPA.

Two-step RT-qPCR to measure the mRNA expression of CDNF in differentiated *SH-SY5Y* cells treated with Lithium (LiCl) and Valproic Acid (VPA). The LiCl treatment was administered at a concentration of 3mM per sample well, and VPA was administered at 1mM concentration. The results display the fold change in CDNF mRNA expression. Both LiCl and VPA treatments increased mRNA expression of CDNF. One-way ANOVA was significant at $p < 0.01$, followed with a Tukey's post-hoc test. (** $p < 0.01$). Sample size: 14, 12, 13 (Control, LiCl, VPA respectively).



n = 14, 12, 13 (Control, LiCl, VPA)

Figure 12. MANF mRNA expression in *SH-SY5Y* cells treated with Lithium and VPA.

Two-step RT-qPCR to measure the mRNA expression of MANF in differentiated *SH-SY5Y* cells treated with Lithium (LiCl) and Valproic Acid (VPA). The LiCl treatment was administered at a concentration of 3mM per sample well, and VPA was administered at 1mM concentration. The results display the fold change in MANF mRNA expression. Both LiCl and VPA treatments significantly increased mRNA expression of MANF. One-way ANOVA was significant at $p < 0.05$, followed with a Tukey's post-hoc test. (* $p < 0.05$). Sample size: 14, 12, 13 (Control, LiCl, VPA respectively).

2.4 Discussion

The endoplasmic reticulum (ER) is the site of protein synthesis, modification, and degradation, spread widely throughout neurons. Impairments in ER functioning due to ER stress, is involved with several chronic conditions. ER stress can occur as a result of various cellular insults including reduction in ER calcium stores, viral infections, changes in protein glycosylation, and unbalanced protein expression (Szegezdi et al., 2006). These factors cause ER stress by negatively impacting protein folding in the ER, leading to an accumulation and aggregation of unfolded proteins in the ER lumen. In response to increased cellular demands in the ER, the unfolded protein response (UPR) is triggered. The UPR acts to increase protein folding capacity and decrease amount of misfolded proteins present in the cell. The UPR acts via several mechanisms to alleviate ER stress, including suppression of protein translation, degradation of misfolded proteins, activation of signaling pathways involved in normal protein folding, and reduction in protein translocation across the ER membrane (Hetz, 2012; Szegezdi et al., 2006). The UPR is responsible for induction of molecular ER chaperones which promote protein folding, as well as induction of ER-associated degradation mechanisms.

In situations where ER stress is prolonged, it can also lead to ER stress-induced apoptosis (Szegezdi et al., 2006). Previous studies have established that MANF and CDFN are both involved in regulating the ER-stress response pathway (Lee et al., 2003; Mizobuchi et al., 2007; Apostolou et al., 2008; Tadimalla et al., 2008, Cheng et al., 2013). MANF has been proven to protect cells *in vitro* against ER-stress induced apoptosis (Apostolou et al., 2008). Additionally, another study found that upon induction of ER-stress by tunicamycin,

CDNF played a neuroprotective role in astrocytes (Cheng et al., 2013). The overexpression of CDNF alleviated ER stress-induced astrocyte damage by reducing the amount of cell lysis. This was observed as a suppression in the percentage of released lactate dehydrogenase (LDH), an enzyme resulting from cell lysis, in response to ER-stress in astrocytes (Cheng et al., 2013).

Additionally, some of the molecular chaperones induced by the UPR include GRP78 (HSPA5 or BiP) and GRP94, which help regulate protein folding in the ER (Hayashi et al., 2009). In normal functioning cells, the splicing of transcription factor XBP1 results in induction of these ER chaperones (Kakiuchi et al., 2003). However, upon induction of ER stress *in vitro* by tunicamycin and thapsigargin in lymphoblastoid (LB) cells derived from BD patients, it was observed that there was a significant attenuation in induction of the spliced form of XBP1 as well as total XBP1 in patients with BD. Additionally, the BD group also showed decreased induction of GRP94 by thapsigargin. The combination of these results provide evidence that BD patients have an impaired ER-stress response (Hayashi et al., 2009). Similarly, a previous DNA microarray analysis looked at the expression of XBP1 and GRP78 in lymphoblastoid (LB) cells derived from two pairs of monozygotic twins, discordant with respect to BD. It was observed that there was down-regulation in expression of both XBP1 and GRP78 in the affected twins (Kakiuchi et al., 2003). This suggests that altered ER-stress response may play an important role in the pathophysiology of BD.

Interestingly, MANF's promoter-region contains an ER stress response element II (ERSEII) sequence that is recognized by spliced XBP1 (Lee et al., 2003, Mizobuchi et al.,

2007). Additionally, MANF calcium-dependently interacts with ER chaperone GRP78, and upon ER stress due to depletion of calcium, it is secreted from the ER (Glembotski et al., 2012, Henderson et al., 2013). These findings suggest that MANF activity is partially controlled by ER calcium levels, and thus allows MANF to play a role in the ER-stress response (Glembotski et al., 2012). MANF's role in the ER-stress response has also been validated based on findings from several studies, where MANF mRNA expression and protein levels were induced by ER stress both *in vitro* and *in vivo* (Apostolou et al., 2008; Glembotski et al., 2012; Hartley et al., 2013; Lee et al., 2003; Lindholm et al., 2008; Mizobuchi et al., 2007; Tadimalla et al., 2008). MANF and CDFN may play a neuroprotective role in the ER-stress response, by facilitating the formation of cysteine bridges and protein folding in the ER (Lindholm and Saarma, 2009). This allows them to reduce ER stress being caused by unfolded and misfolded proteins.

As observed in **figure 11**, treatment of differentiated *SH-SY5Y* cells with Lithium and VPA, caused a significant increase in mRNA expression of CDFN. Similarly, these treatments also significantly increased MANF mRNA expression in *SH-SY5Y* cells (**Figure 12**). Given the role that both MANF and CDFN play in the ER-stress response, it is possible that the mood stabilizers prescribed to BD patients ameliorate their symptoms by managing misfolded proteins. A suggested mechanism of action for the drug treatments used in bipolar disorder is the regulation of ER stress. Lithium and valproic acid are two drug treatments commonly prescribed to BD patients. Both of these mood stabilizers have been shown to upregulate ER-stress related chaperones. In an *in vivo* study, treatment with VPA increased GRP78 expression in rat cerebral cortex (Wang et al., 1999). Additionally,

chronic VPA treatment in rat cerebral cortex and hippocampus, upregulated the expression of GRP78, GRP94, and calreticulin – which is another ER stress protein (Chen et al., 2000). Similarly, a one-week treatment with Lithium also upregulated the mRNA and protein expression of GRP78 and GRP94 in primary cultured rat cerebral cortical cells (Shao et al., 2006). Thus, it is possible that the mechanism of action for these mood stabilizers involves regulation of the UPR through the induction of ER-stress related genes.

Given these findings, it is important to examine the protein expression of MANF and CDNF as a result of the Lithium and VPA drug administration. Additionally, it would be beneficial to further examine the underlying mechanisms involved in these changes. Understanding the cellular and molecular mechanisms underlying these changes will allow us to examine other drug treatments as well as natural compounds, such as curcumin, that can potentially alleviate BD symptoms by directly acting on the expression of NTFs. Additionally, these findings can also play an important role when establishing drug treatments for neurodegenerative diseases such as Alzheimer's disease.

Chapter 3

Investigation of Neurotrophic Factors in an *in vivo* model of Sprague Dawley rats

3.1 Objective

Investigating CDNF and MANF mRNA expression in rats' brain regions treated with lithium chloride and valproic acid

Given the significant findings from the *in vitro* study in chapter 2, the objective of this study is to determine whether the changes in mRNA expression are translatable to an *in vivo* rat model. This study aims to determine whether commonly prescribed mood stabilizers for BD – Lithium and VPA – affect the levels of NTFs in various brain regions of a rat model. It is expected that the drug treatments of lithium chloride (47.5mg/kg) and valproic acid (200mg/kg) will increase the mRNA expression of CDNF and MANF in rat brain regions.

3.2 Materials and Methodology

3.2.1 Rats study 1 – December 2016 (N = 22)

All animal testing was approved by the McMaster Central Animal Facility (CAF) in accordance with guidelines from the Canadian Council on Animal Care. Male Sprague–Dawley rats (300-350g) were purchased from Charles River, Canada and housed individually in standard cages with enrichment at McMaster University CAF. The rats were kept under standard laboratory conditions in a 12-hour light/dark cycle at constant temperature (22°C) and humidity (50%). They were provided food and water *ad libitum*. All animals were given a few weeks to acclimate to their environment, during which they were handled by the experimenters. A cohort of 22 rats were used for this study, and they

were randomly divided into 3 groups with n = 8 per drug treatment group (Lithium and Valproic acid), and n = 6 for the saline control group.

3.2.2 Drug Treatments

All of the rats were injected intraperitoneally (I.P.) twice a day (9 AM and 6 PM) with saline (1ml/kg), lithium (47.5mg/kg), or VPA (200mg/kg), for 14 days. Both lithium chloride and valproic acid were obtained from Sigma Aldrich (Oakville, ON, Canada). The lithium and valproic acid drug treatments were dissolved in saline solution, and injected at a rate of 1ml/kg.

3.2.3 Sacrifice, Blood Collection, and Tissue Dissection

All animals were sacrificed 6 hours after their last injection on day 14. They were heavily anesthetized with isoflurane (Pharmaceutical Partners of Canada Inc, Richmond hill, Ontario, Canada) and rapidly decapitated. Through the neck wound, blood was collected in a SST Blood Collection Vacutainer tube with anti-coagulant. Blood was processed under the following conditions: inverted blood vacutainer 5 times immediately after collection, followed by incubation at room temperature for 30 minutes. The blood was then centrifuged at 2000 rpm for 10 minutes with no break. After the centrifugation, the supernatant (plasma) was collected in 1mL eppendorf tubes, and stored at -80°C. The plasma tubes were then sent for analysis to Dr. Frey's lab at St. Joseph's Healthcare, Hamilton, ON, Canada. Following blood collection, the brain was removed, de-skulled, sectioned, and various brain regions from both sides were dissected including striatum, hippocampus, PFC, and cortex (See **Figures 19 – 22**). Tissues were stored in -80°C for future analysis.

3.2.4 Rats study 2 – March 2017 (N=16)

This study was conducted to replicate and verify the results from animal study 1, following the same protocol with some modifications. This study has a cohort of 16 rats with 6 rats in the saline control group, 6 rats in LiCl treatment group, and 4 rats in the VPA treatment group. The differences in protocol exist in the additional behavioural test which was conducted 2 hours after the last injection on Day 14. Additionally, the rats were sacrificed immediately after the behavioural test was complete. Consequently, rats were sacrificed and blood was collected 2.5 hours after the last injection instead of 6 hours. For this cohort, two additional brain regions – medial prefrontal cortex (mPFC) and amygdala (See **Figures 23, 24**) – were also sectioned and analysed.

3.2.5 Behavioural Test – Open Field Task

Locomotor testing was completed during the dark period of the rodents' light/dark cycle since rats show maximum activity during these hours. The locomotor behaviour of rats was analysed using the open-field task, as described by Frey et al., 2006. The rats were placed in an open field chamber which was 100 cm x 80 cm x 40 cm. The chamber was divided into equal sized squares of 10 cm x 10 cm (**Figure 13**). The total number of squares travelled was analysed as a measure of total distance travelled. Additionally, the amount of time spent exploring the squares in the middle areas was also analysed, along with number of rearings with their front paws. Each rat was tested for 15 minutes, with the first 5 minutes being a habituation period, followed by a 10-minutes testing period of recorded behaviour. Immediately after the locomotor test, the animals were sacrificed.

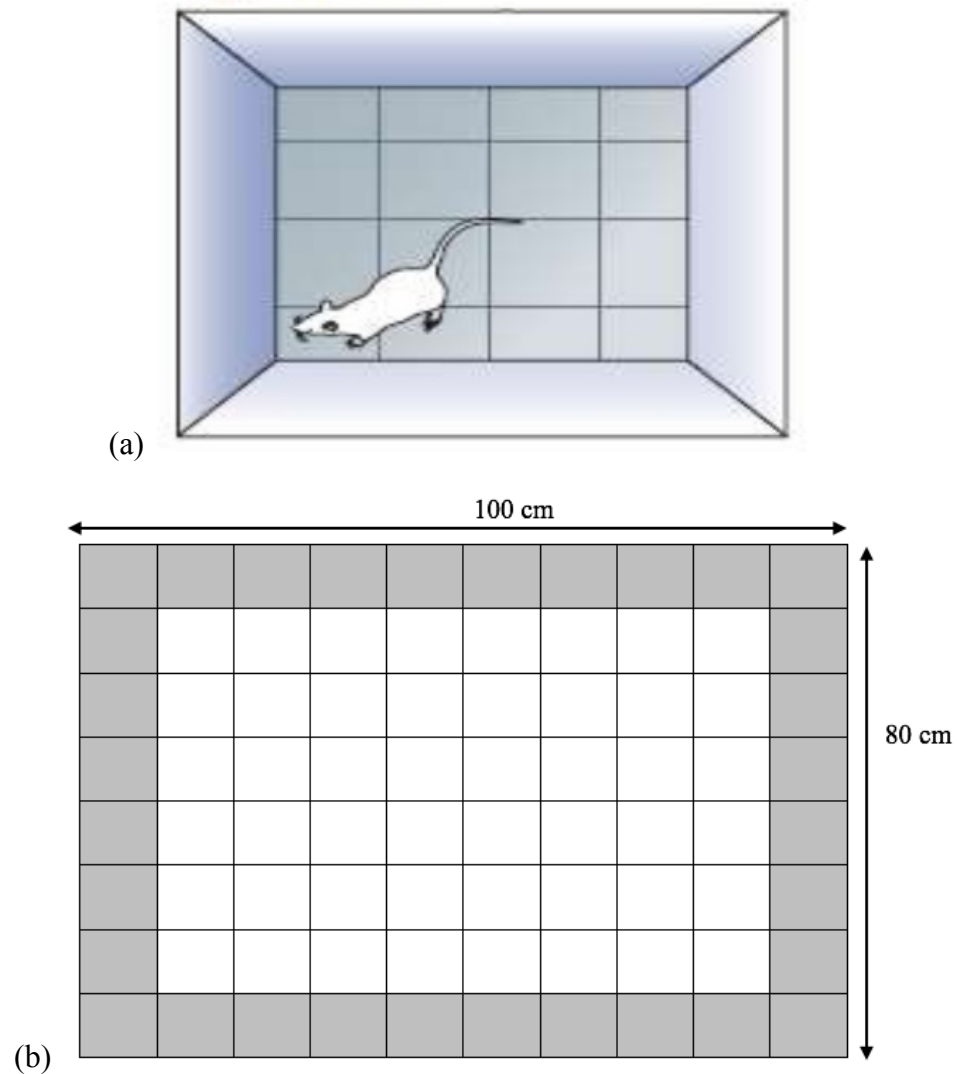


Figure 13. Sample diagram of open-field chamber.

(a) The open-field chamber in use for this study was 100cm x 80cm, with side walls 40cm in height. Rats were placed in the bottom left corner at the beginning of the testing period.

(b) The chamber was divided into squares 10 cm x 10 cm in size. Rats were placed in this chamber for a total of 15 minutes, with the first 5 minutes being a habituation period.

Squares not around the outside perimeter (shaded gray), were considered as areas in the middle.

3.2.6 RNA Extraction from Rat Tissues

Total RNA was extracted using TRIzol reagent (Thermo Fisher Scientific, Catalog# 15596018). Tissues were homogenized in 1mL TRIzol solution with autoclaved plastic homogenizing sticks, until the tissues were completely dissolved in the TRIzol solution and no solid brain regions were visible. The homogenized solution was then incubated at room temperature for 5 minutes. Following the incubation, 0.2ml of chloroform was added per 1 ml of Tri-pure isolation reagent, and shaken for 15 seconds. Samples were then incubated for 15 minutes at room temperature, and then centrifuged at 12000g for 15 minutes at 4°C. Following the centrifugation, the colourless RNA phase was removed and transferred to a 1.5ml eppendorf, and 0.5ml of isopropanol was then added to these eppendorf tubes. Samples were then shaken to mix the components in the tube. Samples were again incubated at room temperature for 10 minutes and then centrifuged for 10 minutes at 12000 g at 4°C. Supernatant was then discarded, and 1ml of 75% ethanol was added to each sample, vortexed thoroughly and centrifuged at 7500g for 5 minutes at 4°C. Supernatant was again discarded and pellet was air-dried for 5-10 minutes. The dried RNA pellet was then resuspended in 40µl of DEPC-Treated RNase-free water, and heated at 60°C for 10 minutes in a pre-heated water bath. The samples were then quickly centrifuged and vortexed before checking their RNA quantity and purity, using a NanoDrop 2000 Spectrophotometer (Thermo Scientific), measuring absorption at 260 nm and 280 nm. The extracted RNA was then treated with DNase I enzyme (ThermoFisher Scientific, Catalog# EN0521) to enhance purity by removing genomic DNA. RNA purity and quantity was again determined using the NanoDrop 2000 Spectrophotometer measuring absorption at

260 nm and 280 nm.

3.2.7 cDNA Synthesis from Rat Tissues' RNA

The DNase-treated RNA was then converted to complementary DNA (cDNA) by reverse transcription (RT) using the qScript cDNA SuperMix (QuantaBio, Catalog# 95048-100). During cDNA synthesis, negative RT controls were also created for randomly chosen samples by using the DNase-treated RNA without the addition of reverse transcriptase enzyme. This acted as a verification for the RT-PCR specificity as well as a check for any DNA contamination. All of the reactions occurred at the following thermal profile conditions: 5 minutes at 25°C, followed by 30 minutes at 42°C, and lastly 5 minutes at 85°C, with a final hold at 4°C.

3.2.8 Reverse Transcription PCR (RT-PCR)

The CDNF, MANF, and GAPDH gene amplicons were detected by amplifying 50 ng of RT product using the Invitrogen Platinum Taq High Fidelity DNA Polymerase (Catalog #: 11304-111) with appropriate primers (listed in **Table 2**). The PCR amplifications were conducted under the following parameters: initial denaturation at 94°C for 2 minutes 30 seconds, followed with 40 cycles of 94°C for 30 seconds, 57°C for 30 seconds, and 72°C for 40 seconds. The amplification ended with a final extension for 7 minutes at 72°C. The primers for MANF, CDNF, and GAPDH were synthesized at MOBIX lab facility (McMaster University, Hamilton, ON), and verified using gel electrophoresis by running the PCR product on a 1.5% agarose gel (**Figure 14**). The bands of interest were then sent for sequencing at the McMaster MOBIX lab. The primers listed in **Table 2** were

used for the RT-PCR analysis. Representative RT-PCR products showed 100% homology with the genes of interest – rat CDNF, MANF, and GAPDH. Concentration of the gene amplicons were then quantified and used for making the absolute standard curve dilutions when running the quantitative RT-PCR.

Primer Sequence (5' → 3')	Product Size	Accession Number
CDNF Fwd: AAAGAAAACCGCCTGTGCTA	199 bp*	NM_001037543.1
CDNF Rev: TCATTTTCCACAGGTCCACA		
MANF Fwd: CGGTTGTGCTACTACATTGGA	129 bp	NM_001108183.1
MANF Rev: CTGGCTGTCTTTCTTCTTCAGC		
GAPDH Fwd: CAACTCCCTCAAGATTGTCAGCAA	118 bp	NM_017008.4
GAPDH Rev: GGCATGGACTGTGGTCATGA		

Table 2. Forward and reverse primer sequences for rats.

These primers were used for RT-PCR and RT-qPCR analysis of CDNF, MANF, and GAPDH genes in several rat brain regions including striatum, hippocampus, cortex, amygdala, mPFC, and PFC. **CDNF primers as described by Niles et al., 2012.* (bp – base pairs).

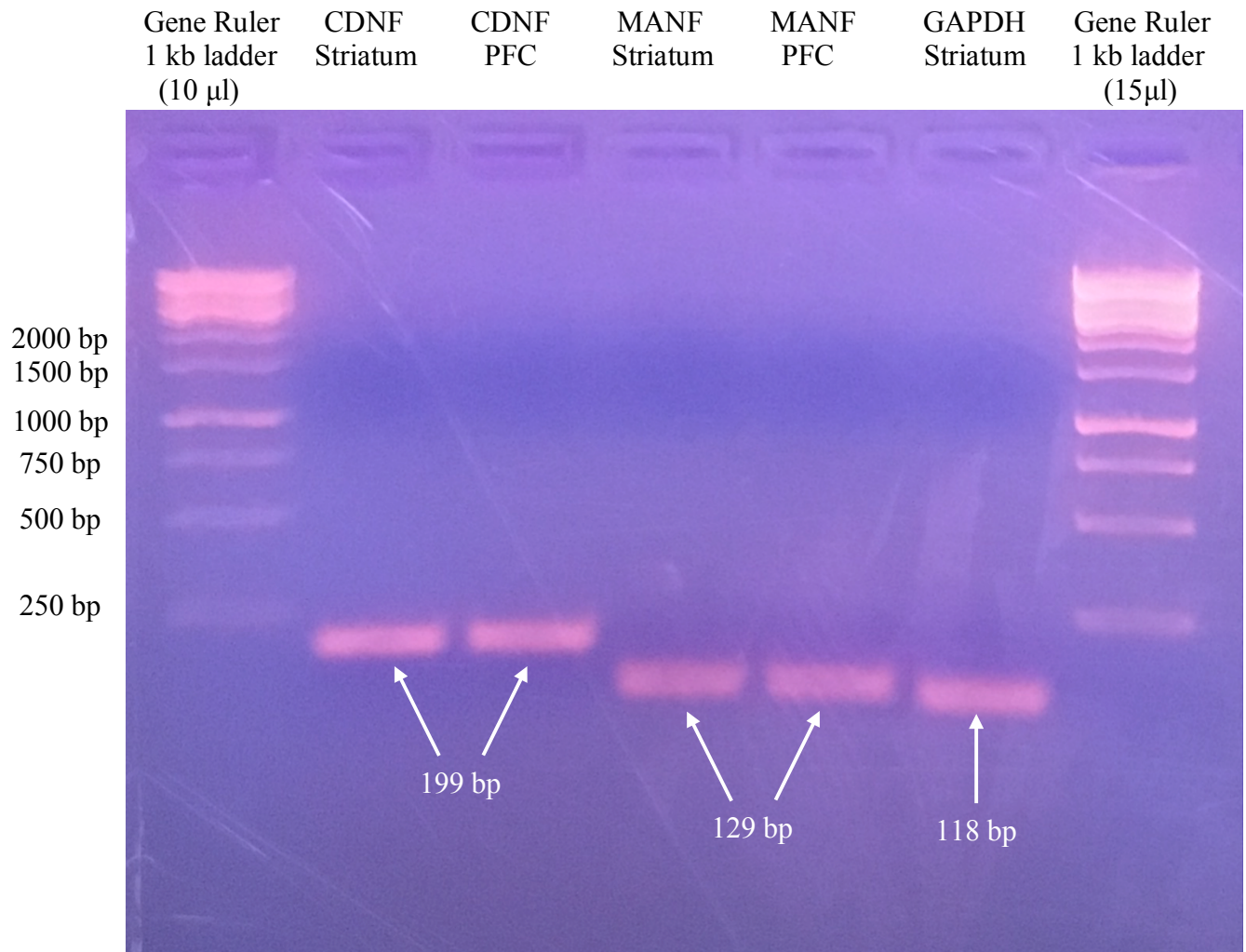


Figure 14. Gel electrophoresis of rat CDNF, MANF and GAPDH genes.

The rat cDNA for striatum and PFC was amplified at 57°C in a polymerase chain reaction, for all three genes of interest. The amplified PCR products for CDNF, MANF, and GAPDH were then run on 1.5% agarose gel. The bands were compared to the 1kb ladder for reference, and NRT controls were run on a separate gel (not shown here). Only one band of interest was observed in all of the lanes. These bands were excised and sent for sequencing.

3.2.9 Real-Time Quantitative Reverse Transcription PCR (RT-qPCR)

The mRNA expression for CDFN and MANF was quantified using RT-qPCR with QuantiFast SYBR Green fluorescent dye PCR kit (Qiagen, Catalog# 204056). The primers listed in **Table 2** were used for the RT-qPCR analysis. The RT-qPCR was used to determine absolute copy numbers of CDFN, MANF, and GAPDH mRNA in the rat brain tissues. The GAPDH mRNA expression was used as an internal control. Additionally, the relative mRNA expression of MANF and CDFN, with regards to the C_t values, were also determined using GAPDH as the housekeeping gene. The cDNA for the rat brain tissues was amplified in triplicates for each sample, using Stratagene MX3000P cycler with an initial PCR activation step at 95°C for 5 minutes. Next, the cDNA was denatured through 40 cycles of denaturation at 95°C for 10 seconds, followed by a combined annealing and extension step for 30 seconds at 60°C. This was followed by melting curve analysis where the qPCR produced a single peak for each product. This allowed for verification of the PCR specificity for each product. Each reaction had a volume of 25µl containing 60ng of total RNA. An absolute standard curve was generated using varying concentrations of cDNA ranging from 1pg to 10ag with 10-fold serial dilutions. Real-time RT-PCR conditions were optimized to ensure amplifications efficiencies remained constant over the course of the run. Components of the RT-qPCR reaction mix were as follows: 12.5ul of QuantiFAST SYBR green (QIAGEN), 5µl each of the 5µM forward and reverse primers (described in **Table 1**), 2µl of sample cDNA, and 0.5µl of nuclease-free water to a final volume of 25µl. **Figures 15 – 18** display a sample of the RT-qPCR output from the MX3000P software.

3.2.10 Statistical Analysis

The resulting C_t (threshold cycle) values for CDNF and MANF were normalized to the GAPDH C_t values, and the data was analyzed using the $\Delta\Delta C_t$ method (as described by Schmittgen and Livak, 2008). The following equation was used to analyze the results:

$$2^{-\Delta\Delta C_t}$$
$$= \left[\frac{((C_T \text{ gene of interest} - C_T \text{ internal control})_{\text{sample A}})}{((C_T \text{ gene of interest} - C_T \text{ internal control})_{\text{sample B}})} \right]$$

MX3000P software performs analysis of data obtained by the RT-qPCR to quantify the copy number of the target sequence in each sample by comparing it with the standard curve copy numbers. Additionally, the MX3000P software provides the C_t values for each sample (**Figure 16**). Real-Time PCR experiments were performed in triplicates, where the three C_t values per sample were averaged prior to analysis. All statistical analyses were conducted using the GraphPad Prism 6.0 software (GraphPad Software, San Diego, California, USA). Outlier detection was performed prior to analyses using GraphPad Outlier Tool. One-way ANOVA with Tukey's post-hoc test was conducted to determine significance between groups, and a p-value of ($p < 0.05$) was considered statistically significant. Data shown is expressed as mean \pm standard deviation.

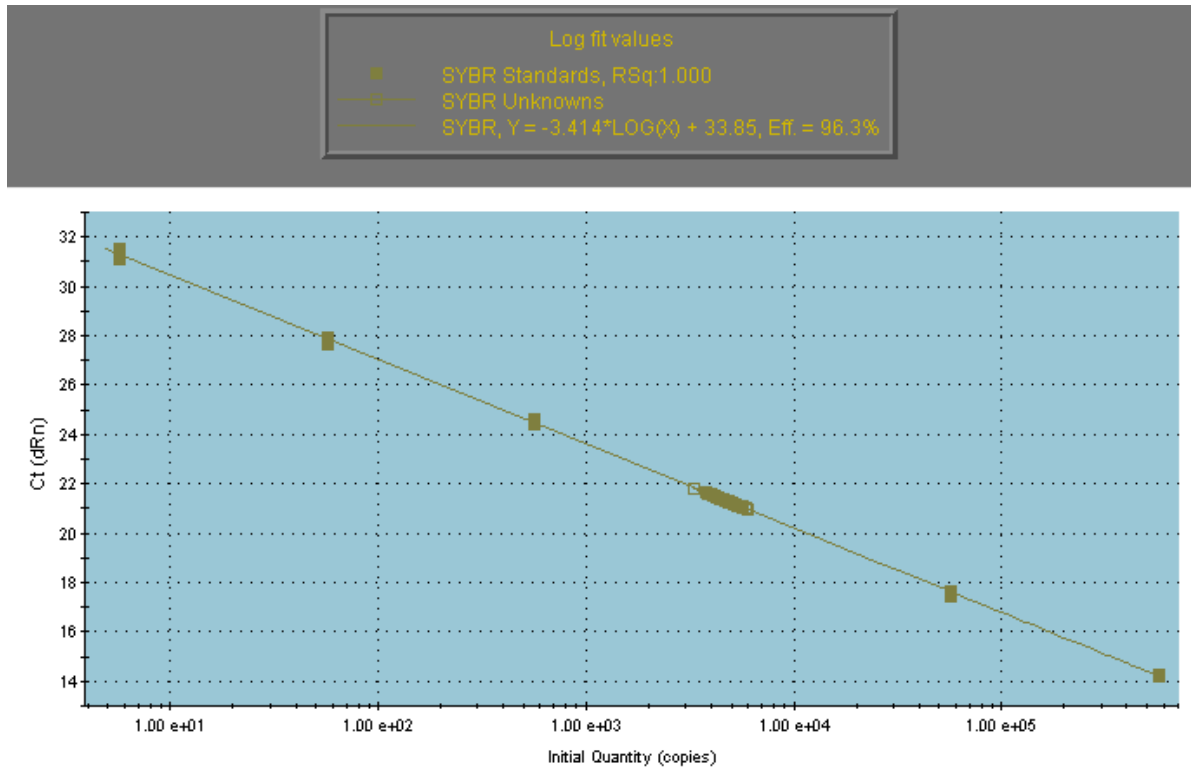


Figure 15. Standard Curve output for RT-qPCR.

The efficiency for all RT-qPCRs was within 90% - 105%. The R-squared values were between 0.95 – 1.00. The x-axis represents the absolute mRNA copy number of the gene of interest. The y-axis represents the C_t value for each sample.

All	1	2	3	4	5	6	7	8	9	10	11	12
A	Standard	Standard	Standard	Unknown	Unknown	Unknown	Unknown	Unknown	Unknown			
	Ref 14.28	Ref 14.19	Ref 14.27	Ref 21.58	Ref 21.43	Ref 21.57	Ref 21.43	Ref 21.44	Ref 21.47			
B	Standard	Standard	Standard	Unknown	Unknown	Unknown	Unknown	Unknown	Unknown			
	Ref 17.55	Ref 17.46	Ref 17.65	Ref 21.41	Ref 21.32	Ref 21.46	Ref 21.30	Ref 21.42	Ref 21.30			
C	Standard	Standard	Standard	Unknown	Unknown	Unknown	Unknown	Unknown	Unknown			
	Ref 21.09	Ref 21.05	Ref 21.13	Ref 21.07	Ref 21.13	Ref 21.23	Ref 21.57	Ref 21.60	Ref 21.84			
D	Standard	Standard	Standard	Unknown	Unknown	Unknown	Unknown	Unknown	Unknown			
	Ref 24.59	Ref 24.99	Ref 24.49	Ref 21.18	Ref 21.29	Ref 21.31	Ref 21.28	Ref 21.28	Ref 21.19			
E	Standard	Standard	Standard	Unknown	Unknown	Unknown	Unknown	Unknown	Unknown			
	Ref 27.63	Ref 27.89	Ref 27.93	Ref 21.19	Ref 21.27	Ref 21.23	Ref 21.65	Ref 21.65	Ref 21.59			
F	Standard	Standard	Standard	Unknown	Unknown	Unknown	Unknown	Unknown	Unknown			
	Ref 31.10	Ref 31.35	Ref 31.52	Ref 20.97	Ref 21.03	Ref 21.08	Ref 21.17	Ref 21.31	Ref 21.18			
G	No RT	No RT	No RT	Unknown	Unknown	Unknown	Unknown	Unknown	Unknown			
	Ref No Ct	Ref 36.31	Ref No Ct	Ref 21.41	Ref 21.58	Ref 21.52	Ref 21.00	Ref 21.17	Ref 21.24			
H	NTC	NTC	NTC	Unknown	Unknown	Unknown	Unknown	Unknown	Unknown			
	Ref 36.86	Ref 34.53	Ref No Ct	Ref 21.50	Ref 21.35	Ref 21.31	Ref 20.97	Ref 21.07	Ref 21.07			

Figure 16. C_t values for RT-qPCR.

MX3000P software provided the C_t -values output above. The samples were run in triplicates as indicated by the triplicate numbers ranging from 1-18, and 30-37. The C_t values for all of the triplicates were within ± 1 cycle per sample. Samples 30 – 35 represent the standard curve values for amplicon serial dilutions from 1pg to 10ag. Triplicate 36 represents the NRT control, and sample 37 represents the no template control (NTC). All samples C_t values fall within the C_t range of the standard curve (C_t 14 – 31). The NRT and NTC C_t values are higher than all of the samples and the standard curve.

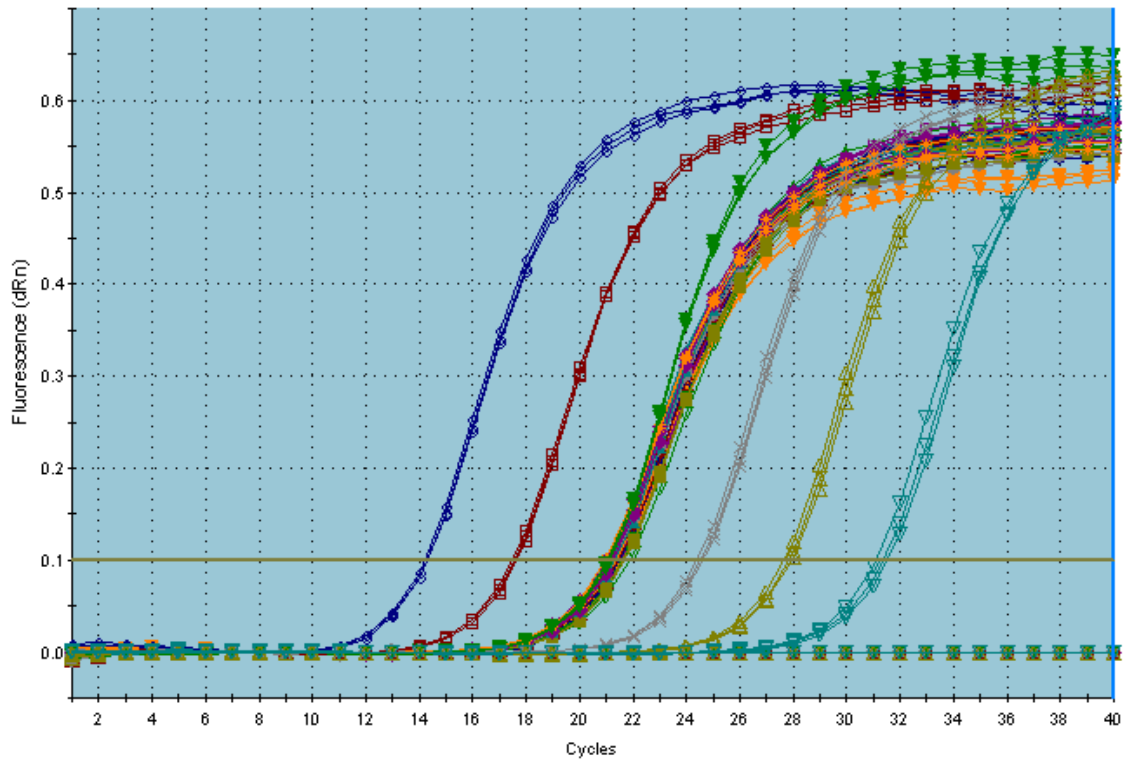


Figure 17. Amplification plot for RT-qPCR.

The x-axis represents the cycle number and the y-axis represents the fluorescence values as a measure of amplification. Each colour represents 3 curves for the sample being run in triplicates. The blue curve represents the amplification curve for 1pg standard, and the light blue curve at the far right represents the amplification curve for the 10ag standard. All of the samples' amplification curves fall between these standard curve ranges.

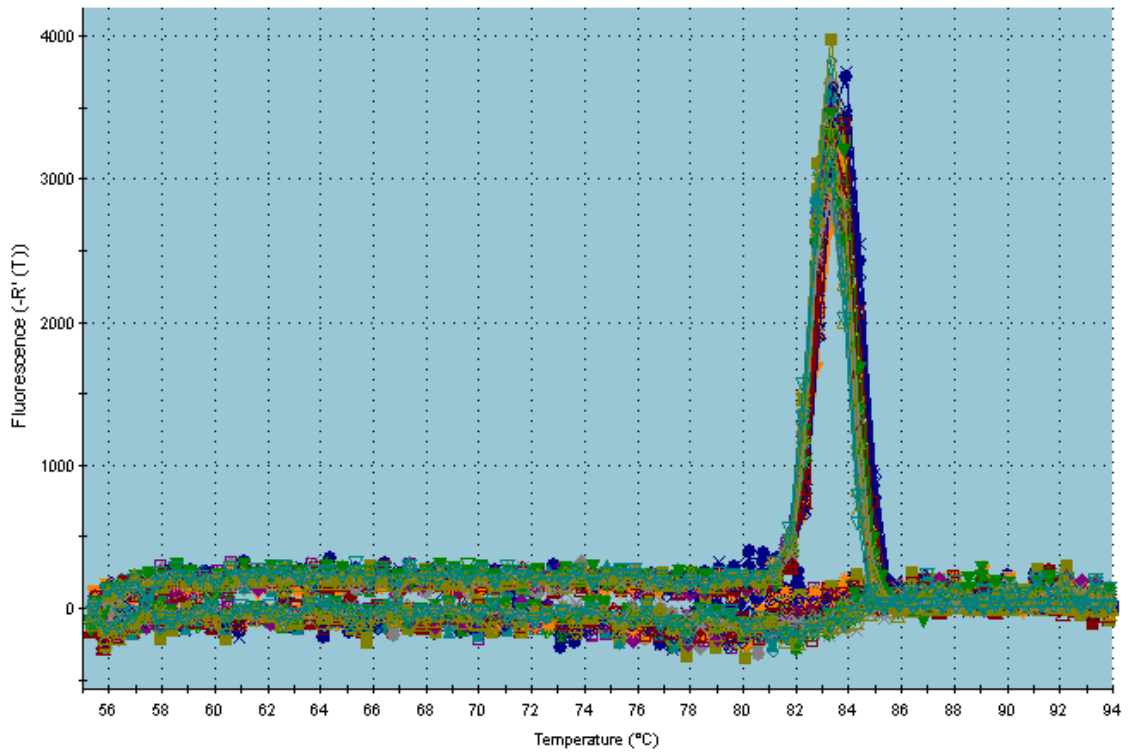


Figure 18. Dissociation curve for RT-qPCR.

The x-axis represents temperature (°C) and the y-axis represents the fluorescence. One single peak in the dissociation curve represents amplification of one single product of interest.

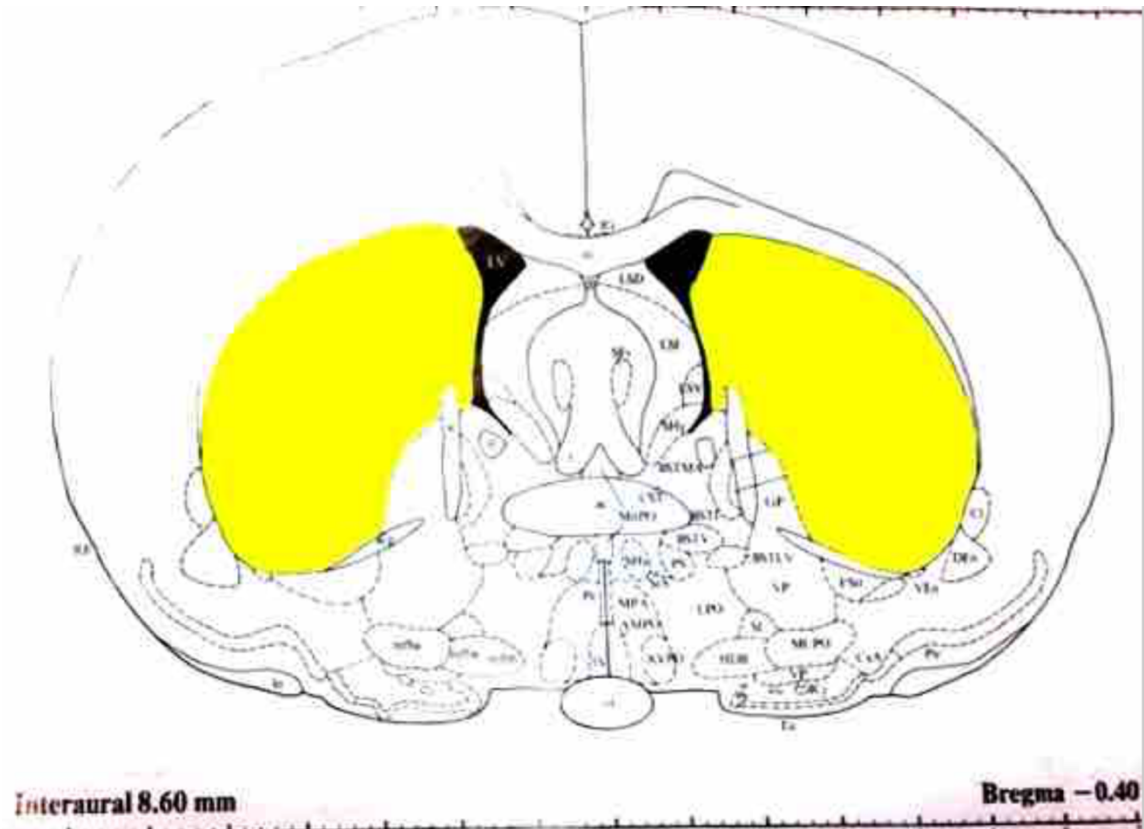


Figure 19. Rat Striatum.

The shaded regions represent the approximate area dissected for the rat striatum sample from both sides of the brain.

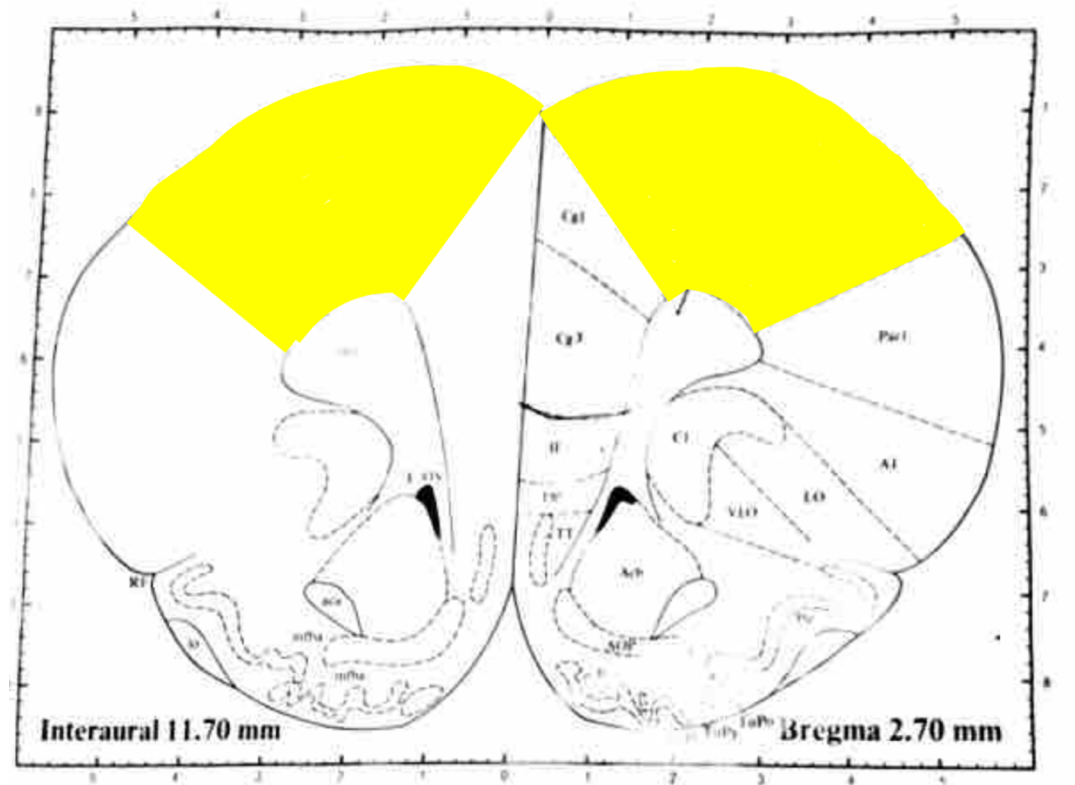


Figure 20. Rat Pre-Frontal Cortex (PFC).

The shaded regions represent the approximate area dissected for the rat PFC sample from both sides of the brain.

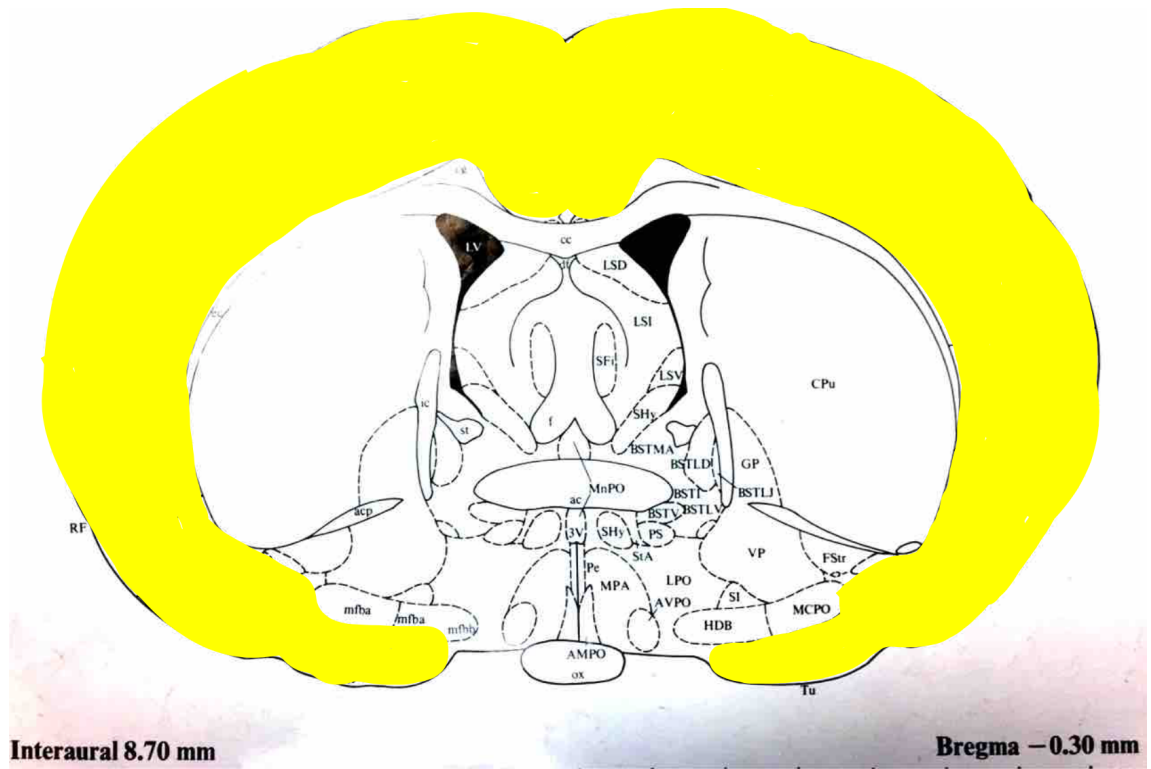


Figure 21. Rat Cortex.

The shaded regions represent the approximate area dissected for the rat cortex sample from both sides of the brain.

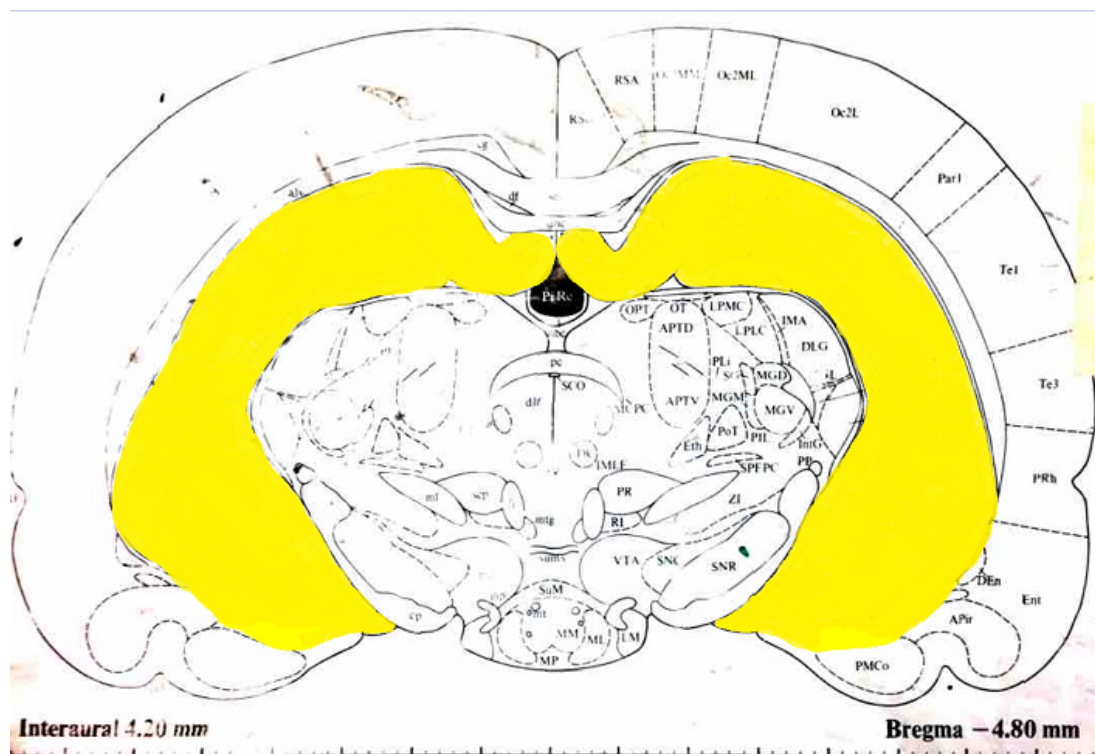


Figure 22. Rat Hippocampus.

The shaded regions represent the approximate area dissected for the rat hippocampus sample from both sides of the brain.

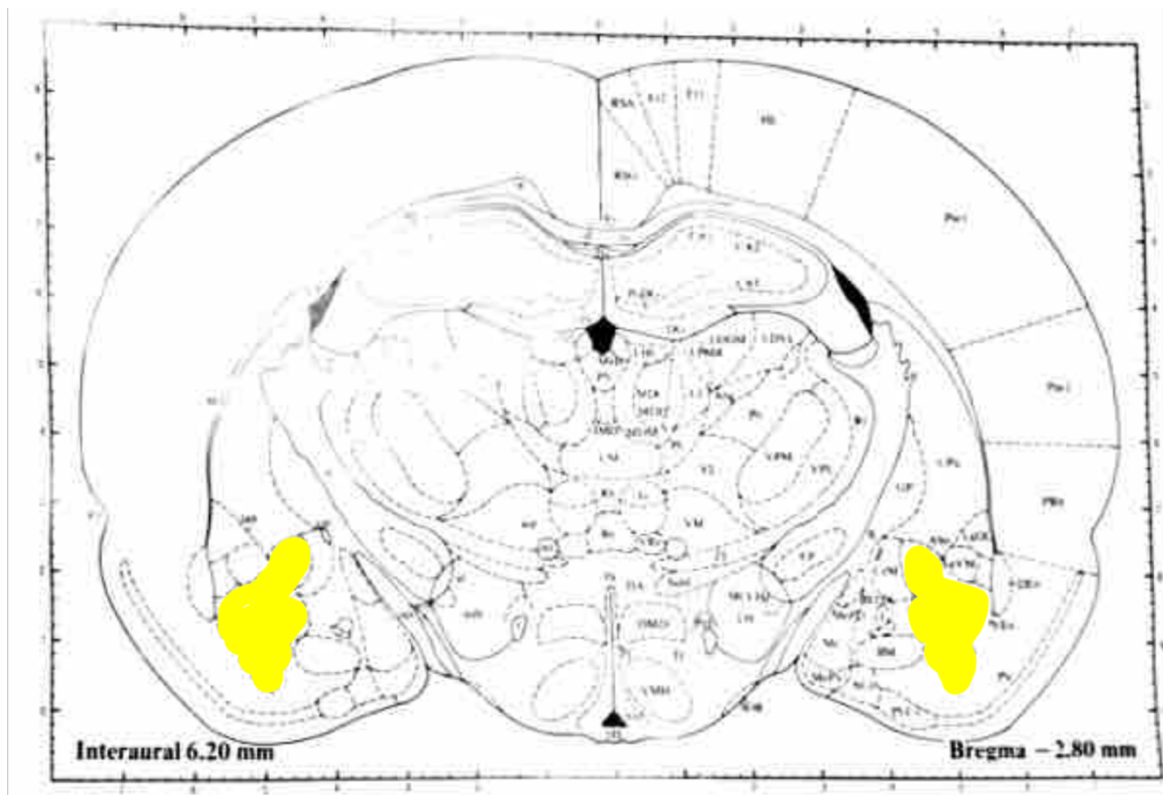


Figure 23. Rat Amygdala.

The shaded regions represent the approximate area dissected for the rat amygdala sample from both sides of the brain.

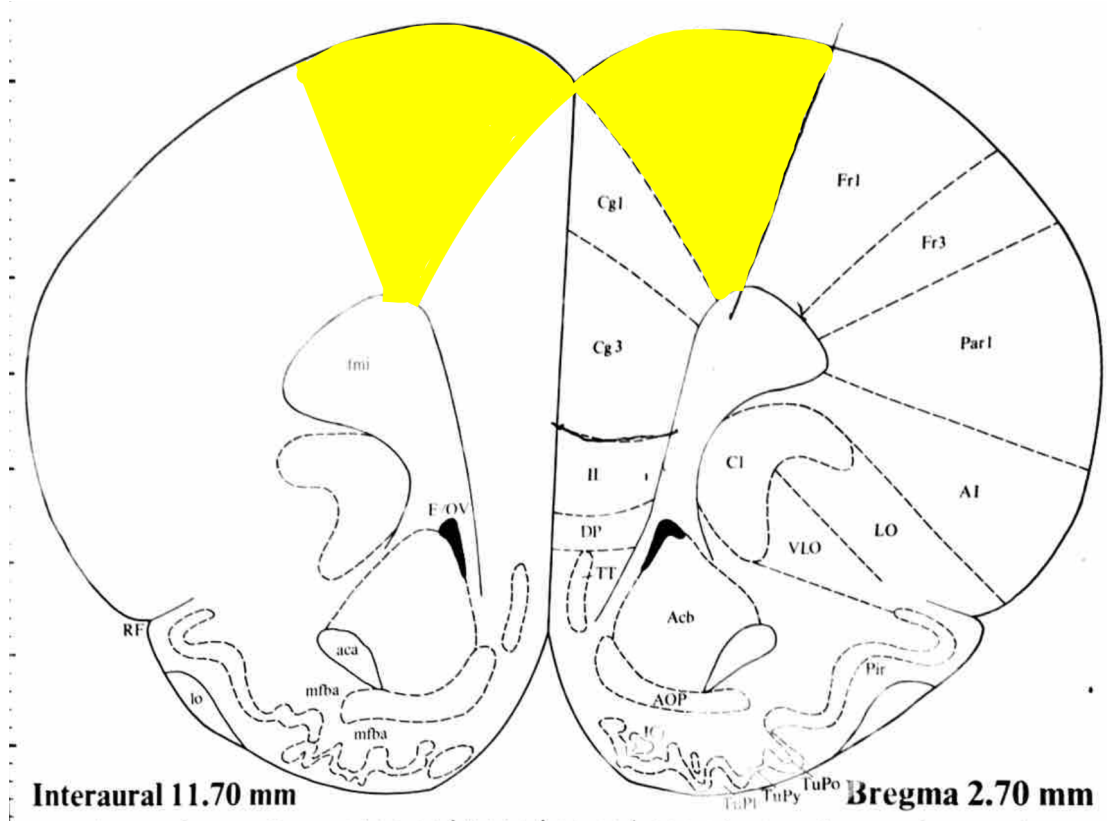
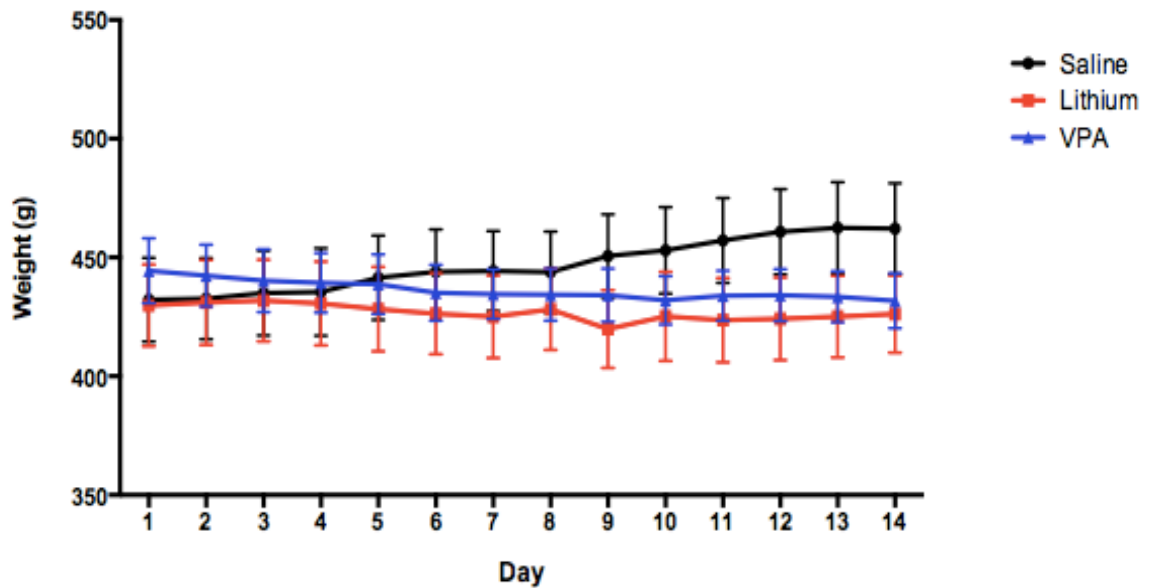


Figure 24. Rat Medial Pre-Frontal Cortex (mPFC).

The shaded regions represent the approximate area dissected for the rat mPFC sample from both sides of the brain.

3.3 Results

3.3.1 Body Weight Change Due to Drug Administration – Cohort 1



n = 6, 8, 8 (Saline, LiCl, VPA)

Figure 25. Effects of Lithium and VPA on rats' body weight.

Results display the changes in weight (y-axis) from Day 1 – 14 (x-axis), for all three treatment groups – Saline, Lithium, and VPA.

3.3.2 Levels of Drug Treatments in Rats' Blood Plasma – Cohort 1

Study ID	Drug Treatment Group	Lithium Chloride Levels (mmol/L)	Valproic Acid Levels (umol/L)
		Therapeutic Range: 0.5-1.1 mmol/L	Therapeutic Range: 350-700 umol/L
S001	Saline	N.D.	N.D.
S002		N.D.	N.D.
S003		N.D.	N.D.
S004		N.D.	N.D.
S005		N.D.	N.D.
S006		N.D.	N.D.
L007	Lithium	0.34	N.D.
L008		0.40	N.D.
L009		0.36	N.D.
L010		0.43	N.D.
L011		0.40	N.D.
L012		0.30	N.D.
L013		0.50	N.D.
L014		0.40	N.D.
V015	Valproic Acid	N.D.	80
V016		N.D.	336
V017		N.D.	79
V018		N.D.	73
V019		N.D.	77
V020		N.D.	63
V021		N.D.	51
V022		N.D.	100

Figure 26. Levels of drug treatments in blood plasma from rats- cohort 1.

Levels of both Lithium and VPA were analyzed in all of the samples to ensure that only one drug was present in each treatment group, and no drugs were present in the saline control group. Blood was collected 6 hours after the last injection on Day 14. (N.D. – Not detected).

3.3.3 Effect of Lithium and VPA on CDNF and MANF mRNA expression in rat PFC

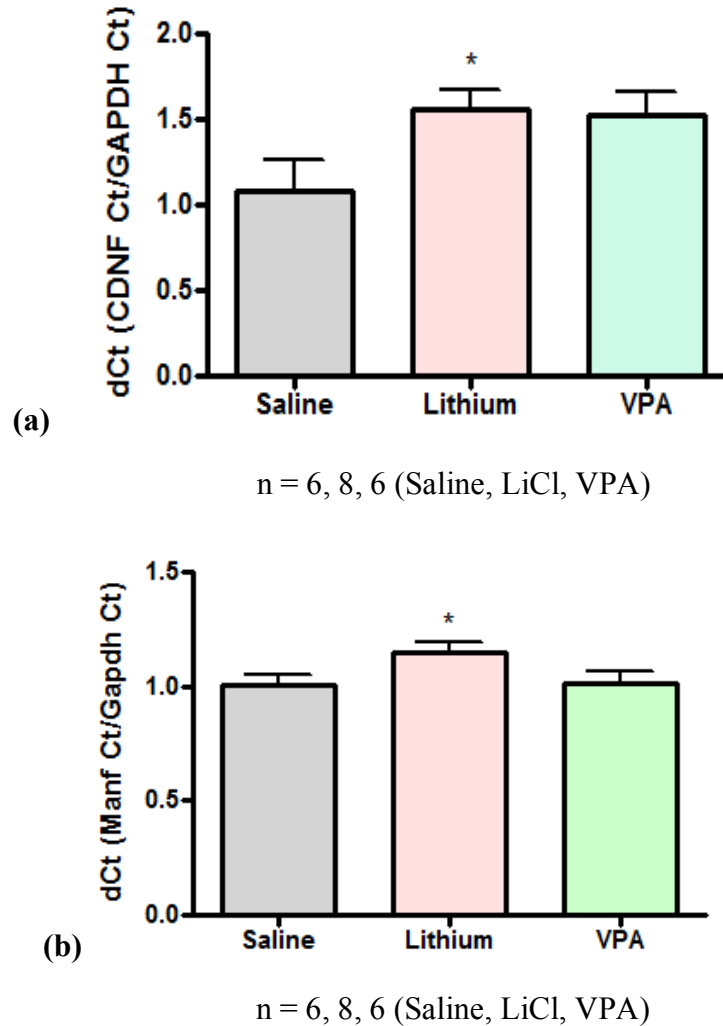


Figure 27. NTFs mRNA expression in PFC of rats treated with Lithium and VPA.

Two-step RT-qPCR to measure the mRNA expression of (a) CDNF and (b) MANF, in the rat PFC, following I.P. injections of Lithium (LiCl) and Valproic Acid (VPA) twice daily for 14 consecutive days. The LiCl treatment was administered at a dosage of 47.5mg/kg per rat, and VPA was administered at 200mg/kg. (a-b) The graphs display the $\Delta\Delta C_t$ values normalized to GAPDH housekeeping gene (y-axis). LiCl treatment significantly increased mRNA expression of CDNF and MANF in PFC (* $p < 0.05$). Sample Size (Saline, Lithium, VPA): 6, 8, 6.

3.3.4 Effect of Lithium and VPA on CDNF and MANF mRNA expression in rat

Striatum

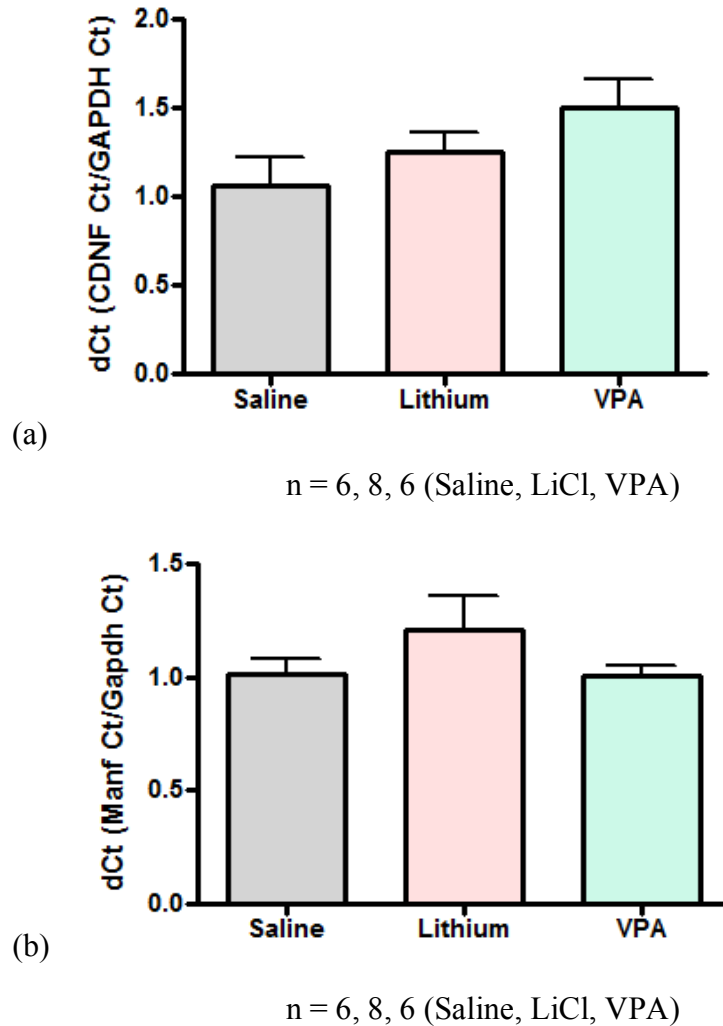


Figure 28. NTFs mRNA expression in striatum of rats treated with Lithium and VPA.

Two-step RT-qPCR to measure the mRNA expression of (a) CDNF and (b) MANF, in the rat striatum, following I.P. injections of Lithium (LiCl) and Valproic Acid (VPA) twice daily for 14 consecutive days. The LiCl treatment was administered at a dosage of 47.5mg/kg per rat, and VPA was administered at 200mg/kg. The y-axis displays the $\Delta\Delta C_t$ values normalized to GAPDH housekeeping gene. Sample Size (Saline, Lithium, VPA): 6, 8, 6.

3.3.5 Effect of Lithium & VPA on Hippocampus CDNF and MANF mRNA expression

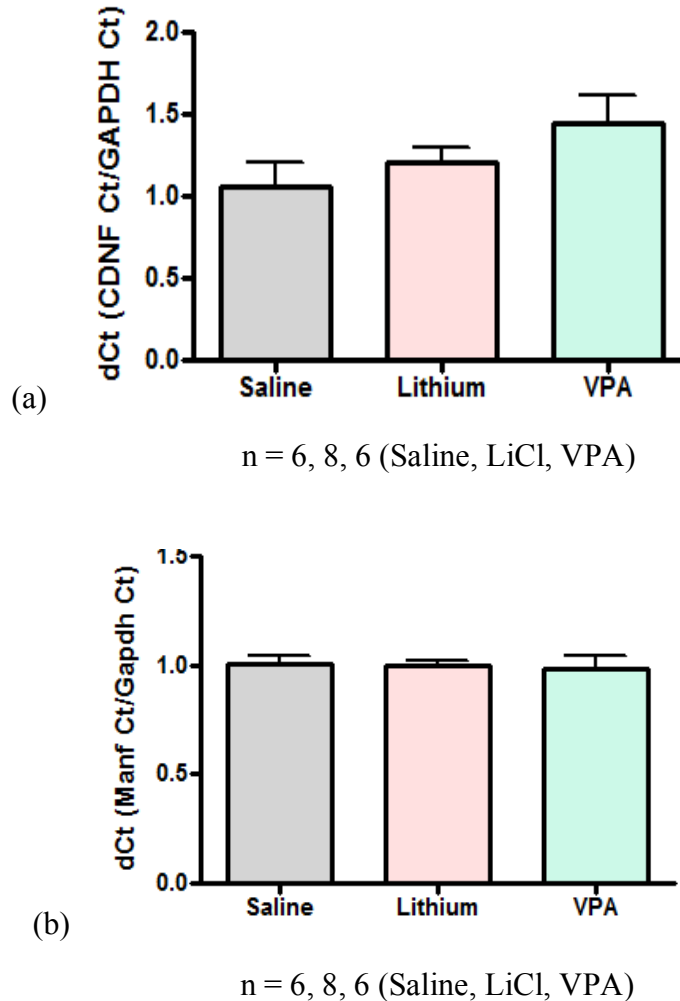


Figure 29. NTFs mRNA expression in rat hippocampus treated with Lithium & VPA.

Two-step RT-qPCR to measure the mRNA expression of (a) CDNF and (b) MANF, in the rat hippocampus, following I.P. injections of Lithium (LiCl) and Valproic Acid (VPA) twice daily for 14 consecutive days. The LiCl treatment was administered at a dosage of 47.5mg/kg per rat, and VPA was administered at 200mg/kg. The y-axis displays the $\Delta\Delta C_t$ values normalized to GAPDH housekeeping gene. Sample Size (Saline, Lithium, VPA): 6, 8, 6.

3.3.6 Effect of Lithium & VPA on CDNF and MANF mRNA expression in rat Cortex

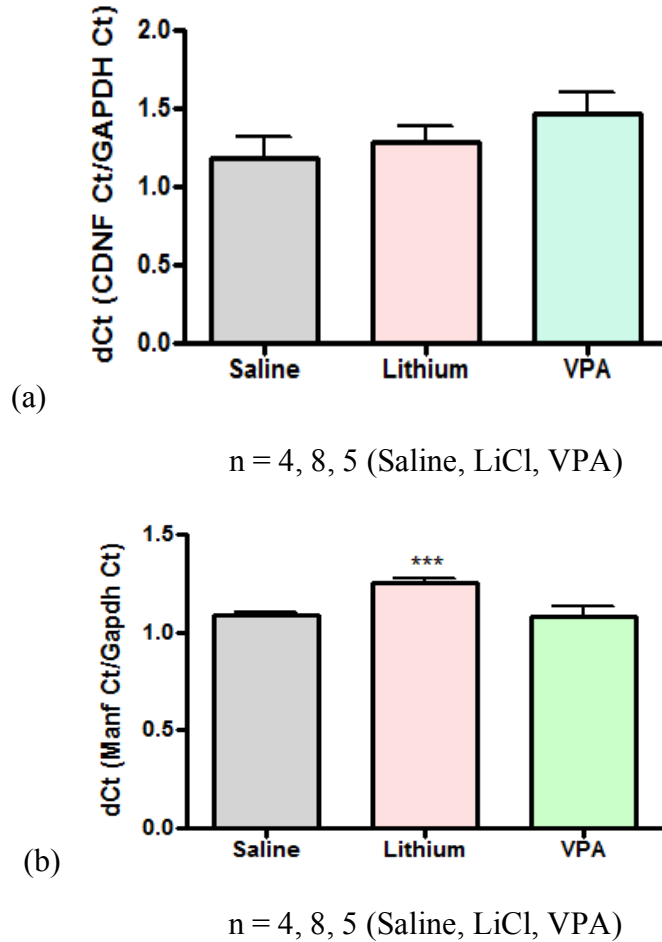


Figure 30. NTFs mRNA expression in Cortex of rats treated with Lithium and VPA.

Two-step RT-qPCR to measure the mRNA expression of (a) CDNF and (b) MANF, in the rat cortex, following I.P. injections of Lithium (LiCl) and Valproic Acid (VPA) twice daily for 14 consecutive days. The LiCl treatment was administered at a dosage of 47.5mg/kg per rat, and VPA was administered at 200mg/kg. The y-axis displays the $\Delta\Delta C_t$ values normalized to GAPDH housekeeping gene. LiCl treatment significantly increased mRNA expression of MANF in Cortex (***p<0.001). Sample Size (Saline, Lithium, VPA): 4, 8, 5.

3.3.7 Effect of Lithium and VPA on GAPDH mRNA expression in Striatum,

Hippocampus, Cortex, and PFC.

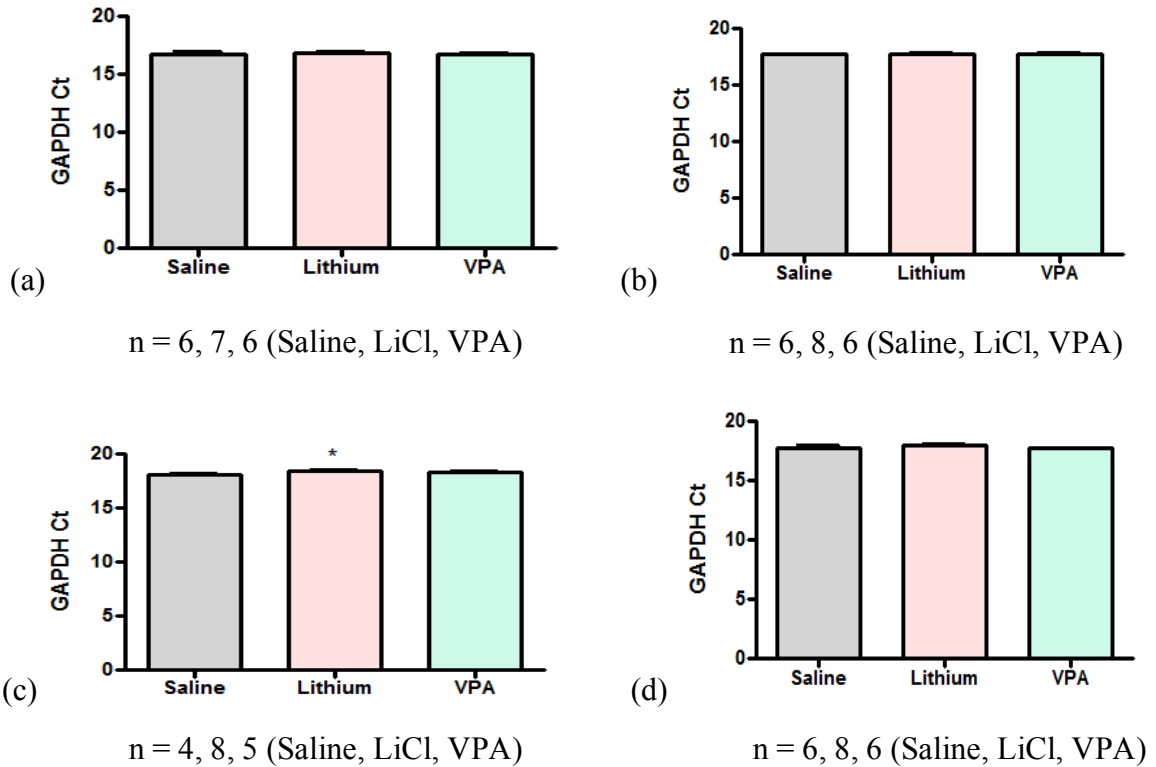


Figure 31. GAPDH mRNA expression in rats treated with Lithium and VPA.

Two-step RT-qPCR to measure the mRNA expression of the housekeeping gene GAPDH in following rat brain regions: (a)Striatum, (b)Hippocampus, (c) Cortex, and (d) PFC, following I.P. injections of Lithium (LiCl) and Valproic Acid (VPA) twice daily for 14 consecutive days. The LiCl treatment was administered at a dosage of 47.5mg/kg per rat, and VPA was administered at 200mg/kg. The results display the Ct values for the GAPDH housekeeping gene. (d) LiCl treatment significantly increased mRNA expression of GAPDH in cortex, other brain regions remain unaffected. (*p<0.05). Sample Size (Saline, Lithium, VPA): (a)Striatum: 6, 7, 6; (b & d) Hippocampus and PFC: 6, 8, 6; (c)Cortex: 4, 8, 5.

3.3.8 Body Weight Change Due to Drug Administration – Cohort 2

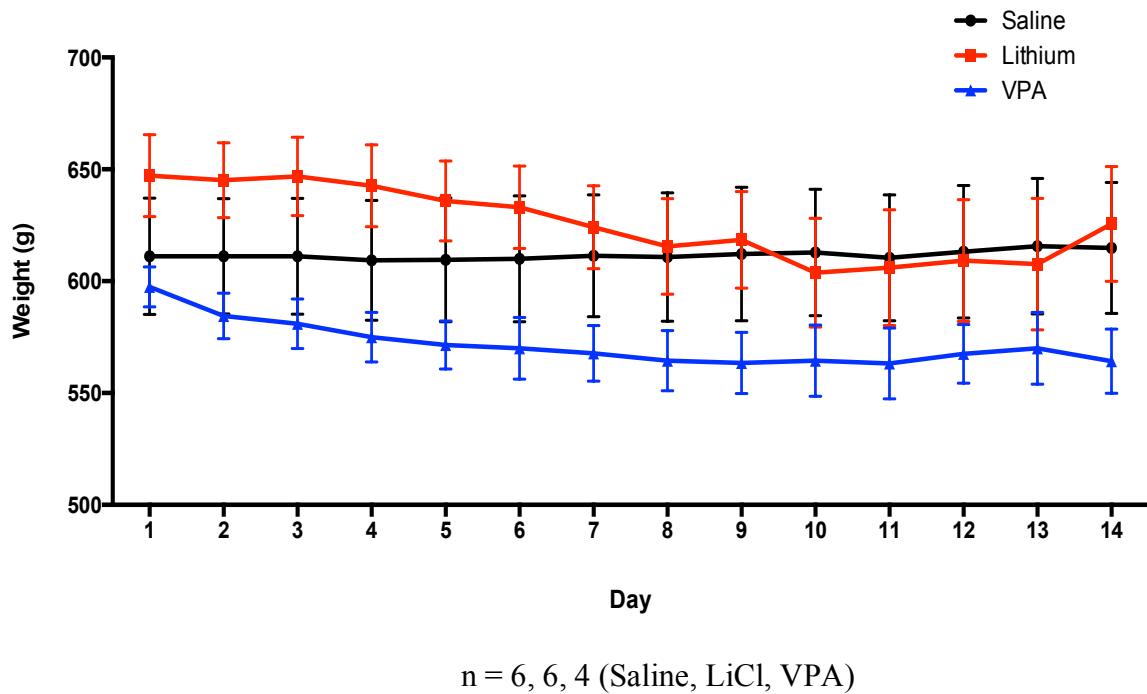


Figure 32. Effects of Lithium and VPA on rats' body weight – cohort 2.

Results display the changes in weight (y-axis) from Day 1 – 14 (x-axis) for all three treatment groups – Saline, Lithium, and VPA.

3.3.9 Levels of Drug Treatments in Rats' Blood Plasma – Cohort 2

Study ID	Drug Treatment Group	Lithium Chloride (mmol/L) Therapeutic Range: 0.5-1.1 mmol/L	Valproic Acid (umol/L) Therapeutic Range: 350-700 umol/L
S001	Saline	N.D.	N.D.
S002		N.D.	N.D.
S003		N.D.	N.D.
S004		N.D.	N.D.
S005		N.D.	N.D.
S006		N.D.	N.D.
L007	Lithium	0.8	N.D.
L008		4.8	N.D.
L009		0.8	N.D.
L010		0.6	N.D.
L011		0.8	N.D.
L012		0.7	N.D.
V013	Valproic Acid	N.D.	263
V015		N.D.	208
V016		N.D.	78
V018		N.D.	374

Figure 33. Levels of drug treatments in blood plasma from rats- cohort 2.

Levels of both Lithium and VPA were analyzed in all of the samples to ensure that only one drug was present in each treatment group, and no drugs were present in the saline control group. Blood was collected 2.5 hours after the last injection on Day 14. (N.D. – Not detected).

3.3.10 Open-Field Task – Behavioural Data

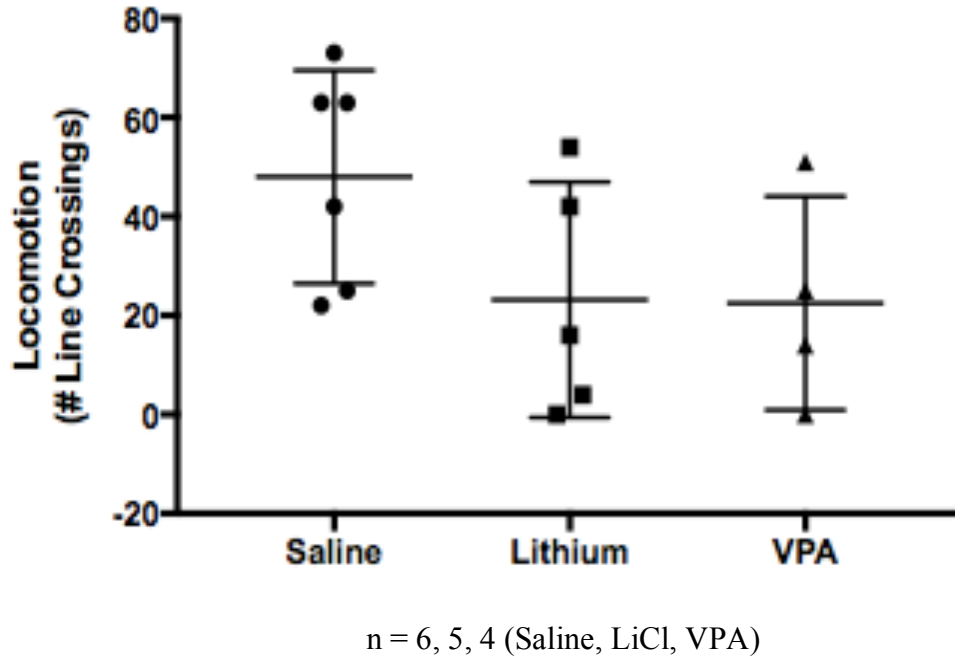


Figure 34. Locomotion data from the open-field behavioural task.

The number of line crossings in the open-field chamber grid was analyzed as a measure of locomotion. Rats were tested for a 5-minute interval, 2 hours after their last injection on Day 14. Sample Size (Saline, Lithium, VPA): 6, 5, 4.

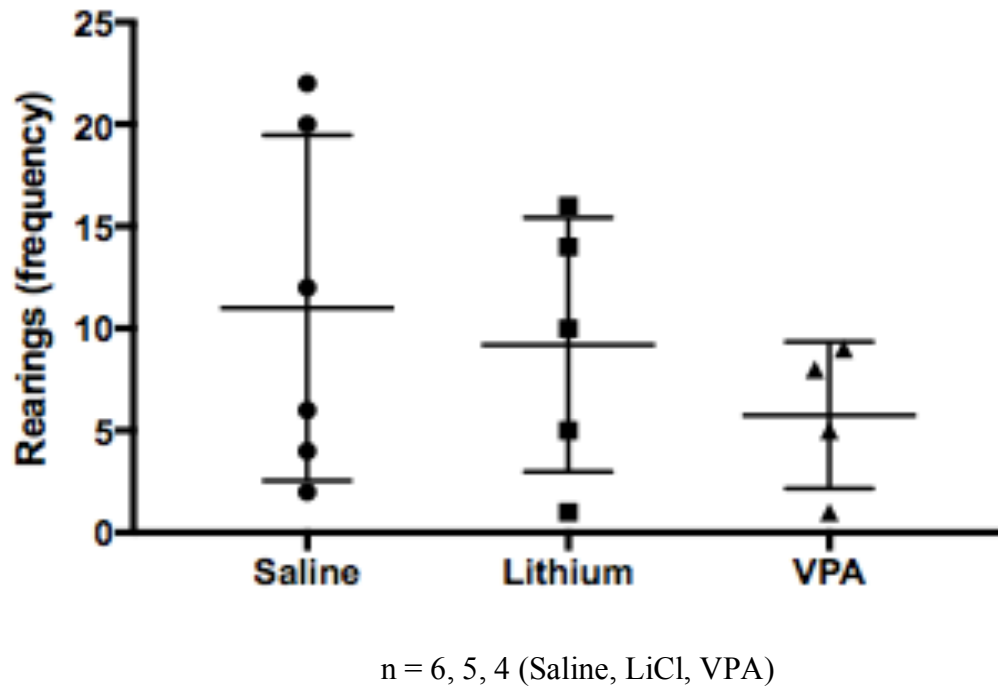
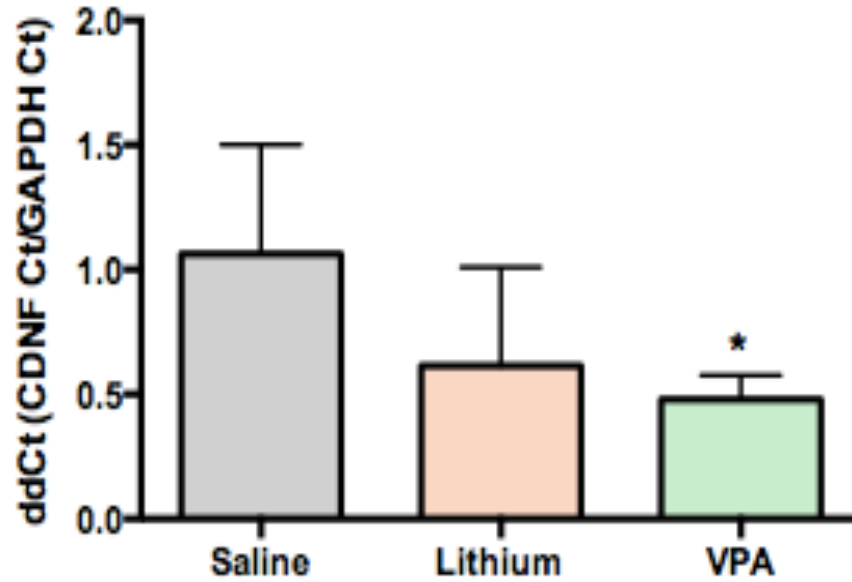


Figure 35. Rearing data from open-field behavioural task.

The number of rearings with their front paws was used as another measure of locomotive behaviour. The rats were tested for a period of 5 minutes individually, 2 hours after their last injection on Day 14. Sample Size (Saline, Lithium, VPA): 6, 5, 4.

3.3.11 Effect of Lithium and VPA on CDNF mRNA expression in rat PFC

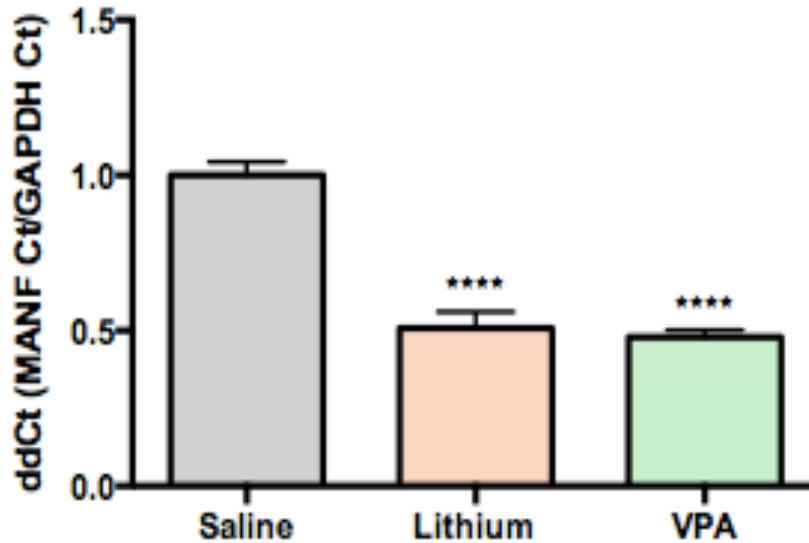


n = 6, 5, 4 (Saline, LiCl, VPA)

Figure 36. CDNF mRNA expression in PFC of rats treated with Lithium and VPA.

Two-step RT-qPCR to measure the mRNA expression of CDNF in the rat PFC, following I.P. injections of Lithium (LiCl) and Valproic Acid (VPA) twice daily for 14 consecutive days. The LiCl treatment was administered at a dosage of 47.5mg/kg per rat, and VPA was administered at 200mg/kg. The y-axis displays the $\Delta\Delta C_t$ values normalized to GAPDH housekeeping gene. VPA treatment significantly decreased mRNA expression of CDNF in PFC. Sample Size (Saline, Lithium, VPA): 6, 5, 4. (* $p < 0.05$).

3.3.12 Effect of Lithium and VPA on MANF mRNA expression in rat PFC



n = 6, 5, 4 (Saline, LiCl, VPA)

Figure 37. MANF mRNA expression in PFC of rats treated with Lithium and VPA.

Two-step RT-qPCR to measure the mRNA expression of MANF in the rat PFC, following I.P. injections of Lithium (LiCl) and Valproic Acid (VPA) twice daily for 14 consecutive days. The LiCl treatment was administered at a dosage of 47.5mg/kg per rat, and VPA was administered at 200mg/kg. The y-axis displays the $\Delta\Delta C_t$ values normalized to GAPDH housekeeping gene. Both Lithium and VPA treatment significantly decreased mRNA expression of CDNF in rats PFC. Sample Size (Saline, Lithium, VPA): 6, 5, 4. (****p<0.0001).

3.3.13 Effect of Lithium and VPA on CDNF and MANF mRNA expression in rat

Hippocampus

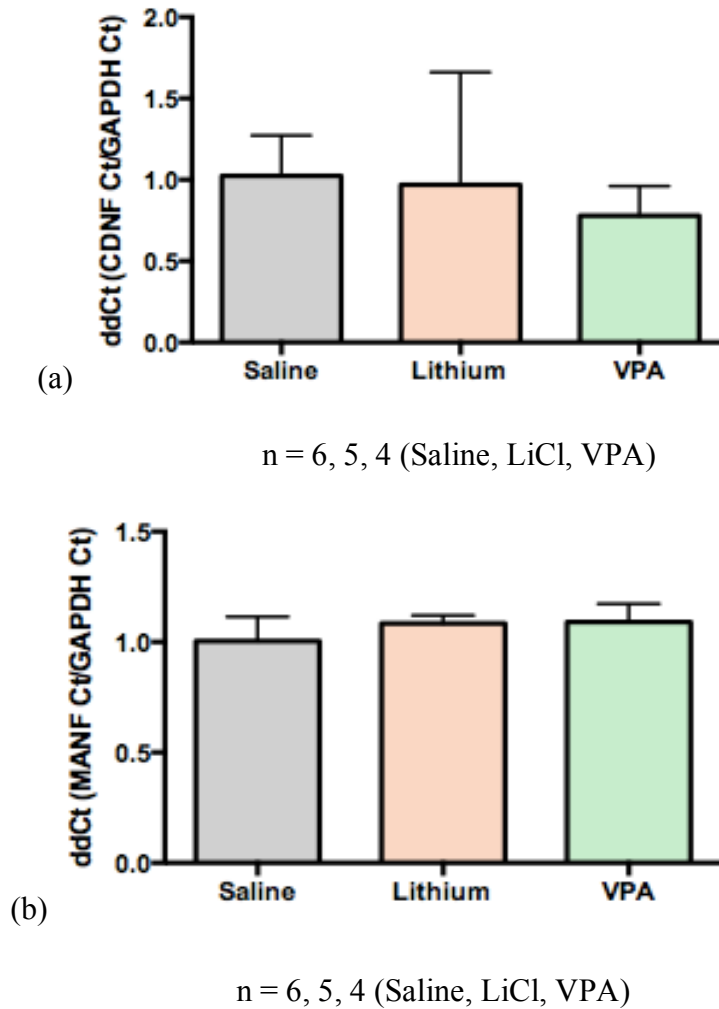
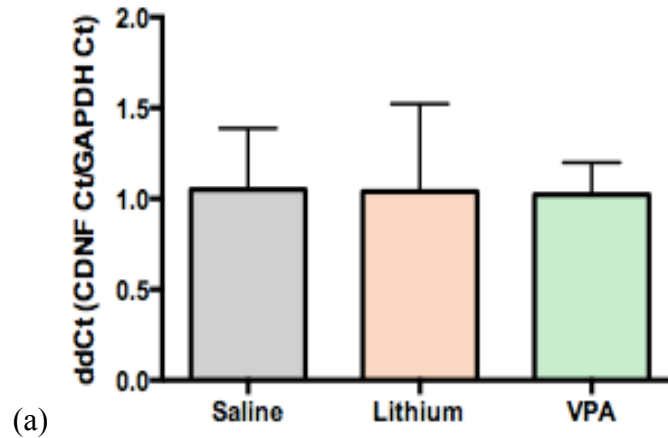


Figure 38. NTFs mRNA expression in rat hippocampus treated with Lithium & VPA.

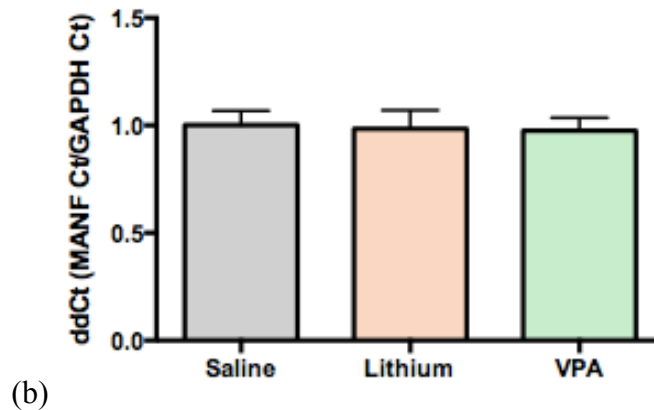
Two-step RT-qPCR to measure the mRNA expression of (a) CDNF and (b) MANF, in the rat hippocampus, following I.P. injections of Lithium (LiCl) and Valproic Acid (VPA) twice daily for 14 consecutive days. The LiCl treatment was administered at a dosage of 47.5mg/kg per rat, and VPA was administered at 200mg/kg. The y-axis displays the $\Delta\Delta C_t$ values normalized to GAPDH housekeeping gene. Sample Size (Saline, Lithium, VPA): 6, 5, 4.

3.3.14 Effect of Lithium and VPA on CDNF and MANF mRNA expression in rat

Striatum



n = 6, 5, 4 (Saline, LiCl, VPA)



n = 6, 5, 4 (Saline, LiCl, VPA)

Figure 39. NTFs mRNA expression in striatum of rats treated with Lithium and VPA.

Two-step RT-qPCR to measure the mRNA expression of (a) CDNF and (b) MANF, in the rat striatum, following I.P. injections of Lithium (LiCl) and Valproic Acid (VPA) twice daily for 14 consecutive days. The LiCl treatment was administered at a dosage of 47.5mg/kg per rat, and VPA was administered at 200mg/kg. The y-axis displays the $\Delta\Delta C_t$ values normalized to GAPDH housekeeping gene. Sample Size (Saline, Lithium, VPA): 6, 5, 4.

3.3.15 Effect of Lithium and VPA on CDNF and MANF mRNA expression in rat

Cortex

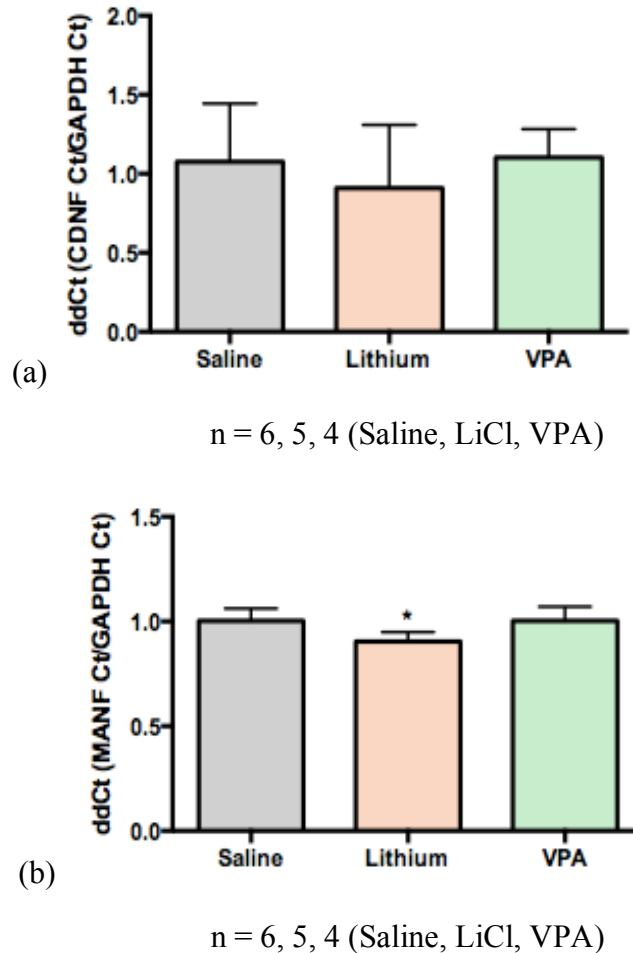


Figure 40. NTFs mRNA expression in cortex of rats treated with Lithium and VPA.

Two-step RT-qPCR to measure the mRNA expression of (a) CDNF and (b) MANF, in the rat cortex, following I.P. injections of Lithium (LiCl) and Valproic Acid (VPA) twice daily for 14 consecutive days. The LiCl treatment was administered at a dosage of 47.5mg/kg per rat, and VPA was administered at 200mg/kg. The y-axis displays the $\Delta\Delta C_t$ values normalized to GAPDH housekeeping gene. Lithium treatment significantly decreased MANF mRNA expression in rat cortex. Sample Size (Saline, Lithium, VPA): 6, 5, 4. (* $p < 0.05$).

3.3.16 Effect of Lithium and VPA on CDFN and MANF mRNA expression in rat

mPFC

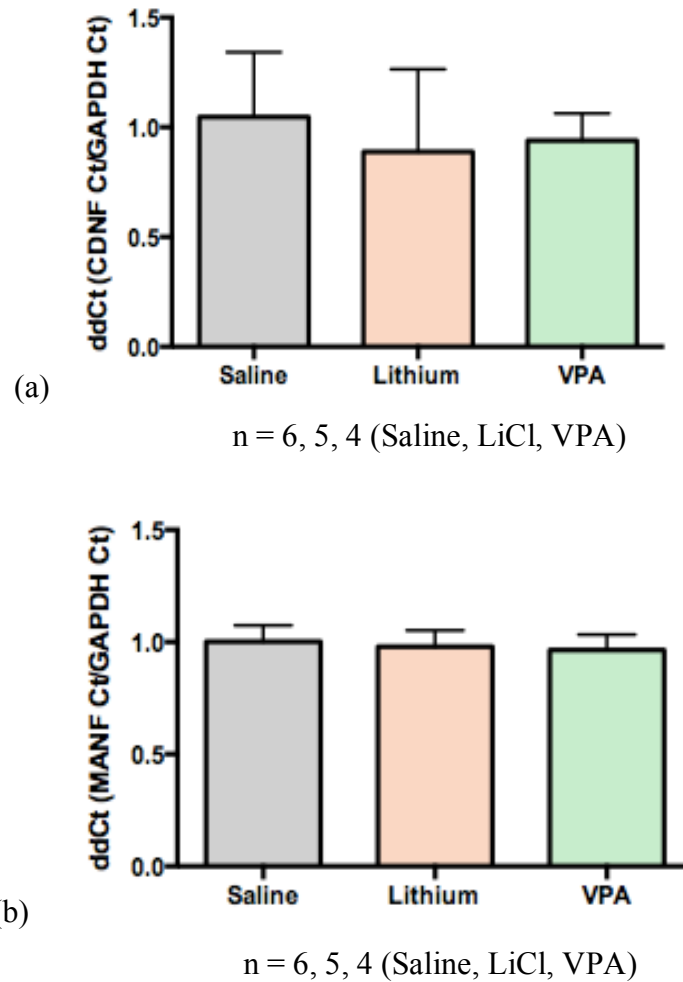


Figure 41. NTFs mRNA expression in mPFC of rats treated with Lithium and VPA.

Two-step RT-qPCR to measure the mRNA expression of (a) CDFN and (b) MANF, in rat mPFC, following I.P. injections of Lithium (LiCl) and Valproic Acid (VPA) twice daily for 14 consecutive days. The LiCl treatment was administered at a dosage of 47.5mg/kg per rat, and VPA was administered at 200mg/kg. The y-axis displays the $\Delta\Delta C_t$ values normalized to GAPDH housekeeping gene. Sample Size (Saline, Lithium, VPA): 6, 5, 4.

3.3.17 Effect of Lithium and VPA on CDNF and MANF mRNA expression in rat

Amygdala

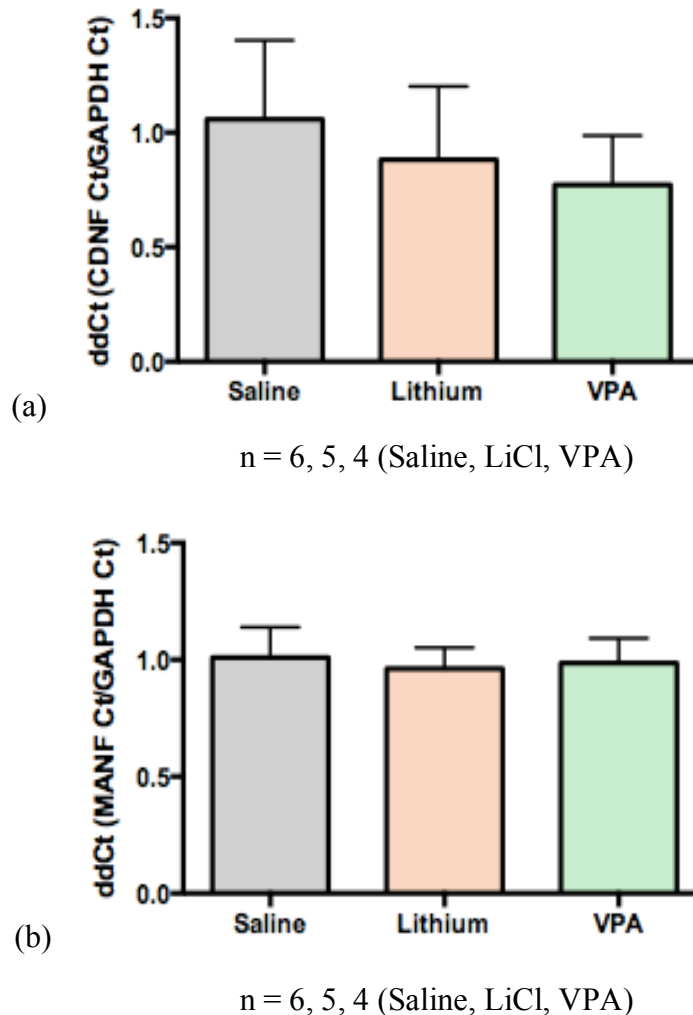


Figure 42. NTFs mRNA expression in amygdala of rats treated with Lithium & VPA.

Two-step RT-qPCR to measure the mRNA expression of (a) CDNF and (b) MANF, in rat amygdala, following I.P. injections of Lithium (LiCl) and Valproic Acid (VPA) twice daily for 14 consecutive days. The LiCl treatment was administered at a dosage of 47.5mg/kg per rat, and VPA was administered at 200mg/kg. The y-axis displays the $\Delta\Delta C_t$ values normalized to GAPDH housekeeping gene. Sample Size (Saline, Lithium, VPA): 6, 5, 4.

3.3.18 Effect of Lithium and VPA on GAPDH mRNA expression in PFC and mPFC

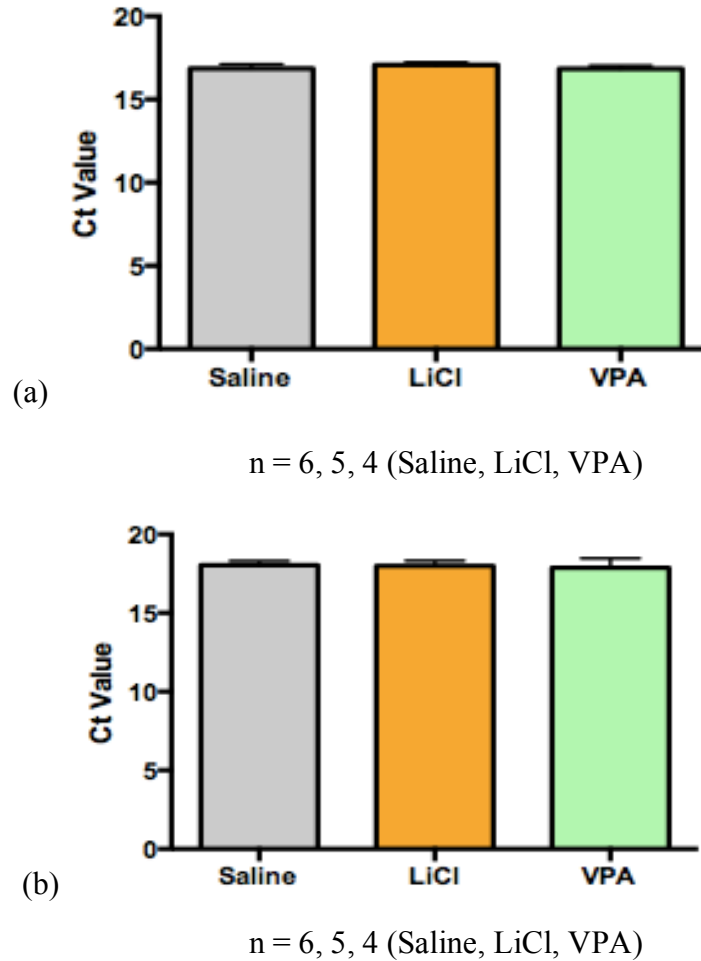


Figure 43. GAPDH mRNA expression in rats PFC & mPFC treated with Lithium and VPA.

Two-step RT-qPCR to measure the mRNA expression of the housekeeping gene GAPDH in (a) PFC, and (b) mPFC, following I.P. injections of Lithium (LiCl) and Valproic Acid (VPA) twice daily for 14 consecutive days. The LiCl treatment was administered at a dosage of 47.5mg/kg per rat, and VPA was administered at 200mg/kg. The results display the Ct values for the GAPDH housekeeping gene. Sample Size (Saline, Lithium, VPA): 6, 5, 4.

3.3.19 Effect of Lithium and VPA on GAPDH mRNA expression in rat Hippocampus

and Amygdala

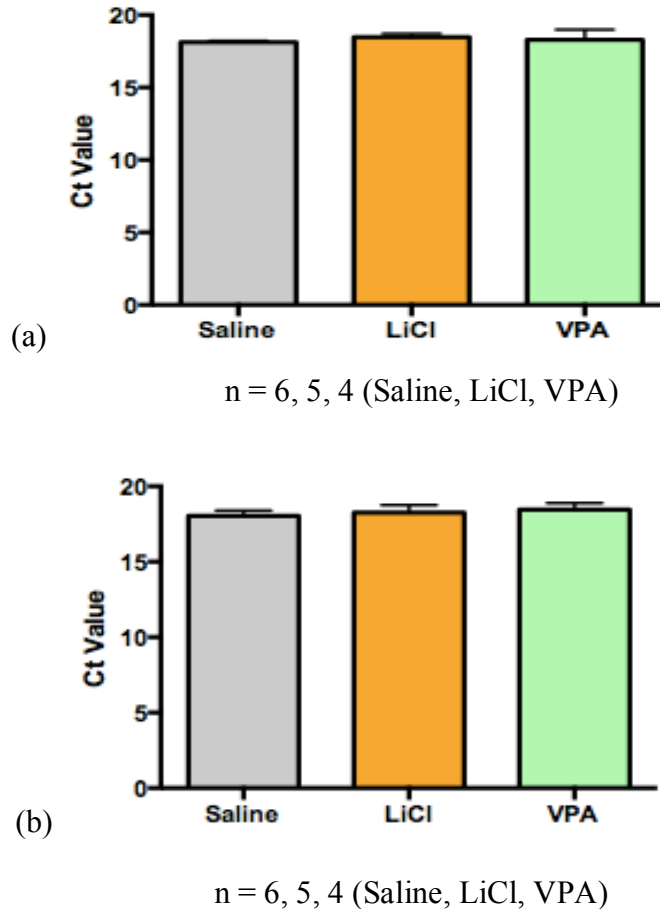


Figure 44. GAPDH mRNA in rats' hippocampus & amygdala treated with Lithium and VPA.

Two-step RT-qPCR to measure the mRNA expression of the housekeeping gene GAPDH in (a) Hippocampus, and (b) amygdala, following I.P. injections of Lithium (LiCl) and Valproic Acid (VPA) twice daily for 14 consecutive days. The LiCl treatment was administered at a dosage of 47.5mg/kg per rat, and VPA was administered at 200mg/kg. The results display the Ct values for the GAPDH housekeeping gene. Sample Size (Saline, Lithium, VPA): 6, 5, 4.

3.3.20 Effect of Lithium and VPA on GAPDH mRNA expression in rat Striatum and

Cortex

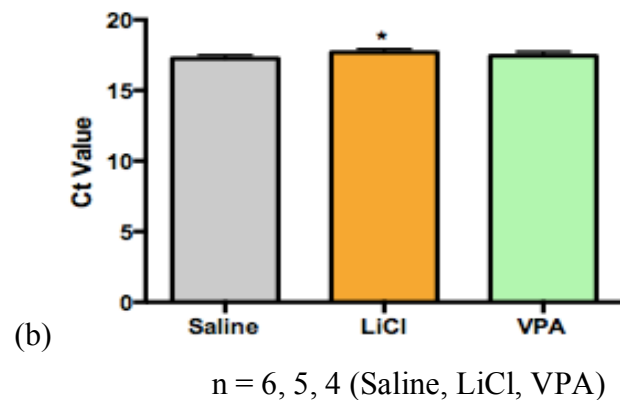
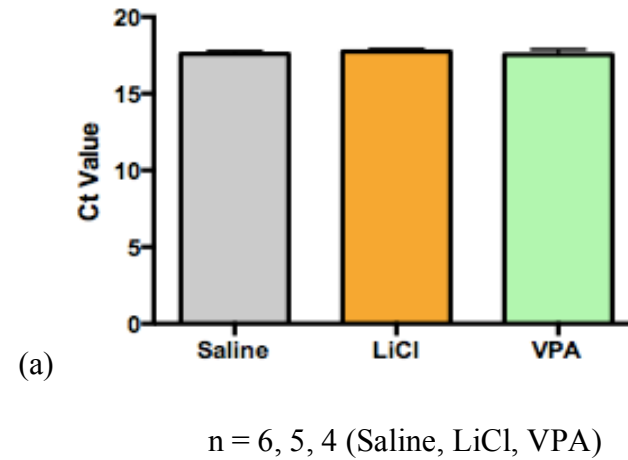


Figure 45. GAPDH mRNA in rats striatum and cortex treated with Lithium and VPA.

Two-step RT-qPCR to measure the mRNA expression of the housekeeping gene GAPDH in (a)Striatum, and (b)Cortex, following I.P. injections of Lithium (LiCl) and Valproic Acid (VPA) twice daily for 14 consecutive days. The LiCl treatment was administered at a dosage of 47.5mg/kg per rat, and VPA was administered at 200mg/kg. The results display the Ct values for the GAPDH housekeeping gene. Lithium significantly increased GAPDH mRNA expression in rat cortex. Sample Size (Saline, Lithium, VPA): 6, 5, 4. (* $p < 0.05$).

3.4 Discussion

Given the increased mRNA expression of MANF and CDFN as a result of lithium and VPA administration to *SH-SY5Y* cells, the aim of this study was to replicate those results. **Figures 25 and 32** display changes in rats' body weight over the duration of the drug administration for cohort 1 and 2 respectively. In both cohorts, lithium and VPA administration caused a significant change in weight, when compared to saline control rats. Lithium and VPA treatment rats have a significantly lower body mass. This decrease in weight is inconsistent with the changes frequently observed in human patients taking these mood stabilizers (Correll, 2007, Biton, 2001). However, rodent models of autism studies have observed that fetal exposure to VPA results in lower body weight of rats (Schneider & Przewłocki, 2005). Thus, it is possible that these mood stabilizers act via different mechanisms, causing different interactions in rats and human patients.

Additionally, the levels of lithium and VPA were measured in the blood plasma, collected from the rats at the time of sacrifice. **Figure 26** displays the values for the first cohort of rats. The measured drug treatment values were not within the therapeutic range for majority of the rats (Lithium: 0.5 – 1.1 mmol/L and VPA: 350-700 umol/L). There was only one exception in the lithium treatment group where rat#13 was within the therapeutic range. However, in the second cohort of rats, upon sacrificing and collecting blood 4 hours earlier, with no other exceptions in the methodology, it was observed that the blood plasma levels of lithium were within the therapeutic range for all of the rats, with one exception (**Figure 33**). The levels of VPA were also closer to the therapeutic range in comparison to the first cohort. As a result, the findings from cohort 1 remain valid since it appears that the

levels of drug treatments observed in that group were due to delay in collecting blood, and not due to other variables.

In the first cohort of rats, it was observed that lithium drug administration significantly increased mRNA expression of both MANF and CDFN in the pre-frontal cortex (**Figure 27**). This is an interesting observation because several *in vivo* studies with human BD patients have also found impairments in neuronal integrity in the pre-frontal cortex (Winsberg et al., 2000, Chang et al., 2003). Given that both MANF and CDFN play an important neuroprotective role, and lithium is the most commonly prescribed mood stabilizer for BD patients, it is suggestive that these drug treatments potentially alleviate BD symptoms by increasing the expression of these neurotrophic factors in the impaired PFC. For a future study, it would be interesting to observe whether these mood stabilizers directly affect the mRNA expression of MANF and CDFN in an *in vivo* study of BD patients (see Chapter 4).

Additionally, lithium treatment also increased mRNA expression of MANF in rat cortex (**Figure 30**). However, the mRNA expression of the housekeeping gene – GAPDH, was also significantly increased by lithium in the rat cortex (**Figure 31**). As a result, the increase in MANF mRNA expression in rat cortex is insignificant. The mRNA expression of GAPDH was not significantly different in the other brain regions as a result of the drug treatment. This suggests that lithium is impacting the mRNA levels of GAPDH differently in the brain regions. It would be beneficial to examine the mRNA levels of another gene such as cyclophilin, in rat cortex, as a means of using it as a different housekeeping gene for comparison. MANF and CDFN mRNA expression was not significantly affected by

lithium and VPA drug treatments in the rat striatum and hippocampus (**Figures 28 – 29**). Similarly, in the second cohort of rats, the mRNA expression of both genes was unaffected by lithium and VPA treatment in the rat hippocampus and striatum (**Figures 38 – 39**).

However, the findings from the first cohort, with respect to the cortex and PFC, were not replicated in the second cohort of rats. In contrast to the initial results, treatment with lithium significantly decreased mRNA expression level of MANF in the PFC (**Figure 37**). Additionally, VPA administration significantly decreased both MANF and CDFN mRNA expression in the PFC (**Figures 36 – 37**). Surprisingly, lithium administration in the cortex also significantly decreased MANF mRNA expression (**Figure 40**). However, similar to the last cohort, the mRNA expression of GAPDH was significantly increased by lithium administration in the cortex (**Figure 45b**). This validates the earlier hypothesis that lithium affects GAPDH mRNA expression differently in the brain regions. Consequently, it is important to determine another housekeeping gene that does not change as a result of the drug treatments, allowing us to validate our cortex MANF findings in the future.

It is imperative to repeat this experiment under controlled conditions, such that it allows us to determine whether these mood stabilizers truly increase or decrease the mRNA expression levels of these neurotrophic factors. Unlike the results observed in the *in vitro* model of differentiated *SH-SY5Y* cells, it appears that lithium and VPA do not have similar effects on the expression of CDFN and MANF. It is possible that the differences in results occurred due to other internal variables such as stress levels. Additionally, the mRNA expression levels of the two neurotrophic factors were also analysed in two other brain regions – mPFC and amygdala. However, similar to the rat hippocampus and striatum, no

significant differences were observed in these brain regions (**Figures 41 – 42**). Furthermore, the levels of GAPDH mRNA expression was not affected in other brain regions, including PFC, mPFC, hippocampus, amygdala, and striatum (**Figures 43, 44, 45a**).

Upon conducting behavioural tests, it was observed that there were no significant differences in locomotion and rearing behavior in rats treated with lithium and VPA (**Figures 34 – 35**). These results are consistent with what we expected as these rats were normal Sprague Dawley strain and not a manic or depressive model of BD. For future studies, it would be beneficial to administer these drug treatments and conduct behavioural tests in a manic or depressive model of BD. This will allow us to gain a better understanding of the effects of these mood stabilizers in the BD population. Additionally, in order to validate the mRNA expression findings, it will be beneficial to analyze the levels of ER stress proteins – GRP78 and GRP94 – in these rat brain regions, in response to drug administration.

Chapter 4

Investigation of Neurotrophic Factors *in vivo* in whole blood samples from Bipolar disorder patients and healthy controls

4.1 Objective

Investigating CDNF, MANF, and GAPDH mRNA expression in whole blood samples from BD patients and age-matched and gender-matched healthy controls

The objective of this study is to determine whether bipolar disorder patients have an altered expression of neurotrophic factors when compared to healthy individuals. Given the findings from the *in vitro* SH-SY5Y cell model, determining a similar correlation between the human BD patients will allow us to validate that the *in vitro* model is a strong predictor of how NTFs expression exists in this neuropsychiatric disorder. For the clinical population, the levels of NTFs mRNA expression will be measured in their blood samples. This study aims to determine the levels of CDNF, MANF, and GAPDH mRNA expression levels in different patient populations including BD adults, BD children, and at risk children, compared to healthy adults and healthy children respectively. It is expected that BD patients will have an elevated level of CDNF and MANF mRNA expression in their blood samples as a result of the mood stabilizers being prescribed to them. It is also expected that the levels of GAPDH mRNA expression will not alter between different patient groups.

4.2 Materials and Methodology

4.2.1 Blood Samples Collection and Preparation

For the clinical studies, whole blood samples were collected from healthy adults and healthy children, as well as patient populations including BD adults, BD children, and children at risk of developing BD. The RNA was then extracted and DNase treated using the PAXgene Blood RNA Kit (Qiagen, Catalog# 762164). The blood collection and RNA extraction was conducted by members of Dr. Frey's laboratory at St. Joseph's HealthCare, Hamilton, ON, Canada.

4.2.2 cDNA Synthesis from Blood RNA

The DNase-treated RNA was then converted to complementary DNA (cDNA) by reverse transcription (RT) using the qScript cDNA SuperMix (QuantaBio, Catalog# 95048-100). During cDNA synthesis, negative RT controls were also created for randomly chosen samples by using the DNase-treated RNA without the addition of reverse transcriptase enzyme. This acted as a verification for the RT-PCR specificity as well as a check for any DNA contamination. All of the reactions occurred at the following thermal profile conditions: 5 minutes at 25°C, followed by 30 minutes at 42°C, and lastly 5 minutes at 85°C, with a final hold at 4°C.

4.2.3 Reverse Transcription PCR (RT-PCR)

The CDNF, MANF, and GAPDH gene amplicons were detected by amplifying 50 ng of RT product using the Invitrogen Platinum Taq High Fidelity DNA Polymerase (Catalog #: 11304-111) with appropriate primers (listed in **Table 3**). The PCR

amplifications were conducted under the following parameters: initial denaturation at 94°C for 2 minutes 30 seconds, followed with 40 cycles of 94°C for 30 seconds, 57°C for 30 seconds, and 72°C for 40 seconds. The amplification ended with a final extension for 7 minutes at 72°C. The primers for MANF, CDNF, and GAPDH were synthesized at MOBIX lab facility (McMaster University, Hamilton, ON), and verified using gel electrophoresis by running the PCR product on a 1.5% agarose gel. The bands of interest were then sent for sequencing at the McMaster MOBIX lab. The primers listed in **Table 3** were used for the RT-PCR analysis. Representative RT-PCR products showed 100% homology with the genes of interest – human CDNF, MANF, and GAPDH. Concentration of the gene amplicons were then quantified and used for making the absolute standard curve dilutions when running the quantitative RT-PCR.

4.2.4 Real-Time Quantitative Reverse Transcription Polymerase Chain Reaction (RT-qPCR)

The mRNA expression for CDNF, MANF, and GAPDH was quantified using RT-qPCR with QuantiFast SYBR Green fluorescent dye PCR kit (Qiagen, Catalog# 204056). The primers listed in **Table 3** were used for the RT-qPCR analysis. The RT-qPCR was used to determine absolute copy numbers of CDNF, MANF, and GAPDH mRNA in the whole blood samples from human patient populations. The GAPDH mRNA expression was used as an internal control. For MANF and GAPDH, the cDNA from the human blood samples was amplified in triplicates for each sample, using Stratagene MX3000P cycler with an initial PCR activation step at 95°C for 5 minutes. Next, the cDNA was denatured through 40 cycles of denaturation at 95°C for 10 seconds, followed by a combined

annealing and extension step for 30 seconds at 60°C. This was followed by melting curve analysis where the qPCR produced a single peak for each product. This allowed for verification of the PCR specificity for each product. Each reaction had a volume of 25µl containing 60ng of total RNA. An absolute standard curve was generated using varying concentrations of cDNA ranging from 1pg to 10ag with 10-fold serial dilutions. Real-time RT-PCR conditions were optimized to ensure amplifications efficiencies remained constant over the course of the run. Components of the RT-qPCR reaction mix were as follows: 12.5ul of QuantiFAST SYBR green (QIAGEN), 5µl each of the 5µM MANF and GAPDH forward and reverse primers (described in **Table 1**), 2µl of sample cDNA, and 0.5µl of nuclease-free water to a final volume of 25µl. For CDNF, one-step RT-qPCR was conducted where 60 ng of RNA was amplified with the primers listed in **Table 3**, under the following conditions: 50°C for 30 minutes (1 cycle), 95°C for 15 minutes (1 cycle), followed by 40 cycles of 94°C for 15 seconds, 52°C for 30 seconds, and 72°C for 45 seconds, and lastly 95°C for 1 minute (1 cycle).

4.2.5 Statistical Analysis

For the human blood samples, the absolute copy numbers of CDNF, MANF, and GAPDH between control groups and patient populations were analyzed. MX3000P software performs analysis of data obtained by the RT-qPCR to quantify the copy number of the target sequence in each sample by comparing it with the standard curve copy numbers. Real-Time PCR experiments were performed in triplicates which were averaged prior to analysis. The whole blood samples results were categorized dependent on gender and three different age groups: <21 years old, 21 – 49 years old, and 49+ years old. This

allowed for the qPCR results to be age-matched and gender-matched between the different patient populations. All statistical analyses were conducted using the GraphPad Prism 6.0 software (GraphPad Software, San Diego, California, USA). Outlier detection was performed prior to analyses using GraphPad Outlier Tool. One-way analysis of variance (ANOVA) with Tukey's post-hoc test was conducted to determine significance between groups, and a p-value of ($p < 0.05$) was considered statistically significant. Data shown is expressed as mean \pm standard deviation (S.D.).

Primer Sequence (5' → 3')	Product Size	Accession Number
CDNF Fwd: AAAGACGCAGCCACAAAGAT	188 bp*	NM_001029954.2
CDNF Rev: AGGATCTGCTTCAGCTCTGC		
MANF Fwd: TCACATTCTCACCAGCCACT	236 bp**	NM_006010.5
MANF Rev: CAGGTCGATCTGCTTGTCATAC		
GAPDH Fwd: GAGTCAACGGATTTGGTCGT	238 bp	NM_001289745.1
GAPDH Rev: TTGATTTTGGAGGGATCTCG		

Table 3. Forward and reverse primer sequences for human samples.

These primers were used for RT-PCR and RT-qPCR analysis of CDNF, MANF, and GAPDH genes in human blood samples. **CDNF primers as designed by Asim Siddiqi for One-step RT-qPCR.* ***MANF primers as described by Cheng et al., 2014.* (bp – base pairs).

4.3 Human Blood Samples – RT qPCR Results

4.3.1 CDNF mRNA Expression in Blood

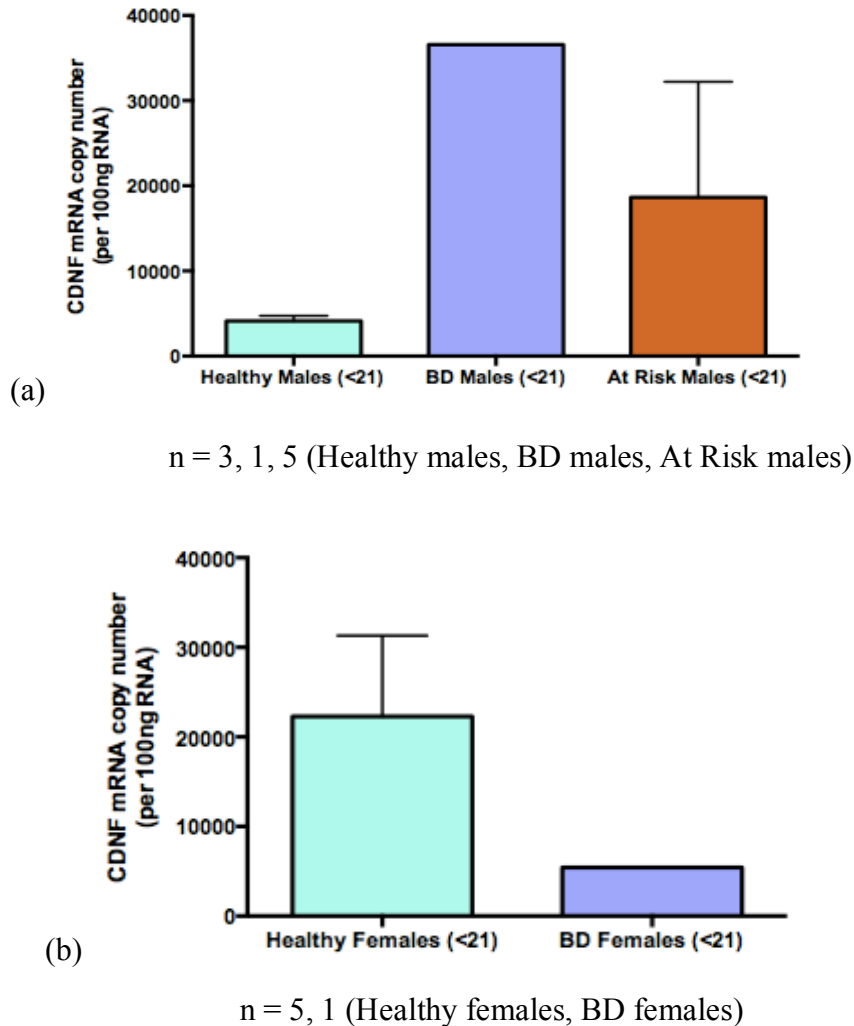


Figure 46. CDNF mRNA expression in human blood samples (<21 years).

One-step RT-qPCR to measure the mRNA CDNF expression in whole blood samples from healthy controls and BD patient populations under the age of 21 years. (a) males (b) females. Y-axis displays the absolute copy number of CDNF in the samples, per 100 ng of RNA. Sample Size (Healthy controls, BD patients, At Risk Children) (a)3, 1, 5 and (b)5, 1.

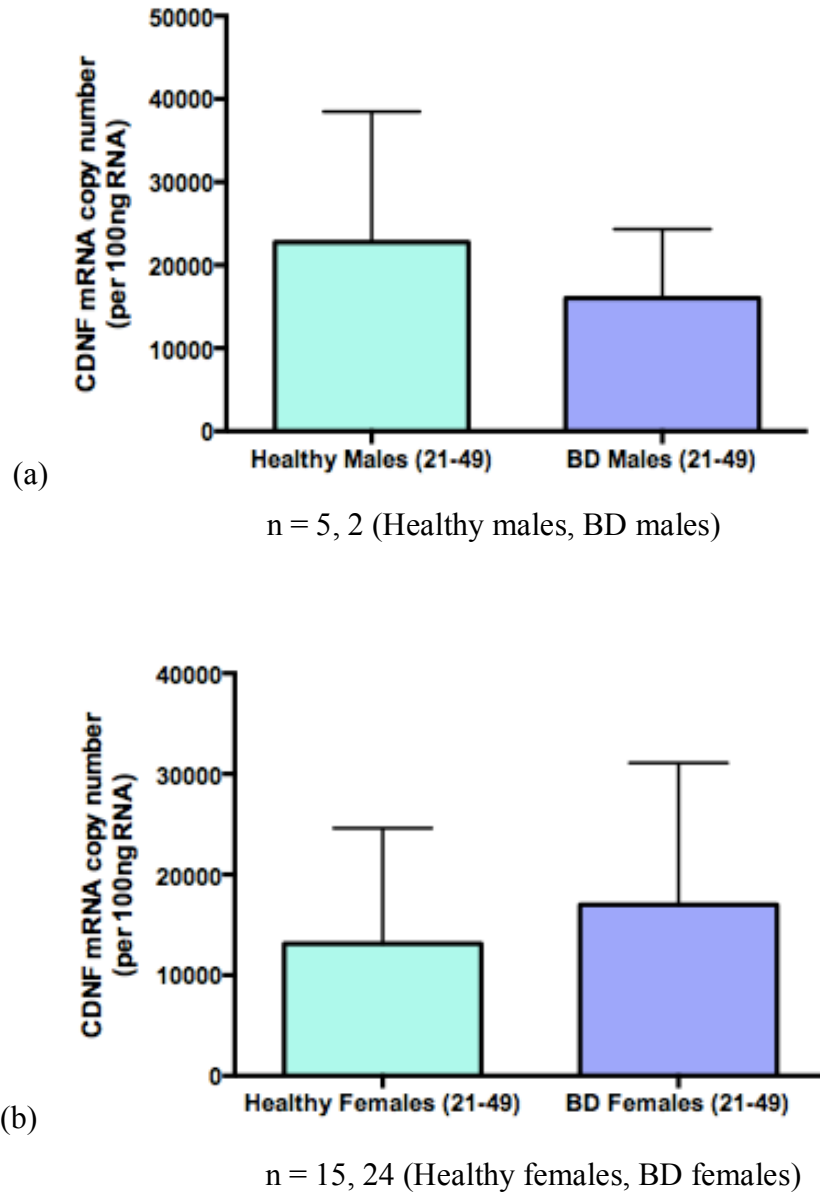


Figure 47. CDNF mRNA expression in human blood samples (21 – 49 years).

One-step RT-qPCR to measure the mRNA CDNF expression in whole blood samples from healthy controls and BD patient populations in the age range 21 – 49 years. (a) males (b) females. Y-axis displays the absolute copy number of CDNF in the samples, per 100 ng of RNA. Sample Size (Healthy controls, BD patients) (a): 5, 2 and (b) 15, 24.

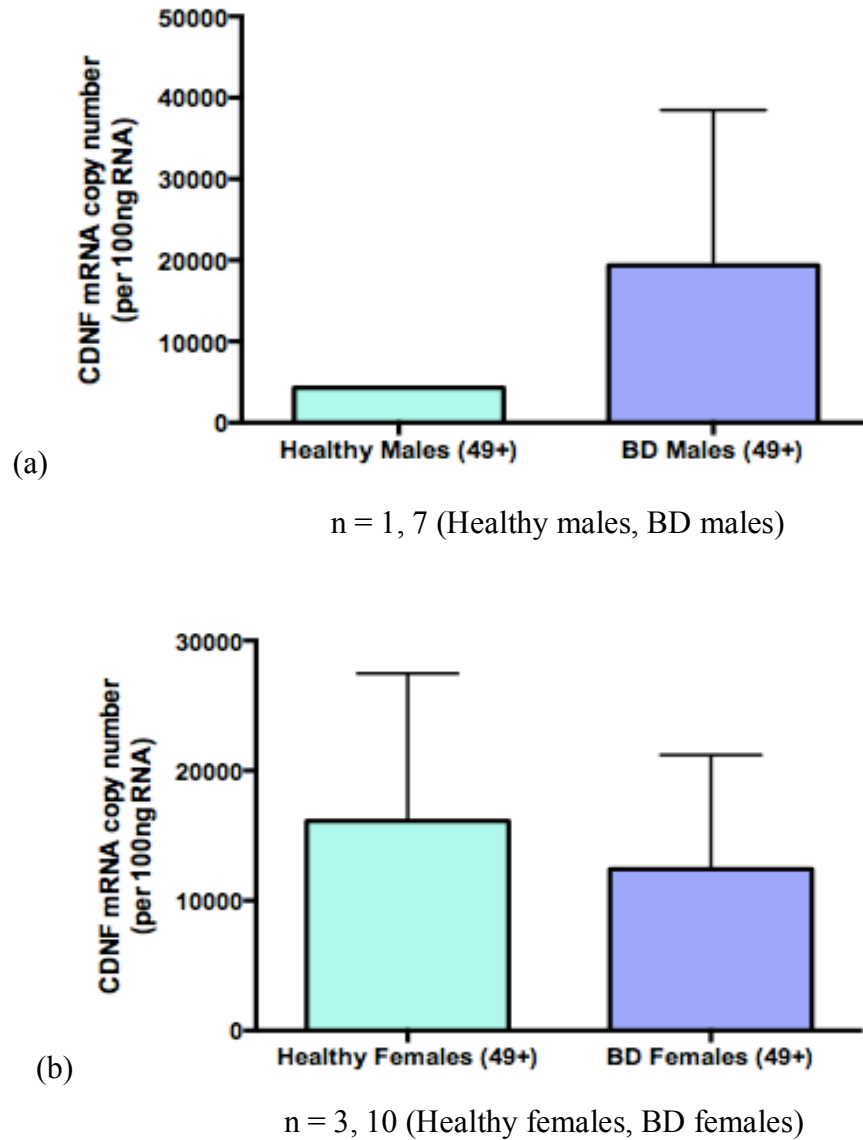


Figure 48. CDNF mRNA expression in human blood samples (49+ years).

One-step RT-qPCR to measure the mRNA CDNF expression in whole blood samples from healthy controls and BD patient populations over the age of 49 years. (a) males (b) females.

Y-axis displays the absolute copy number of CDNF in the samples, per 100 ng of RNA.

Sample Size (Healthy controls, BD patients) (a): 1, 7 and (b) 3, 10.

4.3.2 MANF mRNA Expression in Blood

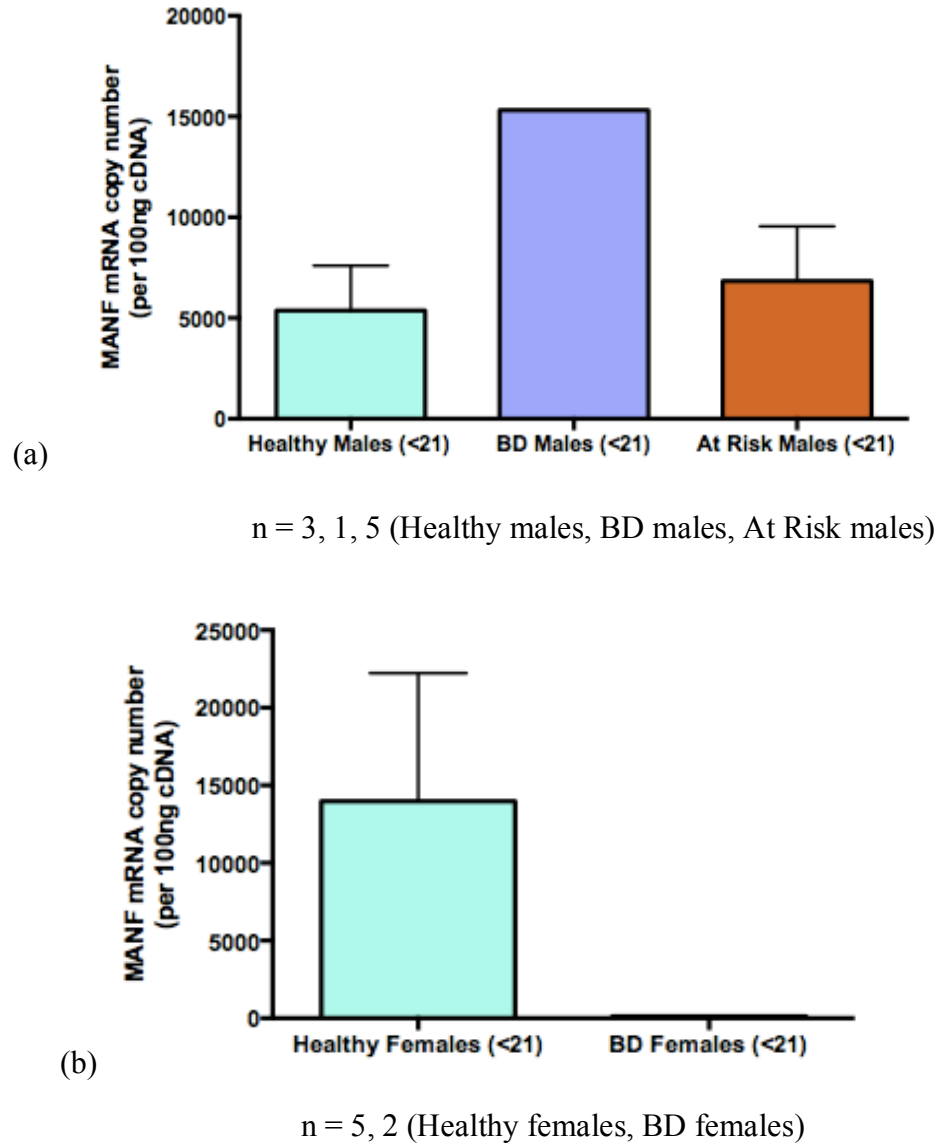


Figure 49. MANF mRNA expression in human blood samples (<21 years).

Two-step RT-qPCR to measure the mRNA expression of MANF in whole blood samples from healthy controls and BD patient populations. (a) males and (b) females. Y-axis displays the absolute copy number of MANF in the samples, per 100 ng of RNA. Sample Size (Healthy controls, BD patients, At Risk Children) (a): 3, 1, 5 and (b) 5, 2.

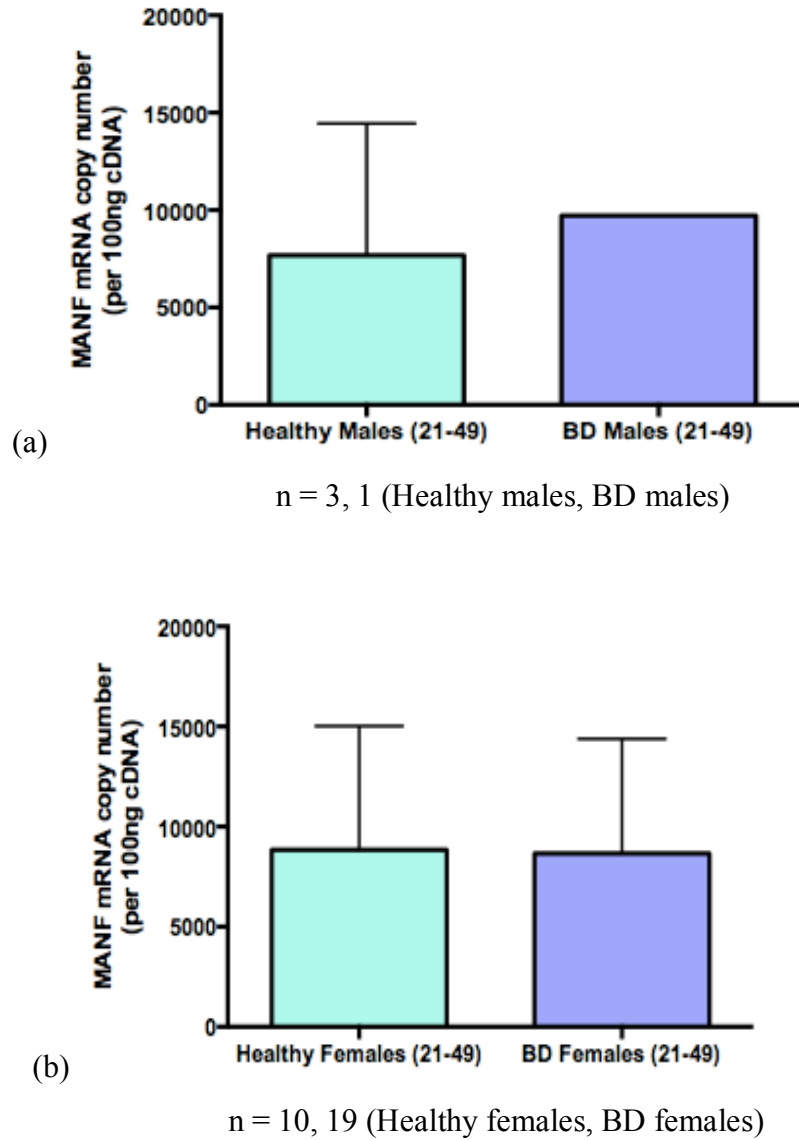


Figure 50. MANF mRNA expression in human blood samples (21 – 49 years).

Two-step RT-qPCR to measure the MANF mRNA expression in whole blood samples from healthy controls and BD patient populations, in the age range 21 – 49 years. (a) males (b) females. Y-axis displays the absolute copy number of MANF in the samples, per 100 ng of RNA. Sample Size (Healthy controls, BD patients) (a): 3, 1 and (b) 10, 19.

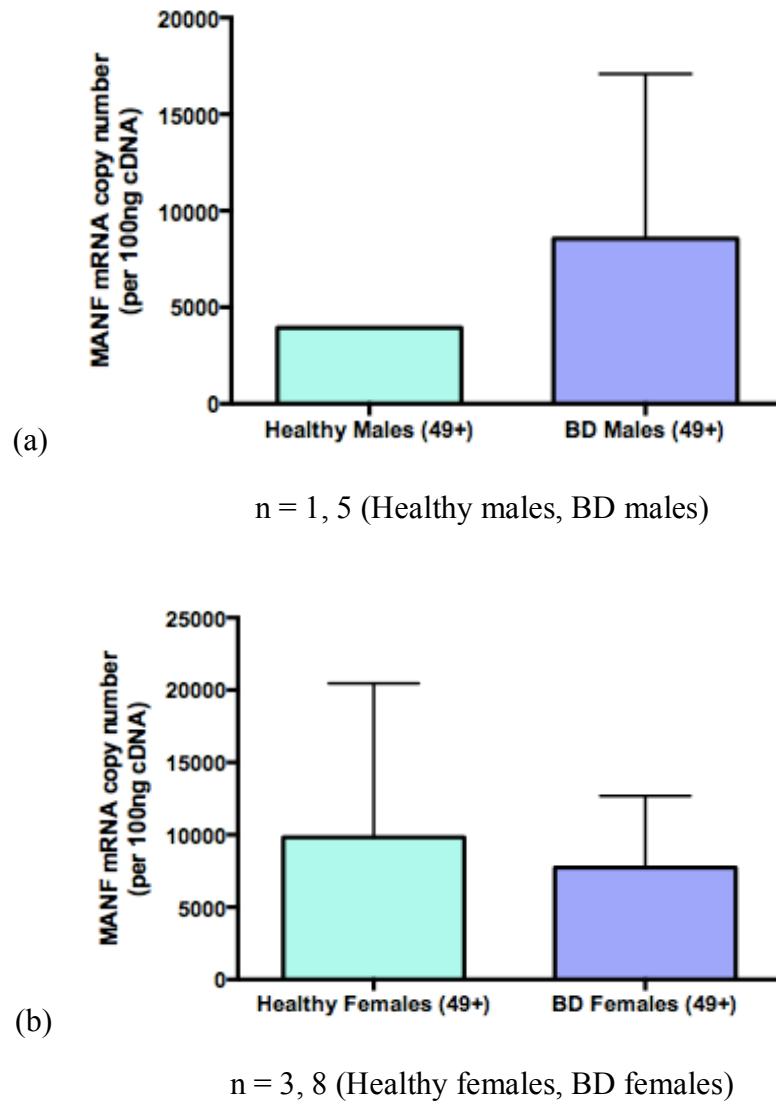


Figure 51. MANF mRNA expression in human blood samples (49+ years).

Two-step RT-qPCR to measure the MANF mRNA expression in whole blood samples from healthy controls and BD patient populations, over the age of 49 years. (a) males (b) females.

Y-axis displays the absolute copy number of MANF in the samples, per 100 ng of RNA.

Sample Size (Healthy controls, BD patients) (a): 1, 5 and (b) 3, 8.

4.3.3 GAPDH mRNA Expression in Blood

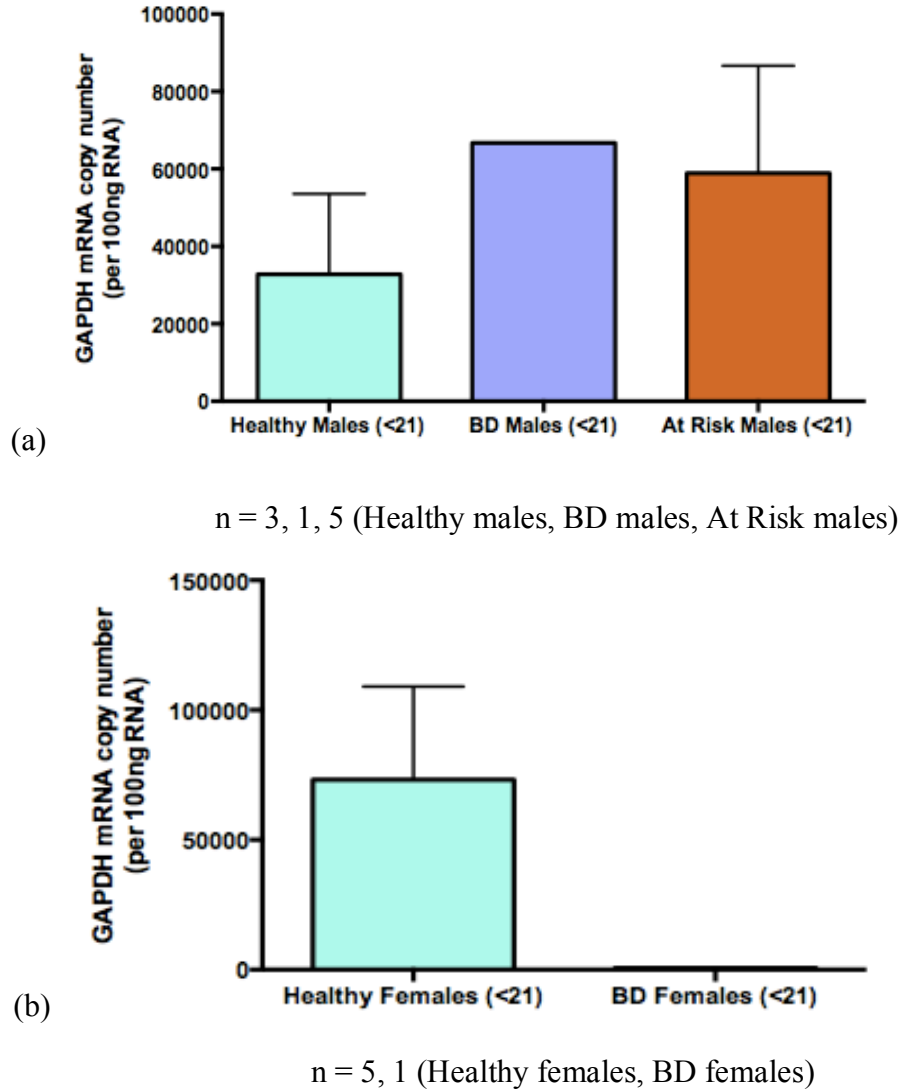


Figure 52. GAPDH mRNA expression in human blood samples (<21 years).

Two-step RT-qPCR to measure the mRNA expression of GAPDH in whole blood samples from healthy controls and BD patient populations. (a) males and (b) females. Y-axis displays the absolute copy number of GAPDH in the samples, per 100 ng of RNA. Sample Size (Healthy controls, BD patients, At Risk Children) (a): 3, 1, 5 and (b) 5, 1.

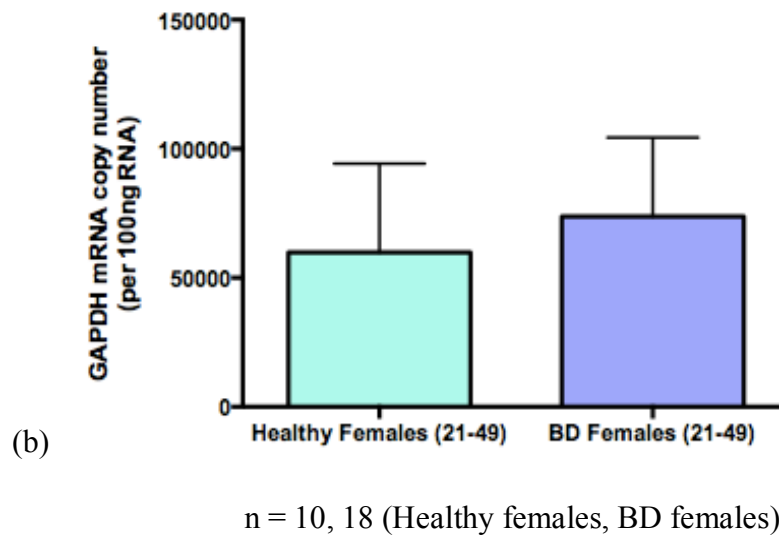
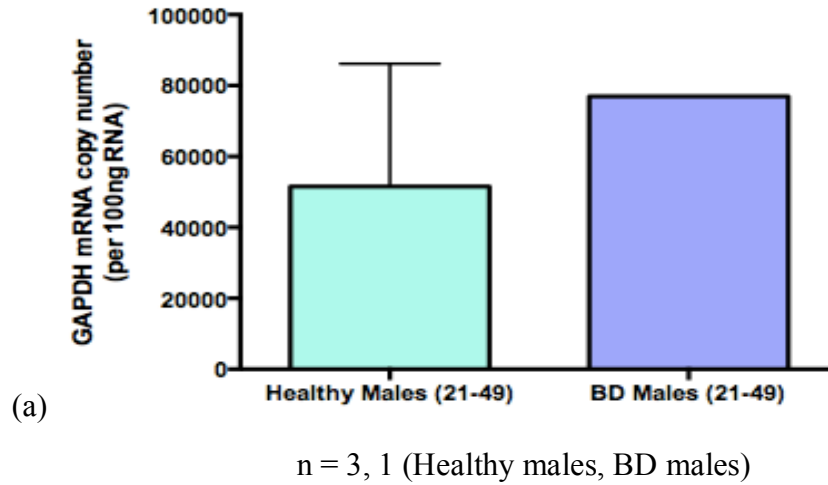
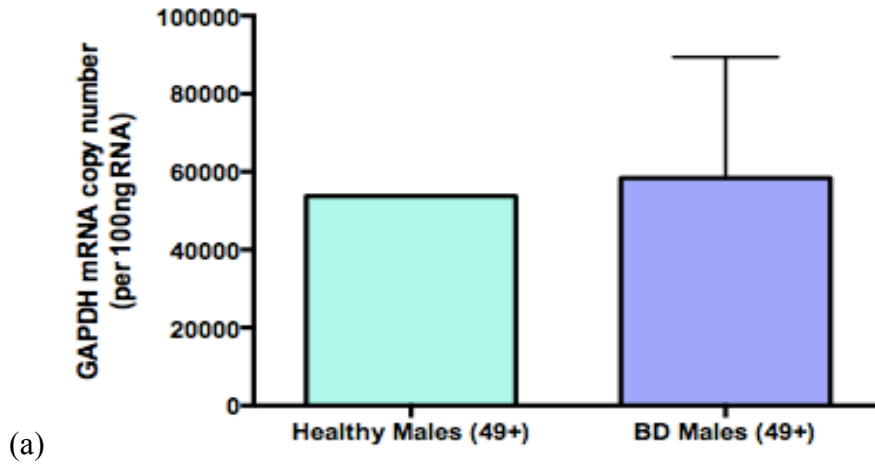
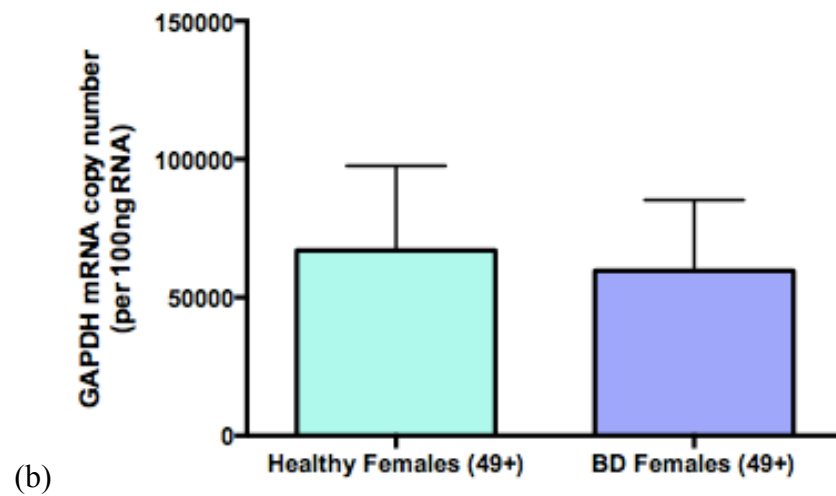


Figure 53. GAPDH mRNA expression in human blood samples (21 – 49 years).

Two-step RT-qPCR to measure the GAPDH mRNA expression in whole blood samples from healthy controls and BD patient populations, in the age range 21 – 49 years. (a) males (b) females. Y-axis displays the absolute copy number of GAPDH in the samples, per 100 ng of RNA. Sample Size (Healthy controls, BD patients) (a): 3, 1 and (b) 10, 18.



n = 1, 5 (Healthy males, BD males)



n = 3, 8 (Healthy females, BD females)

Figure 54. GAPDH mRNA expression in human blood samples (49+ years).

Two-step RT-qPCR to measure the GAPDH mRNA expression in whole blood samples from healthy controls and BD patient populations, over the age of 49 years. (a) males (b) females. Y-axis displays the absolute copy number of GAPDH in the samples, per 100 ng of RNA. Sample Size (Healthy controls, BD patients) (a): 1, 5 and (b) 3, 8.

4.4 Discussion

Given the findings in chapter 2, we know that lithium and VPA treatments significantly increase the mRNA expression of MANF and CDNF *in vitro*. Additionally, several studies have established the role of CDNF and MANF as ER-stress proteins. Lithium and VPA act by upregulating ER chaperones that are decreased in BD patients, including GRP78 and GRP94 (Hayashi et al., 2009). MANF also interacts with these chaperones as well as precursor genes to induct GRP78 (Glembotski et al., 2012). Thus, both the mood stabilizers and neurotrophic factors act in similar ways to reduce ER stress. It was hypothesized that lithium and VPA potentially alleviate BD symptoms by regulating the impaired ER-stress response in BD patients.

In order to determine whether expression of neurotrophic factors is altered *in vivo* as a result of the diseased condition or drug treatments, the mRNA expression of CDNF, MANF, and GAPDH was analysed in whole blood samples from BD patients. Upon matching the results based on gender and age groups, it was observed that neither males or females in any of the age groups have a significant change in their mRNA expression of CDNF, MANF, or GAPDH (**Figures 46 – 54**). These findings are not aligned with the results observed *in vitro*. It was expected that since BD patients are prescribed several mood stabilizers and anticonvulsants including lithium and VPA, the levels of their neurotrophic factors will be altered accordingly. However, one explanation for the insignificant changes in the neurotrophic factors expression is due to the multitude of drug combinations that BD patients are prescribed. In comparison to the *in vitro* study, it is

difficult to find BD patients on monotherapy of lithium or VPA. Consequently, it is possible that these drug treatments act in a similar manner *in vivo*, however, there are drug interactions occurring *in vivo*, causing a change in the effect of lithium and VPA on CDFN and MANF expression.

Several studies have suggested a potential role of increased intracellular calcium concentration in the pathophysiology of BD. In a study conducted *in vivo*, it was observed that platelets and lymphocytes from BD patients had elevated levels of intracellular Ca^{2+} compared to healthy controls (Dubovsky et al., 1992, Emamghoreishi et al., 1997). BD patients also have abnormal phosphatidylinositol (PI) signalling which then results in elevated levels of intracellular Ca^{2+} (Atack et al., 1995, Belmaker et al., 1998). However, lithium regulates the PI signalling cascade by inhibiting enzyme inositol monophosphatase, as well as levels of inositol triphosphate (IP_3) in order to reduce intracellular $[\text{Ca}^{2+}]$ (Atack et al., 1995). IP_3 causes release of Ca^{2+} stores by binding to its surface receptor on the ER. Additionally, it has been suggested that VPA acts on reducing the intracellular $[\text{Ca}^{2+}]$ by inducing ER stress proteins which increase the Ca^{2+} -binding capacity of the ER (Bown et al., 2002). Thus, the regulation of intracellular calcium concentration is another potential mechanism of regulating symptoms in BD. Additionally, MANF also interacts in a calcium-dependent manner in the ER with the ER-stress proteins such as GRP78 (Glembotski et al., 2012, Henderson et al., 2013). Thus it was expected that potentially the drug treatments of lithium and VPA interact with these NTFs to reduce intracellular $[\text{Ca}^{2+}]$, and reduce ER stress in BD patients.

Additionally, one of the major limitations of this study exists in the small sample size of patients. It will be beneficial to increase the human patients sample size in order to determine significant trends. Furthermore, it will be interesting to observe the mRNA expression levels of MANF and CDFN in drug-naïve and at risk populations, as well as patients from a wider age range. This will allow us to determine whether CDFN and MANF can potentially also act as markers to consider when diagnosing patients, as well as while designing therapeutic treatments. Additionally, observing the changes in various age groups will allow us to determine the interaction between these drugs and age-dependent changes in NTFs expression. It will also be useful to determine the protein expression of these neurotrophic factors in the patient populations.

4.5 Conclusion

We have shown that mood stabilizers Lithium and VPA increase *in vitro* mRNA expression of MANF and CDFN. Both of these neurotrophic factors play a role in the ER-stress response pathway, by regulating expression of ER-stress proteins to prevent cell damage and apoptosis. Since BD patients have shown impairments in their ER stress response, it is suggestive that mood stabilizers act on these neurotrophic factors as a mechanism of action. Additionally, our *in vivo* studies with rats treated with mood stabilizers provided incongruent findings. The levels of MANF and CDFN expression were altered in the PFC and cortex. It appears that these mood stabilizers impact neurotrophic factors expression in brain regions shown to have impairments in BD. Thus it is important to further examine the role of these neurotrophic factors in an *in vivo* model. Furthermore, the results from the mRNA expression in human blood samples remain inconclusive due to limited sample size. However, it will be beneficial to determine whether drug-naïve, and at risk BD patient populations express decreased levels of NTFs due to their diseased biological condition. This decrease is then compensated for by their drug treatments. These findings can play a vital role in determining new therapeutic targets for the treatment of BD.

References

- Abukhdeir, A. M., Layden, B. T., Minadeo, N., Bryant, F. B., Stubbs, E. B., & De Freitas, D. M. (2003). Effect of chronic Li⁺ treatment on free intracellular Mg²⁺ in human neuroblastoma SH-SY5Y cells. *Bipolar disorders*, 5(1), 6-13.
- Airaksinen, M. S., & Saarma, M. (2002). The GDNF family: signalling, biological functions and therapeutic value. *Nature Reviews Neuroscience*, 3(5), 383-394.
- Apostolou, A., Shen, Y., Liang, Y., Luo, J., & Fang, S. (2008). Armet, a UPR-upregulated protein, inhibits cell proliferation and ER stress-induced cell death. *Experimental cell research*, 314(13), 2454-2467.
- Aron, L., & Klein, R. (2011). Repairing the parkinsonian brain with neurotrophic factors. *Trends in neurosciences*, 34(2), 88-100.
- Arun, P., Madhavarao, C. N., Moffett, J. R., & Namboodiri, A. (2008). Antipsychotic drugs increase N-acetylaspartate and N-acetylaspartylglutamate in SH-SY5Y human neuroblastoma cells. *Journal of neurochemistry*, 106(4), 1669-1680.
- Atack, J. R., Broughton, H. B., & Pollack, S. J. (1995). Inositol monophosphatase—a putative target for Li⁺ in the treatment of bipolar disorder. *Trends in neurosciences*, 18(8), 343-349.
- Autry, A. E., & Monteggia, L. M. (2012). Brain-derived neurotrophic factor and neuropsychiatric disorders. *Pharmacological reviews*, 64(2), 238-258.

- Belmaker, R. H., Agam, G., van Calker, D., Richards, M. H., & Kofman, O. (1998). Behavioral reversal of lithium effects by four inositol isomers correlates perfectly with biochemical effects on the PI cycle: depletion by chronic lithium of brain inositol is specific to hypothalamus, and inositol levels may be abnormal in postmortem brain from bipolar patients. *Neuropsychopharmacology*, 19(3), 220-232.
- Biton, V., Mirza, W., Montouris, G., Vuong, A., Hammer, A. E., & Barrett, P. S. (2001). Weight change associated with valproate and lamotrigine monotherapy in patients with epilepsy. *Neurology*, 56(2), 172-177.
- Chang, K., Adleman, N., Dienes, K., Barnea-Goraly, N., Reiss, A., & Ketter, T. (2003). Decreased N-acetylaspartate in children with familial bipolar disorder. *Biological psychiatry*, 53(11), 1059-1065.
- Chen, G., Huang, L. D., Jiang, Y. M., & Manji, H. K. (2000). The mood-stabilizing agent valproate inhibits the activity of glycogen synthase kinase-3. *Journal of neurochemistry*, 72(3), 1327-1330.
- Chen, Y. C., Sundvik, M., Rozov, S., Priyadarshini, M., & Panula, P. (2012). MANF regulates dopaminergic neuron development in larval zebrafish. *Developmental biology*, 370(2), 237-249.

- Cheng, L., Zhao, H., Zhang, W., Liu, B., Liu, Y., Guo, Y., & Nie, L. (2013). Overexpression of conserved dopamine neurotrophic factor (CDNF) in astrocytes alleviates endoplasmic reticulum stress-induced cell damage and inflammatory cytokine secretion. *Biochemical and biophysical research communications*, 435(1), 34-39.
- Cheng, Q., Wang, X., Shen, Y., Shen, Y., Zu, B., Xu, J., ... & Wang, J. (2014). Deficiency of IRE1 and PERK signal pathways in systemic lupus erythematosus. *The American journal of the medical sciences*, 348(6), 465-473.
- Cheung, Y. T., Lau, W. K. W., Yu, M. S., Lai, C. S. W., Yeung, S. C., So, K. F., & Chang, R. C. C. (2009). Effects of all-trans-retinoic acid on human SH-SY5Y neuroblastoma as in vitro model in neurotoxicity research. *Neurotoxicology*, 30(1), 127-135.
- Cordero-Llana, Ó., Houghton, B. C., Rinaldi, F., Taylor, H., Yáñez-Muñoz, R. J., Uney, J. B., ... & Caldwell, M. A. (2015). Enhanced efficacy of the CDFN/MANF family by combined intranigral overexpression in the 6-OHDA rat model of Parkinson's disease. *Molecular Therapy*, 23(2), 244-254.
- Correll, C. U. (2007). Weight gain and metabolic effects of mood stabilizers and antipsychotics in pediatric bipolar disorder: a systematic review and pooled analysis of short-term trials. *Journal of the American Academy of Child & Adolescent Psychiatry*, 46(6), 687-700.
- Cousins, D. A., Butts, K., & Young, A. H. (2009). The role of dopamine in bipolar disorder. *Bipolar disorders*, 11(8), 787-806.

- Daniel, E. Di, Mudge, A. W., & Maycox, P. R. (2005). Comparative analysis of the effects of four mood stabilizers in SH-SY5Y cells and in primary neurons. *Bipolar Disorders*, 7(1), 33–41.
- Dereeper, A., Guignon, V., Blanc, G., Audic, S., Buffet, S., Chevenet, F., ... & Claverie, J. M. (2008). Phylogeny. fr: robust phylogenetic analysis for the non-specialist. *Nucleic acids research*, 36(suppl 2), W465-W469.
- Dilsaver, S. C., Chen, Y. W., Swann, A. C., Shoaib, A. M., & Krajewski, K. J. (1994). Suicidality in patients with pure and depressive mania. *The American Journal of Psychiatry*, 151(9), 1312-1315.
- Dubovsky, S. L., & Murphy, J. (1992). Abnormal intracellular calcium ion concentration in platelets and lymphocytes of bipolar patients. *The American Journal of Psychiatry*, 149(1), 118.
- Emamghoreishi, M., Schlichter, L., Li, P. P., Parikh, S., Sen, J., Kamble, A., & Warsh, J. J. (1997). High intracellular calcium concentrations in transformed lymphoblasts from subjects with bipolar I disorder. *American Journal of Psychiatry*, 154(7), 976-982.
- Encinas, M., Iglesias, M., Liu, Y., Wang, H., Muhaisen, A., Cena, V., ... & Comella, J. X. (2000). Sequential treatment of SH-SY5Y cells with retinoic acid and brain-derived neurotrophic factor gives rise to fully differentiated, neurotrophic factor-dependent, human neuron-like cells. *Journal of neurochemistry*, 75(3), 991-1003.

- Frey, B. N., Andreazza, A. C., Houenou, J., Jamain, S., Goldstein, B. I., Frye, M. A., ... & Young, L. T. (2013). Biomarkers in bipolar disorder: a positional paper from the International Society for Bipolar Disorders Biomarkers Task Force. *Australian and New Zealand journal of psychiatry*, 0004867413478217.
- Frey, B. N., Valvassori, S. S., Réus, G. Z., & Martins, M. R. (2006). Effects of lithium and valproate on amphetamine-induced oxidative stress generation in an animal model of mania. *Journal of psychiatry & neuroscience: JPN*, 31(5), 326.
- Geddes, J. R., Goodwin, G. M., Rendell, J., Azorin, J. M., Cipriani, A., Ostacher, M. J., ... & Juszczak, E. (2011). Lithium Plus Valproate Combination Therapy Versus Monotherapy for Relapse Prevention in Bipolar I Disorder (BALANCE): A Randomised Open-Label Trial. *Focus*, 9(4), 488-499.
- Geddes, J. R., & Miklowitz, D. J. (2013). Treatment of bipolar disorder. *The Lancet*, 381(9878), 1672-1682.
- Glembotski, C. C., Thuerlauf, D. J., Huang, C., Vekich, J. A., Gottlieb, R. A., & Doroudgar, S. (2012). Mesencephalic astrocyte-derived neurotrophic factor protects the heart from ischemic damage and is selectively secreted upon sarco/endoplasmic reticulum calcium depletion. *Journal of Biological Chemistry*, 287(31), 25893-25904.
- Goodwin, G.M. (2003). Evidence-based guidelines for treating bipolar disorder: recommendations from the British Association for Psychopharmacology. *Journal of Psychopharmacology*, 17, 149–173.

- Hartley, C. L., Edwards, S., Mullan, L., Bell, P. A., Fresquet, M., Boot-Handford, R. P., & Briggs, M. D. (2013). Armet/Manf and Creld2 are components of a specialized ER stress response provoked by inappropriate formation of disulphide bonds: implications for genetic skeletal diseases. *Human molecular genetics*, 22(25), 5262-5275.
- Hayashi, A., Kasahara, T., Kametani, M., Toyota, T., Yoshikawa, T., & Kato, T. (2009). Aberrant endoplasmic reticulum stress response in lymphoblastoid cells from patients with bipolar disorder. *International Journal of Neuropsychopharmacology*, 12(1), 33-43.
- Hellman, M., Arumäe, U., Yu, L. Y., Lindholm, P., Peränen, J., Saarna, M., & Permi, P. (2011). Mesencephalic astrocyte-derived neurotrophic factor (MANF) has a unique mechanism to rescue apoptotic neurons. *Journal of Biological Chemistry*, 286(4), 2675-2680.
- Henderson, M. J., Richie, C. T., Airavaara, M., Wang, Y., & Harvey, B. K. (2013). Mesencephalic astrocyte-derived neurotrophic factor (MANF) secretion and cell surface binding are modulated by KDEL receptors. *Journal of Biological Chemistry*, 288(6), 4209-4225.
- Hetz, C. (2012). The unfolded protein response: controlling cell fate decisions under ER stress and beyond. *Nature reviews Molecular cell biology*, 13(2), 89-102.
- Hoseki, J., Sasakawa, H., Yamaguchi, Y., Maeda, M., Kubota, H., Kato, K., & Nagata, K. (2010). Solution structure and dynamics of mouse ARMET. *FEBS letters*, 584(8), 1536-1542.

- Itano, Y., Ito, A., Uehara, T., & Nomura, Y. (1996). Regulation of Bcl-2 Protein Expression in Human Neuroblastoma SH-SY5Y Cells: Positive and Negative Effects of Protein Kinases C and A, Respectively. *Journal of neurochemistry*, 67(1), 131-137.
- Kakiuchi, C., Iwamoto, K., Ishiwata, M., Bundo, M., Kasahara, T., Kusumi, I., ... & Sasaki, T. (2003). Impaired feedback regulation of XBP1 as a genetic risk factor for bipolar disorder. *Nature genetics*, 35(2), 171-175.
- Keck Jr, P. E., McElroy, S. L., Strakowski, S. M., West, S. A., Sax, K. W., Hawkins, J. M., ... & Haggard, P. (2003). 12-month outcome of patients with bipolar disorder following hospitalization for a manic or mixed episode. *Focus*, 1(1), 44-52.
- Krishna, A., Biryukov, M., Trefois, C., Antony, P. M., Hussong, R., Lin, J., ... & May, P. (2014). Systems genomics evaluation of the SH-SY5Y neuroblastoma cell line as a model for Parkinson's disease. *BMC genomics*, 15(1), 1154.
- Kovalevich, J., & Langford, D. (2013). Considerations for the use of SH-SY5Y neuroblastoma cells in neurobiology. *Neuronal Cell Culture: Methods and Protocols*, 9-21.
- Kume, T., Kawato, Y., Osakada, F., Izumi, Y., Katsuki, H., Nakagawa, T., ... & Akaike, A. (2008). Dibutyl cyclic AMP induces differentiation of human neuroblastoma SH-SY5Y cells into a noradrenergic phenotype. *Neuroscience letters*, 443(3), 199-203.
- Latge, C., Cabral, K. M., De Oliveira, G. A., Raymundo, D. P., Freitas, J. A., Johanson, L., ... & Foguel, D. (2015). The solution structure and dynamics of full-length human cerebral dopamine neurotrophic factor and its neuroprotective role against α -synuclein oligomers. *Journal of Biological Chemistry*, 290(33), 20527-20540.

- Lee, A. H., Iwakoshi, N. N., & Glimcher, L. H. (2003). XBP-1 regulates a subset of endoplasmic reticulum resident chaperone genes in the unfolded protein response. *Molecular and cellular biology*, 23(21), 7448-7459.
- Lindahl, M., Danilova, T., Palm, E., Lindholm, P., Vöikar, V., Hakonen, E., ... & Rossi, J. (2014). MANF is indispensable for the proliferation and survival of pancreatic β cells. *Cell reports*, 7(2), 366-375.
- Lindahl, M., Saarma, M., & Lindholm, P. (2017). Unconventional neurotrophic factors CDNF and MANF: structure, physiological functions and therapeutic potential. *Neurobiology of Disease*, 97, 90-102.
- Lindholm, P., & Saarma, M. (2010). Novel CDNF/MANF family of neurotrophic factors. *Developmental neurobiology*, 70(5), 360-371.
- Lindholm, P., Peränen, J., Andressoo, J. O., Kalkkinen, N., Kokaia, Z., Lindvall, O., ... & Saarma, M. (2008). MANF is widely expressed in mammalian tissues and differently regulated after ischemic and epileptic insults in rodent brain. *Molecular and Cellular Neuroscience*, 39(3), 356-371.
- Lindholm P, Voutilainen MH, Lauren J, Peranen J, Leppanen VM, Andressoo JO, Lindahl M, et al. (2007). Novel neurotrophic factor CDNF protects and rescues midbrain dopamine neurons in vivo. *Nature*, 448, 73–77.
- Lindström, R., Lindholm, P., Kallijärvi, J., Yu, L. Y., Piepponen, T. P., Arumäe, U., ... & Heino, T. I. (2013). Characterization of the structural and functional determinants of MANF/CDNF in *Drosophila* in vivo model. *PloS one*, 8(9), e73928.

- Lopes, F. M., Schröder, R., da Frota Júnior, M. L. C., Zanotto-Filho, A., Müller, C. B., Pires, A. S., ... & Moreira, J. C. F. (2010). Comparison between proliferative and neuron-like SH-SY5Y cells as an in vitro model for Parkinson disease studies. *Brain research*, 1337, 85-94.
- López-Carballo, G., Moreno, L., Masiá, S., Pérez, P., & Baretino, D. (2002). Activation of the phosphatidylinositol 3-kinase/Akt signaling pathway by retinoic acid is required for neural differentiation of SH-SY5Y human neuroblastoma cells. *Journal of Biological Chemistry*, 277(28), 25297-25304.
- Mätlik, K., Yu, L. Y., Eesmaa, A., Hellman, M., Lindholm, P., Peränen, J., ... & Airavaara, M. (2015). Role of two sequence motifs of mesencephalic astrocyte-derived neurotrophic factor in its survival-promoting activity. *Cell death & disease*, 6(12), e2032.
- Mei, J. M., & Niu, C. S. (2014). Effects of CDNF on 6-OHDA-induced apoptosis in PC12 cells via modulation of Bcl-2/Bax and caspase-3 activation. *Neurological Sciences*, 35(8), 1275-1280.
- Melino, G., Thiele, C. J., Knight, R. A., & Piacentini, M. (1997). Retinoids and the control of growth/death decisions in human neuroblastoma cell lines. *Journal of neuro-oncology*, 31(1-2), 65-83.
- Mizobuchi, N., Hoseki, J., Kubota, H., Toyokuni, S., Nozaki, J. I., Naitoh, M., ... & Nagata, K. (2007). ARMET is a soluble ER protein induced by the unfolded protein response via ERSE-II element. *Cell structure and function*, 32(1), 41-50.

- Nagahara, A. H., & Tuszynski, M. H. (2011). Potential therapeutic uses of BDNF in neurological and psychiatric disorders. *Nature reviews Drug discovery*, *10*(3), 209-219.
- Niles, L. P., Sathiyapalan, A., Bahna, S., Kang, N. H., & Pan, Y. (2012). Valproic acid up-regulates melatonin MT1 and MT2 receptors and neurotrophic factors CDNF and MANF in the rat brain. *International Journal of Neuropsychopharmacology*, *15*(9), 1343-1350.
- Ösby, U., Brandt, L., Correia, N., Ekblom, A., & Sparén, P. (2001). Excess mortality in bipolar and unipolar disorder in Sweden. *Archives of general psychiatry*, *58*(9), 844-850.
- Påhlman, S., Ruusala, A. I., Abrahamsson, L., Mattsson, M. E., & Esscher, T. (1984). Retinoic acid-induced differentiation of cultured human neuroblastoma cells: a comparison with phorbol ester-induced differentiation. *Cell differentiation*, *14*(2), 135-144.
- Palgi, M., Lindström, R., Peränen, J., Piepponen, T. P., Saarma, M., & Heino, T. I. (2009). Evidence that DmMANF is an invertebrate neurotrophic factor supporting dopaminergic neurons. *Proceedings of the National Academy of Sciences*, *106*(7), 2429-2434.
- Palgi, M., Greco, D., Lindström, R., Auvinen, P., & Heino, T. I. (2012). Gene expression analysis of *Drosophila* Manf mutants reveals perturbations in membrane traffic and major metabolic changes. *BMC genomics*, *13*(1), 134.

- Parkash, V., Lindholm, P., Peränen, J., Kalkkinen, N., Oksanen, E., Saarma, M., ... & Goldman, A. (2009). The structure of the conserved neurotrophic factors MANF and CDFN explains why they are bifunctional. *Protein Engineering Design and Selection*, 22(4), 233-241.
- Petrova, P. S., Raibekas, A., Pevsner, J., Vigo, N., Anafi, M., Moore, M. K., ... & Durocher, Y. (2003). Manf. *Journal of Molecular Neuroscience*, 20(2), 173-187.
- Presgraves, S. P., Ahmed, T., Borwege, S., & Joyce, J. N. (2003). Terminally differentiated SH-SY5Y cells provide a model system for studying neuroprotective effects of dopamine agonists. *Neurotoxicity research*, 5(8), 579-598.
- Raykhel, I., Alanen, H., Salo, K., Jurvansuu, J., Nguyen, V. D., Latva-Ranta, M., & Ruddock, L. (2007). A molecular specificity code for the three mammalian KDEL receptors. *The Journal of cell biology*, 179(6), 1193-1204.
- Ryves, W. J., & Harwood, A. J. (2001). Lithium inhibits glycogen synthase kinase-3 by competition for magnesium. *Biochemical and biophysical research communications*, 280(3), 720-725.
- Sawada, M., Hayes, P., & Matsuyama, S. (2003). Cytoprotective membrane-permeable peptides designed from the Bax-binding domain of Ku70. *Nature cell biology*, 5(4), 352-357.
- Schmittgen, T. D., & Livak, K. J. (2008). Analyzing real-time PCR data by the comparative CT method. *Nature protocols*, 3(6), 1101-1108.
- Schneider, T., & Przewłocki, R. (2005). Behavioral alterations in rats prenatally exposed to valproic acid: animal model of autism. *Neuropsychopharmacology*, 30(1), 80-89.

- Shao, L., Sun, X., Xu, L., Young, L. T., & Wang, J. F. (2006). Mood stabilizing drug lithium increases expression of endoplasmic reticulum stress proteins in primary cultured rat cerebral cortical cells. *Life sciences*, 78(12), 1317-1323.
- Singh, T., & Rajput, M. (2006). Misdiagnosis of bipolar disorder. *Psychiatry (Edgmont)*, 3(10), 57.
- Strakowski, S. M., McElroy, S. L., Keck Jr, P. E., & West, S. A. (1996). Suicidality among patients with mixed and manic bipolar disorder. *The American journal of psychiatry*, 153(5), 674.
- Sullivan, A. M., & Toulouse, A. (2011). Neurotrophic factors for the treatment of Parkinson's disease. *Cytokine & growth factor reviews*, 22(3), 157-165.
- Szegezdi, E., Logue, S. E., Gorman, A. M., & Samali, A. (2006). Mediators of endoplasmic reticulum stress-induced apoptosis. *EMBO reports*, 7(9), 880-885.
- Tadimalla, A., Belmont, P. J., Thuerauf, D. J., Glassy, M. S., Martindale, J. J., Gude, N., ... & Glembotski, C. C. (2008). Mesencephalic astrocyte-derived neurotrophic factor is an ischemia-inducible secreted endoplasmic reticulum stress response protein in the heart. *Circulation research*, 103(11), 1249-1258.
- Tohen, M., Vieta, E., Calabrese, J., Ketter, T. A., Sachs, G., Bowden, C., ... & Evans, A. R. (2003). Efficacy of olanzapine and olanzapine-fluoxetine combination in the treatment of bipolar I depression. *Archives of general psychiatry*, 60(11), 1079-1088.
- Williams, R. S., Cheng, L., Mudge, A. W., & Harwood, A. J. (2002). A common mechanism of action for three mood-stabilizing drugs. *Nature*, 417(6886), 292-295.

- Winsberg, M. E., Sachs, N., Tate, D. L., Adalsteinsson, E., Spielman, D., & Ketter, T. A. (2000). Decreased dorsolateral prefrontal N-acetyl aspartate in bipolar disorder. *Biological psychiatry*, 47(6), 475-481.
- Yang, S., Huang, S., Gaertig, M. A., Li, X. J., & Li, S. (2014). Age-dependent decrease in chaperone activity impairs MANF expression, leading to Purkinje cell degeneration in inducible SCA17 mice. *Neuron*, 81(2), 349-365.
- Yuan, P. X., Huang, L. D., Jiang, Y. M., Gutkind, J. S., Manji, H. K., & Chen, G. (2001). The mood stabilizer valproic acid activates mitogen-activated protein kinases and promotes neurite growth. *Journal of Biological Chemistry*, 276(34), 31674-31683.
- Zuccato, C., & Cattaneo, E. (2009). Brain-derived neurotrophic factor in neurodegenerative diseases. *Nature Reviews Neurology*, 5(6), 311-322.